Spectroscopic Studies of Molecular Conformations and Interactions

by

Richard John William Pulham, B. Sc.

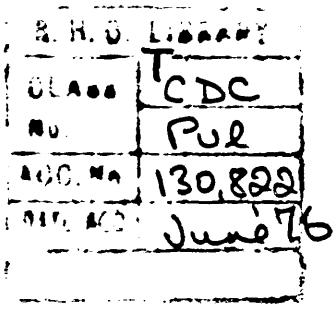

A Thesis presented to the Faculty of Science of the University of London in candidature for the degree of Doctor of Philosophy

Department of Chemistry,
Royal Holloway College,
(University of London),
Egham Hill,
Egham, Surrey.

August 1975

ABSTRACT

The first part of the thesis shows how nuclear magnetic resonance can be used to determine the energy difference between the two conformers of mono-substituted cyclohexanes or tetrahydropyrans.

Proton magnetic resonance and ^{13}Carbon magnetic resonance were used and the recently introduced Fourier transform ^{13}Carbon magnetic resonance was assessed to see if it was suitable for this kind of work.

It was found that the halogeno tetrahydropyran molecules studied have similar free energy differences to those of their cyclohexane analogues.

Force field refinement work was carried out using biphenyl and fluorinated and deuterated derivatives including a new compound, 4-4' difluoro biphenyl d^8. The restriction that all ring C-C stretch force constants should be the same was lifted and the geometry used in the calculations was improved. The dihedral angle of 4-4' difluoro biphenyl d^8 in solution was estimated.

Finally variable temperature studies were carried out on the infrared band shape of the γ_{CH} mode of p-difluorobenzene in cyclohexane and acetonitrile. The band was found to be broader in acetonitrile and to show a much smaller temperature dependence in the polar solvent. This is interpreted as due to vibrational relaxation governing the band width in the polar situation.

Acknowledgements

Many thanks are due to Derek Steele and Duncan Gillies for their invaluable help and encouragement during my stay at Royal Holloway College.

Thanks also to Valerie Eaton, Ian Hill, Ellis Gill, and Donald Owens who helped in various ways and to all Academic and Technical Staff who have helped me.

A grant from the Science Research Council is gratefully acknowledged.

Contents

CHAPTER ONE

NUCLEAR MAGNETIC RESONANCE - THEORY AND METHODS

1.1 The n.m.r. experiment

The existence of nuclear spin was first suggested by Pauli in 1924 in order to explain hyperfine structure in atomic spectra. The proton has a spin quantum number, I, of 1/2 as does the neutron. For nuclei other than ^{1}H the spin angular momenta of the individual nucleons couple (together with their orbital-type angular momenta) to give the observed total.

The facts that ^{12}C and ^{16}O have zero values for I and that n.m.r. depends on the existence of nuclear spin have meant that the spectra of many complex organic chemicals are easy to interpret being attributable to hydrogen nuclei (protons) alone.

As this thesis contains n.m.r. spectra of only two nuclei (^{1}H and ^{13}C) both of which have I = 1/2, this is the only value of I which will be considered here.

A nucleus possessing the spin quantum number of I = 1/2 has two spin states which in the absence of a magnetic field are equally populated. However, when a magnetic field of strength B is applied in a direction defined as z, there is an energy difference between the states, and the populations are no longer equal.

Any motion of a charged particle has an associated magnetic field. In the nucleus the possible angular momenta values are quantised, therefore, so are the associated magnetic moments. In the case of I = 1/2, there are two spin states characterised by $m_I = \pm 1/2$. Because $m_I = +1/2$ aligns with, and $m_I = -1/2$ opposes, the applied field the two energy levels are formed, (Fig. 1.1).

Fig. 1.1 Effect of a magnetic field on the energy levels of a proton.

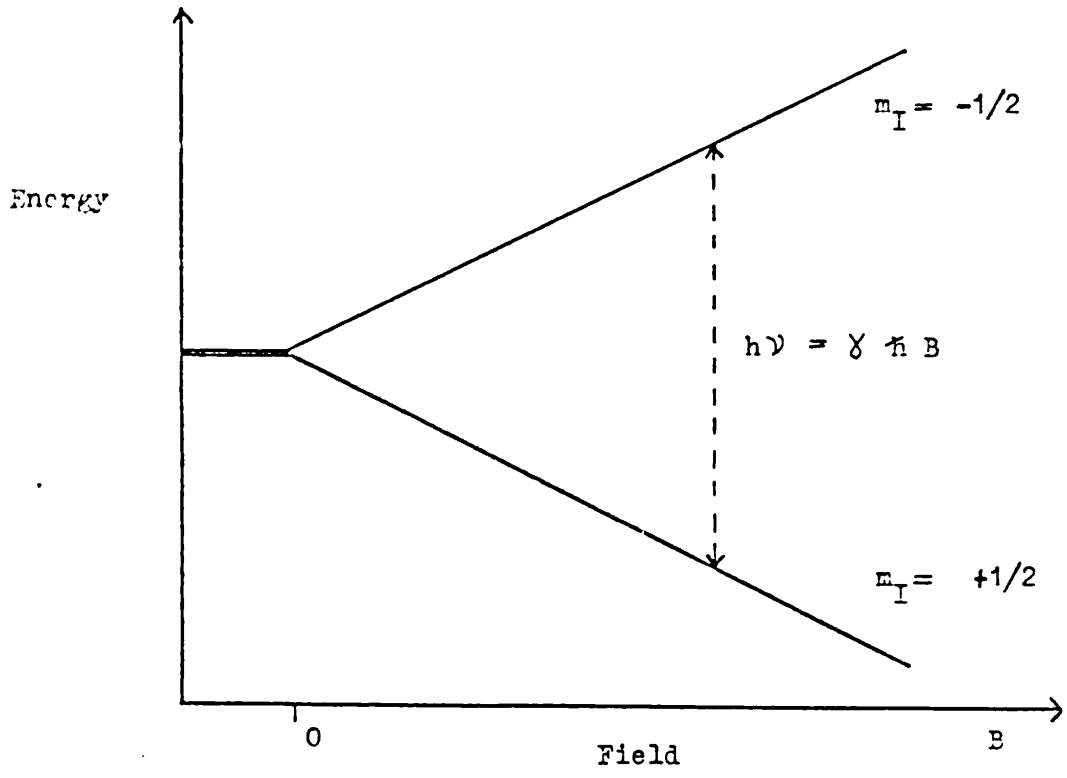

The tendency of nuclei to align with the field and thus drop into the lowest energy level is opposed by thermal motions, which tend to equalise the populations of the two levels. The resultant equilibrium distribution is the usual compromise predicted by the Boltzmann equation

$$\frac{n+}{n-} = \exp\left(-\frac{\Delta E}{kT}\right) = \exp\left(\frac{-\gamma \hbar B_o}{kT}\right)$$

where n+ and n- are the populations of the upper and lower energy levels, $\hbar$ is $h/2\pi$, where h is Planck's constant, and γ, the magnetogyric ratio, which is defined as the ratio of the magnetic moment to the angular momentum. The population excess in the lower energy level is about 10^{-5} times the total population in that level at room temperature. This very small difference in population occurs because the energy difference between the levels is of the order of 10^{-26} Joules.

It is possible to induce transitions between these levels by the use of appropriate electromagnetic radiation. Such transitions will be governed by the Bohr frequency condition, whereby energy is transferred when ΔE, the difference in energy between the levels is equal to $h\nu$, where ν is the frequency of the radiation.

$$h\nu = \left|\gamma \hbar B\right|$$

$$\text{or} \qquad \nu = \left|(\gamma/2\pi)B\right|$$

The magnetic fields are normally in the range 1-5T and the transition frequencies are therefore of the order of tens of MHz and these are in the radio frequency range of the spectrum.

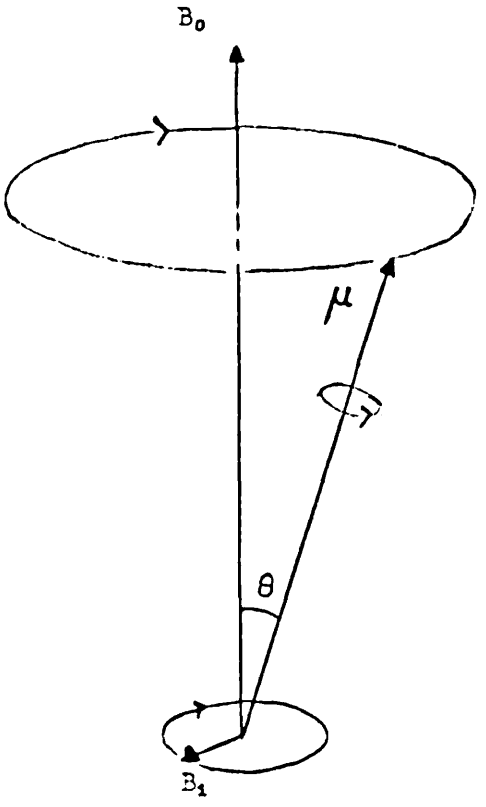

Fig. 1.2 Precession of magnetic moment in the magnetic fields B_0 and B_1.

a) Radiofrequency does not equal Larmor frequency.

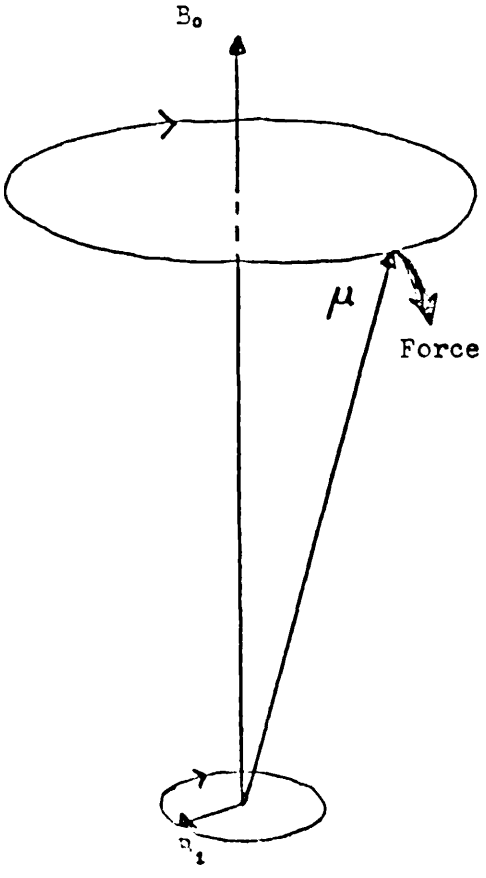

b) Radiofrequency does equal Larmor frequency.

Since the resonance frequency is proportional to the magnetic field, either ν or B may be varied to achieve resonance, but it is more convenient to vary ν. This type of experiment where the frequency range is swept linearly with respect to time is known as continuous wave n.m.r.

1.2 Precession

It can easily be shown by classical mechanics that the torque exerted on a magnetic moment μ by a magnetic field inclined at any angle θ relative to the moment causes the nuclear magnetic moment to precess about the direction of the field with a frequency given by the well known Larmor equation

$$\nu = -\gamma B/2\pi$$

where ν is the Larmor frequency.

If a smaller magnetic field B_1 is introduced, which is of constant magnitude and perpendicular to the original field B_o but is rotating about that direction, such a field will also exert a torque on μ tending to change the angle θ between μ and B_o, (Fig. 1.2a). If B_1 is rotating at some frequency other than the Larmor frequency it will alternately try to increase and decrease θ as μ precesses. Since B_1 is weak the net effect will be a slight wobbling in the precession of μ. If B_1 is rotating about B_o with the same frequency as the precession of μ its orientation with respect to μ will always to constant. Suppose this orientation is such that B_1 is always perpendicular to the plane containing B_o and μ. Then the torque exerted on μ by B_1 will always be away from B_o. Consequently a large effect on μ is possible (Fig. 1.2b).

Fig. 1.3 The relationship between the macroscopic nuclear magnetisation M and individual nuclear moments.

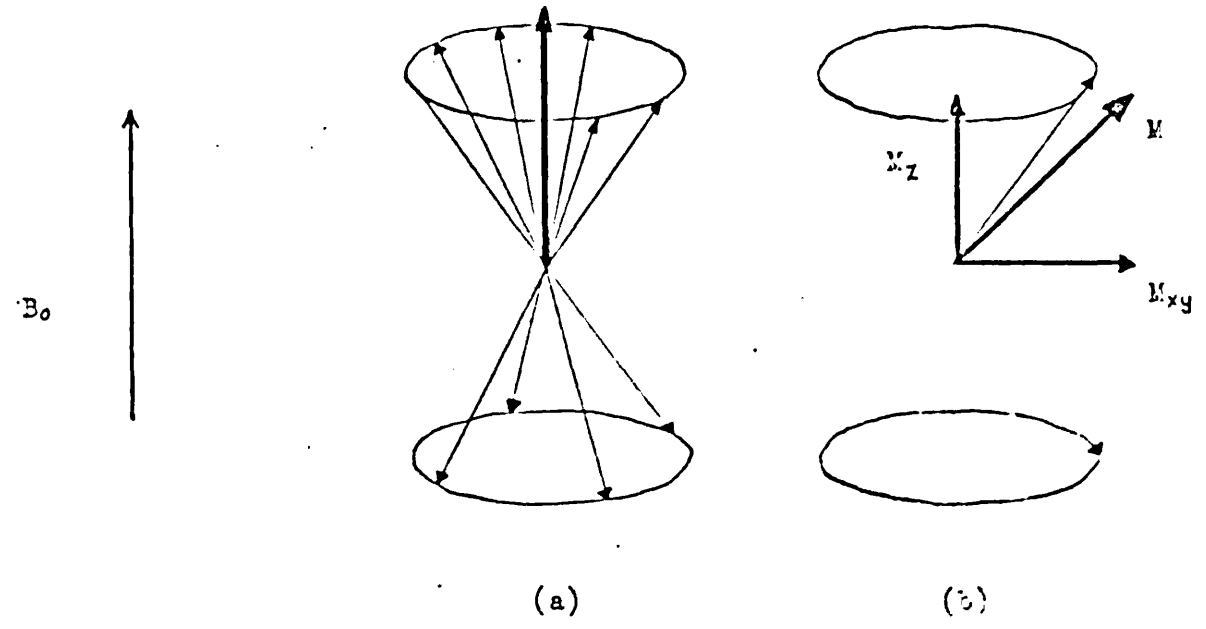

It is more illuminating however to study an ensemble containing a large number of identical nuclei rather than a single nuclear moment. In the absence of resonance the moments of the nuclei precess at the same, Larmor, frequency and with random phase. The Boltzmann distribution slightly favours the lower energy state, so there are more nuclei aligned in the direction of B_0 than opposed to it. Thus there is a net macroscopic magnetisation (M) which is orientated along the z axis (Fig. 1.3a).

An imposed rf field B_1 will have no appreciable effect unless its frequency is the Larmor frequency. In this case two effects are seen. Firstly some nuclei flip by absorbing energy from B_1 so that the populations become more nearly equal thus decreasing M_z. Secondly the nuclei are forced by the rf field to precess in phase, thus creating a component of magnetisation M_{xy} in the xy plane (Fig. 1.3b).

After resonance the nuclei gradually get out of phase with respect to each other. The lifetime for this loss of phase coherence depends on T_2, the spin-spin relaxation time (Fig. 1.3c). The lifetime for the reversion to the Boltzmann distribution between the two energy levels depends on T_1, the spin lattice relaxation time (Fig. 1.3d, e).

1.3 The rotating frame

In order to understand 90° and 180° pulses, it is necessary to consider a frame of reference which rotates in the laboratory frame about the z axis with a frequency equal to the Larmor frequency. The new axes are designated x' y' and z' and this is called the rotating frame (Fig. 1.4a).

Fig. 1.4 The rotating frame.

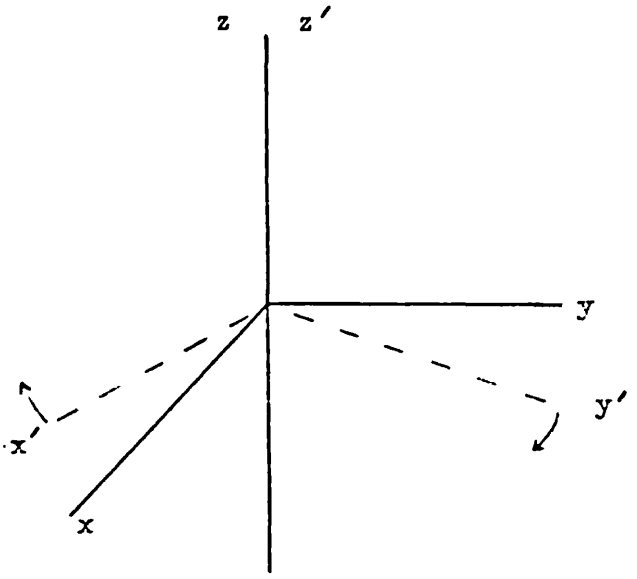

a) Comparison with laboratory frame.

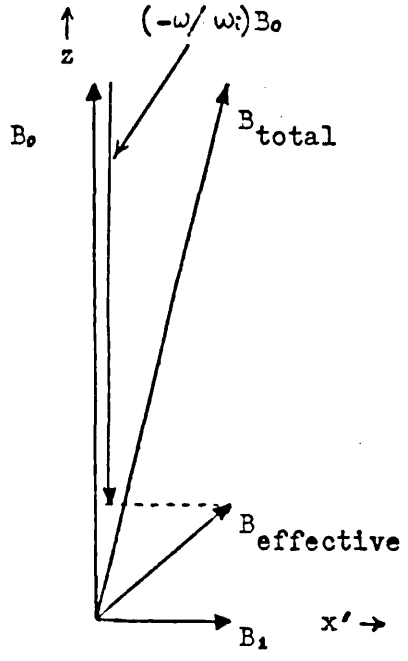

b) Effect on magnetic field.

As the rate at which the frame is rotating increases the precession rate appears to decrease, so an increase in the frequency of rotation has the same effect as decreasing the strength of the static field (Fig. 1.4b).

It can be seen from the diagram that if the frame rotates at the Larmor frequency the angle between the effective field and the z axis increases with increasing radiofrequency until it is entirely in the x' direction at resonance, the static field having been completely cancelled out and the effective field being equal to B_1.

In the rotating frame the magnetisation precesses about the effective field and at resonance it precesses in a circle in the zy' plane, giving a large signal.

From the Larmor equation the magnetisation precesses about the field at a frequency γB_1 and the angle through which M precesses in time t is given by

$$\Theta = \gamma B_1 t \text{ radians}$$

From this expression it is easy to calculate the length of pulse required to induce a precession of the magnetisation by any angle required.

1.4 Nuclear spin relaxation

After excitation the macroscopic magnetisation may be split into two components, M_z along the z axis and $M_{y'}$ along the y' axis. These components decay exponentially to their equilibrium values at rates governed by T_1 and T_2 respectively.

The nuclei interact with fluctuating localized magnetic fields caused for instance by the motions of magnetic moments of surrounding nuclei. Only those components of the magnetic fields fluctuating in the xy plane at the Larmor frequency are effective in exchanging energy with the lattice.

The decay of M_y' is associated with those mechanisms which tend to distribute the magnetic moment directions randomly over a cone with symmetry axis B_o, but negligibly affect the total magnetic energy. An important mechanism for this spin-spin, as well as spin-lattice, relaxation is the dipolar interaction between a nucleus and the surrounding nuclear dipoles. Although the average value is zero in the liquid situation, contributions arise from the non zero value of the mean square amplitude. Another important factor influencing dephasing of magnetisation in the xy plane is inhomogeneity in the magnetic field.

1.5 Saturation

In the presence of an rf field the probability of a transition from one energy level to the other is proportional to the population of the original level. Thus there is slightly more chance of a transition from the lower to the upper energy level than for the reverse and so a net absorption of energy takes place. The population of the upper energy level increases but relaxation processes attempt to reestablish the equilibrium situation.

If a large rf power is used it is possible to excite the nuclei faster than they can relax. The intensity of the absorption spectrum decreases owing to the reduction in the difference in population between

the two levels. If saturation is suspected a faster scan speed or lower rf power must be used. Both tend to degrade the spectrum however and a compromise is often required.

1.6 The typical spectrum

Although each type of nucleus has a characteristic resonance frequency a typical spectrum will contain a number of lines. These arise for two reasons.

Nuclei are screened from the applied static field by their surrounding electrons. The effective field at the nucleus may be lower or higher than the applied field. The amount by which it is changed depends on the chemical environment of the nucleus and the frequency difference is measured in relation to a standard compound (Tetramethylsilane for proton magnetic resonance) in parts per million and is called the chemical shift. This screening effect may vary with orientation of the molecule but an average value is seen in liquids.

Peaks distinguished by different screening effects may be further split into two or more lines by interactions with adjacent magnetic nuclei. In the absence of second order effects, a nucleus with spin I causes its neighbour to exhibit $2I + 1$ lines each separated by J Hz, the coupling constant.

1.7 ^{13}C Nuclear magnetic resonance

The ^{13}C experiment is much less sensitive than proton magnetic resonance (p.m.r.) for two reasons. Firstly ^{13}C has a natural abundance of 1.1%. This natural abundance is low enough to make lines due to ^{13}C - ^{13}C spin-spin coupling interactions very small in normal spectra of

unenriched compounds yet large enough to be considered practical for n.m.r. Secondly the magnetogyric ratio γ of ^{13}C nuclei is about one quarter that of protons. Since the sensitivity of a nucleus in a magnetic resonance experiment is proportional to the cube of γ, each excited ^{13}C nucleus gives rise to 1/64 the signal produced by a proton. Combined, these factors lower the sensitivity by a factor of about six thousand relative to the p.m.r. experiment.

1.8 Fourier transform n.m.r.

The development of Fourier transform n.m.r. has made versatile ^{13}C n.m.r. studies not only practical but also nearly comparable with p.m.r. in terms of experimental ease and quality of results.

The biggest disadvantage of continuous wave (c.w.) n.m.r. is the fact that only one frequency can be observed at one time. For example, a reasonable sweep width for a 20 MHz ^{13}C spectrometer is 4000 Hz. Therefore each 1 Hz wide band is only observed for 1/4000 of the scanning time. By simultaneously exciting all ^{13}C nuclei we can observe the total response of the sample at one time.

The Fourier transform (FT) experiment starts with a short rf pulse. A continuous rf would obviously produce excitation at only one frequency but because a pulse is used a finite bandwidth of frequencies is excited. If the pulse is short enough (about 50 μsec), then the bandwidth of excitation can be greater than 5000 Hz, sufficient to simultaneously excite all ^{13}C nuclei in a sample. In order to strongly excite the sample in this short period of time very high rf power is required.

After the pulse the pattern detected by the receiver is called a free induction decay (FID).

Fig. 1.5 Free induction decay and Fourier transform of 4 - chloro T.H.P.

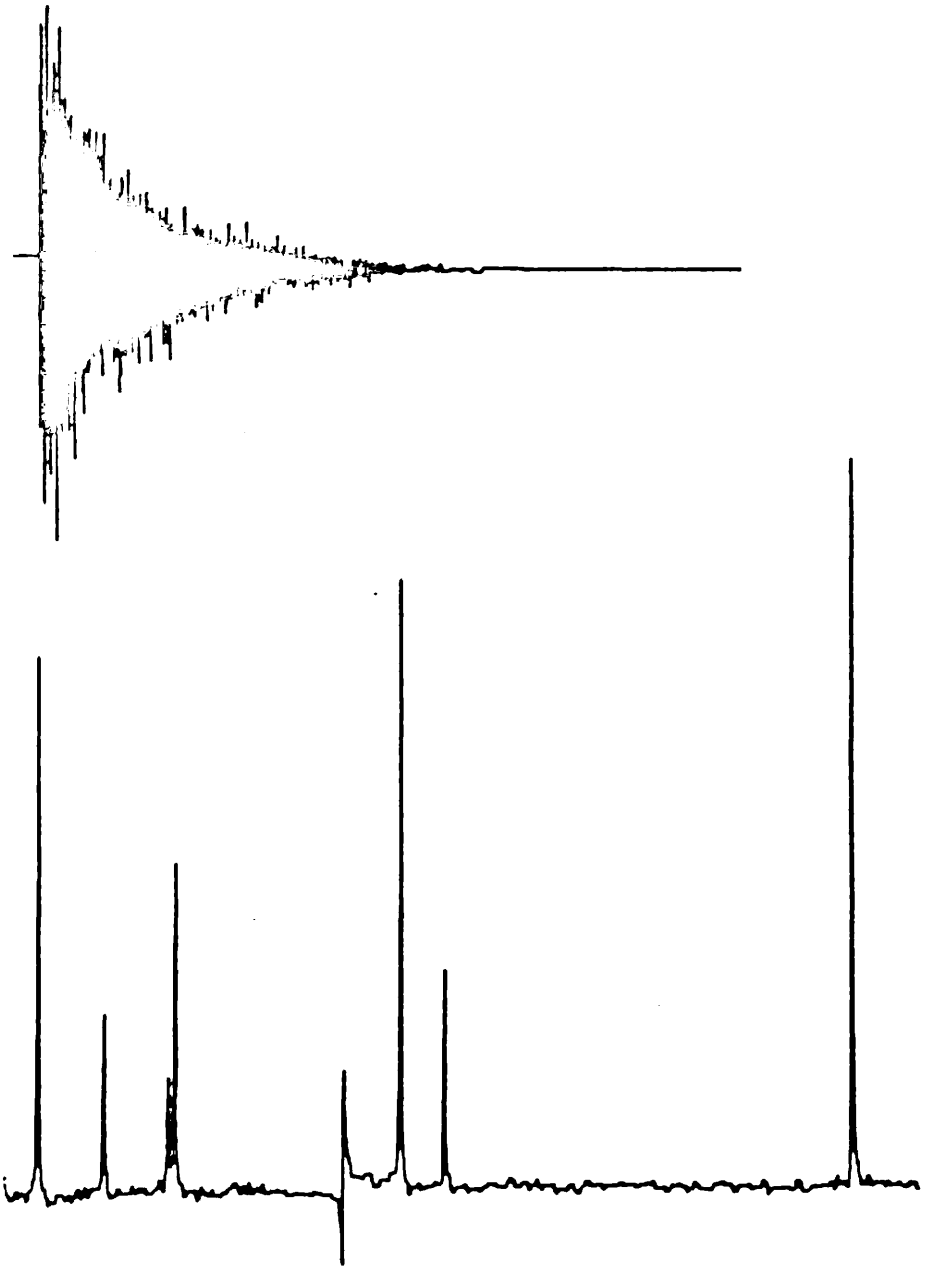

Suppose a 90^{o} pulse is applied along the x' axis. Following the pulse the magnetisation lies entirely in the y' direction. If the rf equals the Larmor frequency, the decay of $M_{y'}$ is exponential, and the FID records an exponential decay since the detector is referenced in phase to the rf. This reference is called the carrier frequency. The FT of this FID consists of absorption and dispersion parts, the absorption line shape being Lorentzian.

If we consider the ^{13}C nucleus in a different environment the Larmor frequency will now be different. The $M_{y'}$ vector will now rotate in the x'y' plane at a frequency equal to the difference between the frequency of the applied field and the Larmor frequency. Now the exponential decay has a sine function superimposed with periodicity equal to the frequency difference. The FT of this pattern has a Lorentzian absorption part which is offset from the carrier frequency by the appropriate amount.

Thus the detector receives a signal which is a complex wave form consisting of signals generated by each type of nucleus in the system and is a function of time (Fig. 1.5). Fourier transformation of this leads to a function of frequency the absorptive part of which is identical to the c.w. spectrum. In practice, it is usual to choose a carrier frequency to one side of the region where resonances are expected to be.

By multiplying the FID by an exponential of the form exp (kt) we can reduce noise at the expense of some artificial broadening of the lines ($k < 0$) or alternatively can enhance resolution by artificially narrowing the lines but with a reduction of signal to noise ($k > 0$) (1).

1.9 Proton Decoupling

Each carbon resonance in an organic molecule is spin-coupled not only to directly attached protons ($J_{CH} > 125$ Hz) but also to protons 2-4 bonds distant ($J < 20$ Hz). These effects broaden carbon resonances and can result in overlap of multiplets. Wide-band proton decoupling allows simultaneous decoupling of all protons in a sample causing each multiplet to collapse to a singlet (in the absence of other magnetic nuclei). The sensitivity increase caused by the collapse of the multiplets to singlets is also enhanced by the Nuclear Overhauser effect.

1.10 Nuclear Overhauser effect

The Nuclear Overhauser effect (NOE) is a direct result of the saturation of the proton nuclei in the decoupling experiment. The carbon nuclei react to the equilisation of proton energy level populations by changing their own energy level populations. This results in an equilibrium excess in the lower ^{13}C energy level relative to that required for the Boltzmann distribution. This allows a bigger absorption of rf energy and hence an increase in peak heights. The enhancement may be up to 2.988 times the expected value but the amount of enhancement is rather unpredictable. This is a problem in conformational work where the enhancement can vary from conformation to conformation as well as from nucleus to nucleus.

CHAPTER TWO

CONFORMATIONAL ANALYSIS OF SIX-MEMBERED RINGS

2.1 Introduction

The term "Conformation" was introduced by Haworth (2) to denote the different spatial arrangements of the atoms in a classical organic structure (Configuration). The different arrangements of the atoms are produced solely by rotation about bonds without any bonds being broken.

Conformational analysis (3) is the study of physical and chemical properties of a compound in terms of its preferred conformations.

It is well known that cyclohexane rapidly interconverts between two identical chair conformations. Each chair has six axial and six equatorial hydrogens. If one of these is replaced by a substituent, the conformers are no longer identical and there is a stability difference between the two. Repulsions between the 1, 3, 5 axial atoms cause the conformer with the axial substituent to be unstable with respect to the equatorial conformer to the extent that derivatives with large substituents can only exist in the equatorial form.

Cyclohexane derivatives have been studied extensively over the past fifteen years, partly because these molecules are freely available and partly because they form a basic unit of many natural products.

Surprisingly little work has been done on their tetrahydropyran (T.H.P.) analogues although a vast amount of work has been carried out on carbohydrates containing the T.H.P. ring.

Fig. 2.1 Interconversion between conformers.

(a) Cyclohexane derivatives.

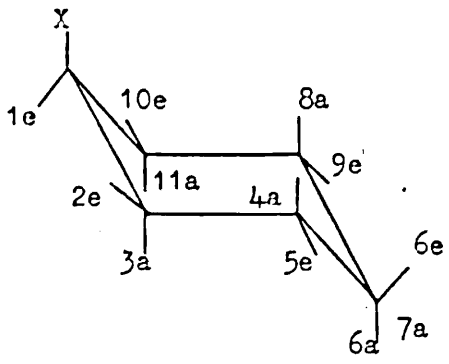

axial

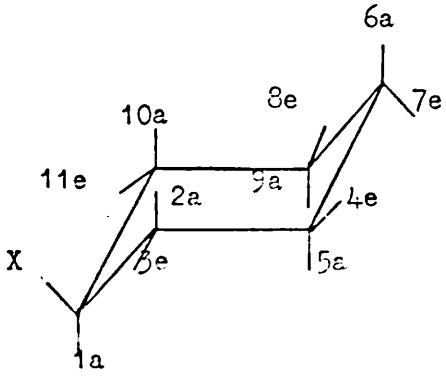

equatorial

(b) Tetrahydropyran derivatives.

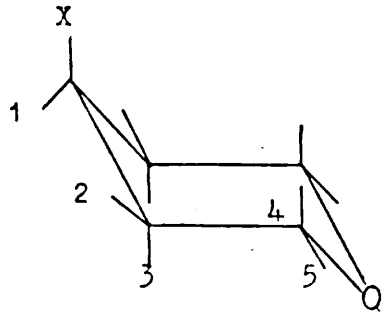

axial

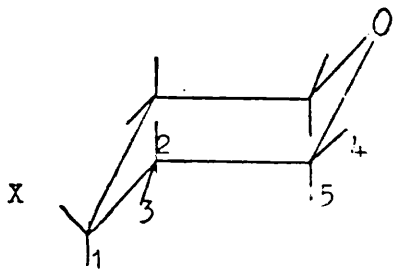

equatorial

Dr. R. Barrett (4) prepared and analysed two mono-halogenated T.H.P. derivatives. It is thought that the presence of an oxygen atom in the ring would have little effect on the energy difference between the two conformers, but this assumption was not endorsed by the results obtained. Part of the current work was to prepare the other mono-halogenated derivatives with the intention of explaining the anomalous result obtained for 4 - chloro T.H.P.

A wide variety of conformational studies have been carried out using n.m.r. In some cases a variety of assumptions have been introduced into the calculations of the results which have eventually proved to have been unjustified. Another aspect of this work was to compare the validity of the methods used to calculate conformational stabilities of equatorial over axial conformers particularly those methods made available by the introduction of Fourier transform ^{13}C n.m.r. During the interconversion between the two chair forms it can be seen from Fig. 2.1 that each proton changes its environment from axial to equatorial or vice versa. At room temperature this interconversion is fast compared with the n.m.r. time scale and an average spectrum is recorded. As the temperature is reduced the spectrum broadens out then eventually sharpens up to give the spectra of both axial and equatorial conformers.

The n.m.r. parameters of the room temperature spectrum are a function of the conformer populations at that temperature and this is an important method of calculating these populations. Information can also be obtained from the line shapes of the spectra obtained at intermediate temperatures.

At present these methods can only be used on simple spectra and could not be used to study the molecules of interest here.

2.2 Methods used to calculate the free energy values.

If K is the constant for the equilibrium between the two conformations,

$$K = x/(1-x)$$

where x is the mole fraction of equatorial conformer, then the standard free energy difference, ΔG°, between the conformers at absolute temperature T is given by

$$\Delta G^{\circ} = -RT\ln K$$

where R is the gas constant.

The standard free energy difference is affected by

1) The size of the substituent (Van der Waal's repulsion).

2) The polarisability of the substituent (London forces of attraction).

3) The length of the bond joining the ring carbon to the first atom of the substituent.

4) The nature of the solvent.

The standard free energy difference is derived from an experimental value for the equilibrium constant. This can be obtained using the following methods.

a) Peak areas

This method employs the use of a low temperature spectrum in which there is no averaging and the peaks are completely resolved. Under these conditions the peak areas are proportional to the population of conformer present (5).

The spectrum was traced on to paper which was cut out and weighed. The experiment was repeated a number of times and the results were found to be sufficiently consistent. The areas were also measured by counting the squares enclosed by the peak on the spectrum. This method is more time consuming but is of comparable accuracy. The use of automatic integrals plotted by the machine are not sufficiently accurate to be considered here.

The use of areas is limited by the following considerations

1) The assignment of each peak considered to its appropriate nucleus must be obvious.

2) The peak must not overlap another.

3) Low temperature measurements are required and the temperature range and the accuracy of the temperature calibration may impose further limitations.

4) The energy of activation for the interconversion must be sufficiently high for the resolved conformers to be measured in the temperature range available.

5) The sample must be liquid at this temperature. This normally requires the use of a solvent. Carbon disulphide was used as this was less likely to affect the equilibrium constant than polar solvents or those which might induce hydrogen bonding.

6) Rf power and sweep rate must be chosen to avoid differential saturation of one conformer. It has been shown (6) that the longer lifetime of the more stable isomer makes it more susceptable to saturation and the

peak areas associated with it may be reduced relative to that of the less stable isomer.

7) If the ^{13}C spectra are proton decoupled there is the likelihood of Nuclear Overhauser enhancement affecting the peak areas. It may differentially affect different nuclei in one molecule or the same nucleus in the different conformers. There is evidence for this latter effect (7) in ^{19}F spectra.

b) Chemical shifts.

Firstly the spectrum is analysed as fully as possible at room temperature and at low temperature. Because the environment of axial and equatorial protons are different these protons have different shifts and coupling constants. When the rate of inversion in s^{-1} is appreciably greater than the chemical shift difference in Hz the observed shift for each proton will be an average of its shifts in the axial and equatorial environments (8) according to the formula

$$\delta = x\,\delta_e + (1-x)\,\delta_a$$

From this the equilibrium constant can be obtained

$$K = \frac{x}{1-x} = \frac{\delta-\delta_a}{\delta_e-\delta}$$

This method when applied to proton spectra assumes that the shifts of the conformers are temperature independent otherwise there is no way of knowing what the shifts are at room temperature. However, a method has been devised to derive shifts at room temperature. This requires the preparation of tertiary butyl derivatives which lock the compound into either the axial or equatorial conformation. The derivatives must be homogeneous and the derivative group must have no effect on the shifts.

However there is evidence that this latter assumption cannot be guaranteed.

Initial evidence that the t- butyl group affects the shifts of the α- proton (9) was discounted because the author was unaware that the chemical shift of a proton was not necessarily at the geometric centre of a symmetrical signal (10). However, more recent evidence (11) clearly shows the t- butyl group effect on the shifts.

c) Vicinal couplings constants.

This method is similar to the previous one in that the room temperature coupling constants are a function of the coupling constants of the individual conformers and the populations of the conformers. Again it is assumed that they are temperature independent, but there are two additional problems. The difference in coupling constants is much smaller than the difference in shifts and second order effects mean that the coupling constants cannot be read directly from the spectrum so they must be obtained by computer analysis.

Evidence has been published that coupling constants are solvent dependent (12, 13) and temperature dependent (14, 15).

d) Line widths

For the X portion of an AA'BB'X spin system the distance between the outer lines is independent of $\nu_A - \nu_B$ and equals $2J_{AX} + 2J_{BX}$. If the H_X resonance is an unresolved hump then an accurate value for this is not available but a rough value can be obtained from the width of the band at a quarter the maximum height of the band.

Because the axial - axial coupling constant is large compared with the other vicinal coupling constants it is possible by this means to assign the band with the greater width to the axial proton.

2.3 A review of n.m.r. studies

The first measurements were carried out on bromocyclohexane (8) by Eliel. He found that he could not reach a sufficiently low temperature and so could not obtain separate spectra. He resorted to the use of locked conformers and recorded an equilibrium constant of 1.5 ± 0.2 equivalent to a standard free energy change of 240 ± 90 cal mol $^{-1}$ (1000 ± 380 J mol $^{-1}$) at room temperature. This value was shown to increase in chloroform and 87% ethanol probably because of preferential hydrogen bonding between the equatorial bromine and the solvent.

Reeves and Stromme achieved spectral separation using carbon disulphide as solvent (16). They derived standard free energy values of 511 cal mol $^{-1}$ (2138 J mol $^{-1}$) for bromocyclohexane and 406 cal mol $^{-1}$ (1700 J mol $^{-1}$) for chlorocyclohexane by measurement of the α proton areas and an activation energy of about 11000 cal mol $^{-1}$ (46000 J mol $^{-1}$).

^{19}F n.m.r. has been used to derive a value of 242 cal mol $^{-1}$ (1013 J mol $^{-1}$) for fluorocyclohexane. This paper (17) also pointed out the fact that the geometric centre of a peak may not necessarily be taken as the shift position.

A point of some importance overlooked in the paper is that there is an intrinsic temperature dependance in the ^{19}F chemical shift of the equatorial conformer.

The equilibrium constant calculated by areas around -50°C is 1.75 and at -87.6°C is 1.96. Their calculation using shifts at 29°C is 1.29. However by extrapolating the lowest values for the individual conformers to room temperature I calculated it to be 1.46. This corresponds to a ΔG^{o} value of 229 cal mol $^{-1}$ (958 J mol $^{-1}$) compared with 154 cal mol $^{-1}$ (644 J mol $^{-1}$) for 1.29. By extrapolating the averaged shifts at high temperature down to -50°C a value of 1.80 is obtained which is in good agreement with the value obtained by areas.

Unfortunately the earlier paper (16) on chloro- and bromocyclohexane gives very little experimental data. The shifts for the bromocyclohexane conformers appear to be temperature independent. It is more difficult to judge the chlorocyclohexane results as only two low temperatures are quoted but the shifts change with temperature in each case despite their claim to the contrary. However, in this case, the experimental error probably justified the assumption but in the case of the ^{19}F n.m.r. paper the trend seems to be much more apparent. If this correction is accepted their value of 1.05 e.u. (4.39 J mol $^{-1}$ K $^{-1}$) for ΔS^{o} may be reduced to about 0.1 e.u. (0.4 J mol $^{-1}$ K $^{-1}$). Another example of the temperature effect on fluorine shifts is given in reference 7.

ΔS^{o} values for chlorocyclohexane (18) have been assessed as being between 0.25 and 0.49 e.u. (1.05 and 2.05 J mol $^{-1}$ K $^{-1}$) depending on solvent and for bromocyclohexane between 0.40 and 0.51 e.u. (1.67 and 2.13 J mol $^{-1}$ K $^{-1}$), but there is no evidence that these results are any more accurate than the previous one. Indeed, since no low temperature spectra were run the fact that the shifts are a function of temperature is unlikely to have been considered.

A fine paper by Jensen and Beck (11) showed by direct comparison that the shifts of the α - proton in the two conformers of some cyclohexane derivatives at low temperature do not correspond to their 4 - tertiary butyl equivalents. They were also able to show between -80°C and -105°C that the effect of temperature on these shifts were the same and concluded that although it could not be proven that this was the case at higher temperatures, that it was a better method than that previously used whereby the room temperature 4 - tertiary butyl derivative shifts were assumed to be the same as the inaccessible shifts of the unlocked parent compounds.

Even the method of measuring peak areas is known to be fraught with hidden dangers (6). In cases where a definite conformational preference exists then the half-life of a molecule in the less stable conformation is shorter than that of a molecule in the more stable form. By the process of interconversion the molecules of the less stable conformer are replaced by unsaturated molecules faster than those of the more stable isomer;

therefore, the peaks which correspond to the less stable conformer will tend to saturate less readily than those of the more stable form causing the apparent equilibrium constant to decrease as power is increased. Current relaxation studies indicate that the differences in relaxation time between the conformers is small.

The paper also indicates that the ΔS^{o} values should be less than 1 e.u. (4 J mol $^{-1}$ K $^{-1}$) for all the cyclohexyl halides.

The newest development in this field has been the availability of low temperature ^{13}C F.T. n.m.r. (19, 20).

One paper (21) quotes ΔG^{o} values obtained from ^{13}C spectra for cyclohexyl halides. These are similar to earlier values but are not as close as might be expected. No mention was made about the effect of temperature on the chemical shifts.

Generally, however, taking all the information available, we can deduce an order for the free energy differences between the conformers of the cyclohexyl halides such that

$$Cl > Br > I > F$$

These differences can be rationalised in terms of internuclear distances, covalent radii and polarisabilities of the electron clouds. In a series of comparable atoms arranged in order of increasing radii, the contributions to steric interactions due to increased size and increased polarisability should be in opposite directions. These effects are roughly counterbalanced in the chloride, bromide and iodide derivatives.

Table 2.1 Literature determinations of ΔG° values.
p.m.r. results unless otherwise stated.

Compound	ΔG°(cal mol^{-1}) area	shift	ΔG°(J mol^{-1}) area	shift	Conditions	Reference
C_6H_{11}-X						
Br		240		1004	RT locked	8
Br	511		2138		173°K; CS_2	16
Cl	406		1699			
F	250	241	1046	1008	180°K; CS_2	24
Cl	513	478	2146	2000	192°K; CS_2	
Br	480	439	2008	1837		
I	431	407	1803	1703		
Cl	777		3251		198°K; CS_2	25
Br	722		3021			
I	692		2895			
F	244		1021		218°K	17
F	249		1042		185°K ^{19}F; CCl_3F	
F		229*		958*	302°K	
F	273		1142		182°K CS_2	
Cl		389-448		1628-1874	309°K various solvents. locked.	18
Cl		371-486		1552-2033	412°K	
Br		393-421		1644-1761	308°K	
Br		441-472		1845-1975	412°K	

Table 2.1 (continued).

Compound	ΔG (cal mol^{-1}) area	ΔG (cal mol^{-1}) shift	ΔG (J mol^{-1}) area	ΔG (J mol^{-1}) shift	Conditions	Reference
C_6H_{11}-X						
Cl	490	350	2050	1464	193°K; CS_2	11
Cl		550**		2301**		
Br	530	390	2218	1632		
Br		570**		2385**		
F	276 ± 15		1155 ± 63		187°K; CS_2	6
Cl	528 ± 19		2209 ± 79		192°K	
Br	476 ± 13		1992 ± 54		192°K	
I	468 ± 21		1958 ± 88		192°K	
F	360 ± 25		1506 ± 105		180°K; ^{13}C; CF_2Cl_2	21
Cl	620 ± 40		2594 ± 167		200°K	
Br	585 ± 25		2448 ± 105		200°K	
I	455 ± 25		1904 ± 105		180°K	
C_5H_9O-X						
Cl	704/855		2946/3577		300°K; CS_2	4
Br	467		1954			

* Allowing for temperature dependence of shifts. See text.

** Allowing for temp. dependence of shifts of locked conformers.

The deformation of the electron cloud of fluorine should occur with the most difficulty, but fluorine is a small atom and the internuclear distances appear to be sufficiently great that steric interactions are small.

The replacement of a methylene group in cyclohexane by an - O - grouping gives the parent heterocyclic molecule, T.H.P. The shape is expected to be slightly different because the C - O bond length (1.42×10^{-10} m) is somewhat smaller than the C - C bond length (1.52×10^{-10} m). This causes an increase in some of the 1, 3 diaxial non-bonded interactions. However it has been shown that the inversion rate of T.H.P. (22) is similar to that of cyclohexane (23) and the general trend for the free energy differences between the conformers of the 4 - halo tetrahydropyrans is expected to be the same. Consequently, the free energy difference values derived by Dr. Barrett (4) cannot be explained by the above considerations and evidence has been produced in the course of this work which indicates that the value for 4 - chloro T.H.P. is much lower.

A survey of the data obtained using n.m.r. is given in table 2.1.

2.4 Calculation of n.m.r. spectra

The program used for these calculations was UEA NMR BASIC, attributed to C.M. Woodman and R.K. Harris of the University of East Anglia. The program accepts an arbitary set of chemical shifts and coupling constants and generates an ordered table of frequencies and intensities of the lines expected in the n.m.r. spectrum.

Each line is given a line identification number, which is related to the energy level diagram.

The program automatically performs magnetic equivalence factoring, treating an X_3 group, for example, as occupying either a quartet state with spin 3/2 or a doublet state with spin 1/2, and multiplying the calculated intensities by the appropriate weighting factor.

If different types of nuclei are present, with large differences in resonance frequency, further factorisation is performed for each type of nucleus.

The spectrum of each type of spin state and of each type of nucleus is printed separately.

The program may also be used to calculate the spectra of molecules containing nuclei with spin greater than 1/2.

The program can handle any seven spin - 1/2 system and certain larger systems with magnetic equivalence.

PLOTTING. In each case a Lorentzian line shape (cut off at ten half-widths) is assigned to each line, and the intensity at 1000 equally spaced points across the plotted region is calculated. These points are plotted as a continuous curve of frequency against intensity. The width of the grid on which each spectrum is plotted is 50cm. The heights of the peaks can be increased or decreased at will. If the scaling factor is greater than 1.0 the largest peaks are truncated at 1.0 at the top of the plot.

The following amendments were introduced into the program during the course of this work.

The maximum height could be scaled to less than 1.0 (rather than $\geqslant 1.0$ as it was before). This was found useful for comparing spectra of compounds mixed together in different quantities, in this case axial and equatorial conformers.

The intensities were calculated for 1000 points and so if the plotting region is, for example, 1000 Hz the plotting interval is 1 Hz. Consequently the maximum intensities derived from these values are only accurate to the nearest 1 Hz. A facility was introduced whereby the intensities were recalculated at 0.1 Hz intervals for 1 Hz on either side of these maxima so that the new maxima were accurate to the nearest 0.1 Hz.

In order to save paper it is possible to plot spectra one half the normal size.

INPUT

Card 1 NC, NN, NWANT, NISO, NAME FORMAT(4I3,10A6)

NC - arbitary case number.

NN - number of nuclei, or magnetically equivalent groups of nuclei. $NN \leqslant 7$

NWANT - number of ISO values for which calculated spectrum is required.

NISO - number of different ISO values (not greater than 4)

NAME - arbitary title or compound name.

Card 2 FR1, FR2, AMIN FORMAT(3F 10.0)

FR1 - lower limit of frequency range

FR2 - upper limit of frequency range

AMIN - minimum intensity of lines for which a print-out is required.

Card 3 ISO(I), I = 1,7, I(I), I = 1,7, KHS(I) = 1,7 FORMAT(21I1)

Each nucleus is given an ISO value. Nuclei with small chemical shift differences relative to their coupling constants are given the same ISO value.

L(I) is the maximum multiplicity (2I+1) for each group.

KHS(I) is used for nuclei with spin greater than 1/2.

Card 4 W(I), I = 1, NN FORMAT(7F10.0)

W(I) is the chemical shift of the I^{th} nucleus or group, in Hz.

Card 5 to (4+NN) FORMAT(7F10.0)

These cards contain coupling constants in Hz as follows,

Card 5 J(1,2), J(1,3) ... J(1,NN)

Card 6 J(2,3), J(2,4) ... J(2,NN) etc.

Card 5+NN 1 in first column

PLOTTING INPUT

Card 1 1 in first column for full size plot or 0 for half size

Card 2 NC, NISO, TITLE FORMAT(2I3,10A6)

NC - arbitary case number

NISO - Iso value to be plotted

TITIE- arbitary title which appears on the plot 9 in column 80 recalculates maximum intensities as described in the previous section.

Card 3 W, FR1, FR2, SCUP FORMAT(4F10.0)

W - full width at half height in Hz

FR1 - lower limit of frequency range to be plotted

FR2 - upper limit of frequency range to be plotted

SCUP - scaling of maximum intensity

Further plots can be obtained by further pairs of cards (Card 2 and Card 3) and two blank cards terminate the program.

2.5 Methods of preparation

3 - butene - 1 - ol

3 - butene - 1 - ol was prepared by selective reduction of vinyl acetic acid (3 - butenoic acid) (26).

Lithium aluminium hydride (105 g, 2.76 mole) was placed in a five litre three - necked flask equipped with reflux condenser, dropping funnel and mechanical stirrer. Calcium chloride tubes were connected to the condenser and dropping funnel to protect the apparatus from atmospheric moisture.

Sodium - dried diethyl ether (1400ml) was added to the flask, which was ice - cooled. A solution of vinyl acetic acid (Koch - Light) (232 g, 2.70 mole) in ether (800ml) was added via the dropping funnel at such a rate as to produce a steady reflux. On completion, water was cautiously added to decompose excess hydride. The mixture was neutralised by the addition of 3160ml of 10% sulphuric acid with further cooling and the product was extracted with ether. The extracts were dried with anhydrous magnesium sulphate. A crude product was obtained on rotary evaporation which was distilled under vacuum to give 3 - butene - 1 - ol (b.pt. 113°C (760mm), yield 60%)

Tetrahydropyran - 4 - ol

T.H.P. - 4 - ol was prepared by a Prin's cyclisation outlined by Hanschke (27).

3 - butene - 1 - ol (268 g, 3.72 mole) and 360 ml of a freshly prepared saturated paraformaldehyde solution (prepared by refluxing paraformaldehyde and distilled water overnight) were added to a five litre three - necked flask equipped with a condenser, dropping funnel and mechanical stirrer. The flask was heated on an oil bath to 80°C. Concentrated sulphuric acid (54ml) was added, slowly, to reduce the amount of charring as much as possible. The mixture was heated for a further four hours and then neutralised with 2N sodium hydroxide solution. The product was extracted with ether and the extracts dried over anhydrous magnesium sulphate.

After rotary evaporation the crude product was distilled under vacuum. The first fraction was 3 - butene - 1 - ol which could be used again. The second fraction was tetrahydropyran - 4 - ol (b.pt. 86°C (11mm), n_D^{20} 1.4606).

Tosyl derivative of T.H.P. - 4 -ol

Tetrahydropyran - 4 - ol (17g, 0.17 mole) was dissolved in 150ml dry pyridine, which had been dried by distilling from sodium hydroxide pellets. The solution was cooled in an ice - salt bath to -5°C. Tosyl chloride (34g) was slowly added, the mixture being swirled until each addition had dissolved. The flask was left overnight in a refrigerator, during which time crystals had formed showing that the reaction was complete. A small amount of water (1ml) was added with shaking and the mixture was poured into 150ml water. The product forms as crystals which are filtered off and the filtrate is extracted with chloroform, which when rotary evaporated to dryness gives another yield of product. The crystals are recrystallised to constant melting point (54.5°C) in ethanol.

Purification of p - toluenesulphonyl chloride (28)

Tosyl chloride (200g, Koch - Light) was dissolved in the minimum amount of dry chloroform (about 500 ml) and the resulting solution diluted with five volumes of petroleum ether (40 - 60°). The impurities were filtered off and the filtrate treated with activated charcoal, concentrated on a steam bath to about 800ml which was then rotary evaporated to dryness to give pure p - toluenesulphonyl chloride (m.pt. 67.5 - 68.5°C).

Tetra - n - butylammonium fluoride

A 40% aqueous hydrogen fluoride solution (3 - 4ml) was placed in a polythene beaker and was titrated with 40% aqueous tetra - n - butylammonium hydroxide solution to pH 6-7 using pH indicator paper. The mixture was diluted to three times its volume with distilled water and then cooled in ice. Tetra - n - butylammonium fluoride crystals were deposited which were filtered on a water pump, washed with a small volume of cold water, air dried, then transferred to a round - bottomed flask. The crystals were melted (40 - 50°C) under reduced pressure on a rotary evaporator. This temperature was maintained until no more water would evaporate from the solution which was then poured into a crystallising dish. This was placed in a vacuum desiccator over phosphorus pentoxide. It was necessary to break up the solid which formed to allow as much water to be removed as possible. After a few days the drying is complete and the product is extremely hygrosocpic.

Concentration of the mother liquors from the first filtration to about one third of the original volume followed by cooling will yield a further crop of crystals.

4 - fluoro tetrahydropyran

Several attempts were made to prepare this previously unreported compound but it was not possible to isolate it.

The tosylate of T.H.P. - 4 - ol (10g, 0.04 mole) was dissolved in 100 ml pure dry acetonitrile. A slight excess of tetra - n - butylammonium fluoride (15g, 0.06 mole), weighed under dry conditions, was quickly added to the mixture, which was refluxed for three hours.

After leaving overnight the solution was distilled under vacuum leaving a treacle coloured compound as residue. G.L.C. and M.S. analysis indicated three components having molecular weights of 104, 84, and 41, corresponding to 4 - fluoro tetrahydropyran, 2, 3 - dihydro - α - pyran, and acetonitrile, there being less than 5% of the fluoride.

Various attempts at fractional distillation were carried out but the compound only distilled over in the presence of solvent and was clearly losing hydrogen fluoride to form 2, 3 - dihydro -α- pyran. Dimethyl-formamide and propionitrile were also used as solvent, the mixture being heated to about 80°C in each case. Again it was not possible to separate the compound.

4 - chloro tetrahydropyran

3 - butene - 1 - ol (50g, 0.71 mole) was placed in a 500ml three - necked flask equipped with a condenser, mechanical stirrer and bleed together with 100ml saturated formaldehyde solution in the presence of excess para-formaldehyde powder (4). Hydrogen chloride from a small lecture bottle was bubbled at a steady rate through the contents of the flask, cooled in an ice - bath, until the solution was saturated (i.e. all the paraformaldehyde had dissolved), care being taken to avoid sudden suckback. The flask was then surrounded by ice, the solution neutralised with aqueous sodium hydroxide, then extracted with diethyl ether. The extracts were dried with anhydrous magnesium sulphate.

The ether was removed by rotary evaporation to give a crude product which was distilled to give 4 - chloro tetrahydropyran (b.pt. 42° at 12mm of Hg).

4 - iodo tetrahydropyran

Tetrahydropyran - 4 - ol (6.56g, 0.064 mole) was placed in a 100ml flask equipped with a mechanical stirrer, condenser and thermometer, together with 88% orthophosphoric acid (15ml) and potassium iodide (36g)(29, 30). The mixture was stirred and heated on an oil bath at 110 - 120°C for 4-5 hours. The stirred mixture was allowed to cool and 16ml of water and 30ml of ether were added. The ether layer was separated, shaken with 50ml of 10% sodium thiosulphate solution, washed with 22ml of cold saturated sodium chloride solution and dried with 6g anhydrous sodium sulphate. The ether was removed by rotary evaporation, and the product, purified by vacuum distillation, was stored by refrigeration.

This compound was previously unreported but gave mass spectrometric and n.m.r. results consistant with 4 - iodo tetrahydropyran.

Cyclohexyliodide

This compound was prepared using the same method as for 4 - iodo tetrahydropyran. The preparation was carried out on a larger scale, however, as the starting material, cyclohexanol, was freely available.

2.6 Results obtained by n.m.r.

a) Proton magnetic resonance

Calculations were originally carried out on 4 - iodo T.H.P. and the standard free energy difference value obtained was similar to that of cyclohexyl iodide. As it had already been shown that the values for cyclohexyl bromide and 4 - bromo T.H.P. were similar further data were collected to check the unexpected value obtained for 4 - chloro T.H.P. This new calculation yielded a much lower value which was more in keeping with the value for cyclohexyl chloride.

An attempt was made to derive all the coupling constants and chemical shifts for each conformer and for the average spectrum. Expected values for these parameters were fed into the computer program previously described and the calculated spectrum obtained was compared with the experimental spectrum. Initial assignments were made on the basis of expected chemical shifts, expected coupling constants and integrated intensities.

In order to carry out the n.m.r. calculations it was necessary to introduce one approximation. The program used was only capable of handling seven types of nucleus. Because there are nine protons in each of the molecules considered it was necessary to divide the molecule about its plane of symmetry and to consider the protons in only one half. These are labelled 1-5 in Fig. 2.1. This is a good approximation as long range couplings are unlikely to be apparent in the spectrum. However it does introduce two artifacts into the computed spectrum of the proton attached to the substituted carbon.

Firstly its intensity is double what it should be and secondly the splittings caused by the protons on the adjacent carbon in the half not considered are not computed.

A long series of calculations were carried out, gradually changing the parameters to get the best fit. Naturally it was found most difficult to compute spectra when chemical shifts differences were small because of the lack of information obtainable from these parts of the experimental spectra, and likewise in the low temperature spectra where there were overlapping resonances.

Generally, however, it would be fair to say that the calculated shifts are sufficiently accurate for calculating standard free energy differences except when there are two shifts very close together to the extent that second order effects are dominant.

Further problems arise when estimating coupling constants. The coupling constants are small and are thus more susceptible to recording errors. In the absence of second order effects the separation between the outside lines of a resonance equals the sum of the coupling constants. This separation can be reasonably accurately measured but there can be slight differences in the individual couplings which still give the same sum. For example, the sum of 2.8, 3.4 and 7.8 or 3.0, 3.1, and 7.9 is 14.0 in both cases. This error is reduced if confirmation of these coupling constants appear elsewhere in the spectrum.

Table 2.2a 4-iodo T.H.P. Data for calculated spectra in Hz.

AVERAGE

Nucleus	1	2	3	4	5
220 MHz shift	953.8	462.0	454.7	815.1	746.9
100 MHz shift	433.4	210.0	206.7	370.1	339.6

J_{12}	6.8	J_{13}	6.4	J_{14}	0.0	J_{15}	0.0
J_{23}	-12.0	J_{24}	4.3	J_{25}	5.9		
J_{34}	4.3	J_{35}	5.5				
J_{45}	-11.5						

Table 2.2b 4-iodo T.H.P. Data for calculated spectra in Hz.

EQUATORIAL

Nucleus	1	2	3	4	5
220 MHz shift	912.2	490.0	475.0	814.5	719.0
100 MHz shift	413.8	224.5	217.2	370.5	326.3

J_{12}	8.8	J_{13}	7.3	J_{14}	0.0	J_{15}	0.0
J_{23}	-12.0	J_{24}	3.4	J_{25}	8.6		
J_{34}	3.4	J_{35}	4.8				
J_{45}	-12.0						

AXIAL

Nucleus	1	2	3	4	5
220 MHz shift	1044.8	403.5	411.5	810.0	802.0
100 MHz shift	473.6	185.5	190.0	368.8	366.8

J_{12}	3.0	J_{13}	3.0	J_{14}	0.0	J_{15}	0.0
J_{23}	-12.0	J_{24}	3.0	J_{25}	3.0		
J_{34}	7.1	J_{35}	3.0				
J_{45}	-11.8						

Table 2.2c 4-chloro T.H.P. Data for calculated spectra.

AVERAGE

Nucleus	1	2	3	4	5
220 MHz shift	897.9	396.7	446.8	849.5	749.6
100 MHz shift	406.7	180.3	203.1	386.1	340.7

J_{12}	8.6	J_{13}	4.2	J_{14}	0.0	J_{15}	0.0
J_{23}	-12.7	J_{24}	4.5	J_{25}	8.4		
J_{34}	4.5	J_{35}	3.0				
J_{45}	-11.8						

Table 2.2d 4-chloro T.H.P. Data for calculated spectra.

EQUATORIAL

Nucleus	1	2	3	4	5
220 MHz shift	854.7	397.6	441.9	851.0	718.3
100 MHz shift	389.4	180.7	200.9	387.4	324.3

J_{12}	11.6	J_{13}	4.9	J_{14}	0.0	J_{15}	0.0
J_{23}	-12.6	J_{24}	4.3	J_{25}	11.8		
J_{34}	1.5	J_{35}	3.0				
J_{45}	-11.6						

AXIAL

Nucleus	1	2	3	4	5
220 MHz shift	988.6	383.5	464.5	808.0	798.0
100 MHz shift	450.1	174.3	211.1	367.0	361.5

J_{12}	2.8	J_{13}	2.8	J_{14}	0.0	J_{15}	0.0
J_{23}	-12.8	J_{24}	4.9	J_{25}	2.2		
J_{34}	7.0	J_{35}	3.0				
J_{45}	-12.0						

The fact that the resonance of proton 1 is not calculated is not a serious disadvantage because the shifts are generally well clear of the remainder of the spectrum and the splittings are due to only two types of coupling constant. This is the region of the spectrum which is normally used for this type of calculation.

The values of coupling constants where good agreement was obtained were accurate to within ± 0.1 Hz. A larger error in the chemical shifts is acceptable because of the larger differences involved but these were considered accurate within ± 1 Hz.

Table 2.2 shows the data used to produce the best fit between calculated and experimental spectra. Although 220 MHz and 100 MHz spectra were calculated the coupling constants were found to be the same for both and are consequently only detailed once.

Comparison between individual calculated spectra and their experimental equivalents.

The numbers 1 - 5 in this section refer to the proton labels already discussed.

4 - iodo T.H.P. 220 MHz (Fig. 2.2)

Average (Fig. 2.3)

The shifts and coupling constants for protons 1, 4 and 5 give good agreement, but overlap of the resonances of protons 2 and 3 means that little information can be obtained from this region.

Fig. 2.2 . 220 MH z spectrum of 4-iodo tetrahydropyran in CS_2.

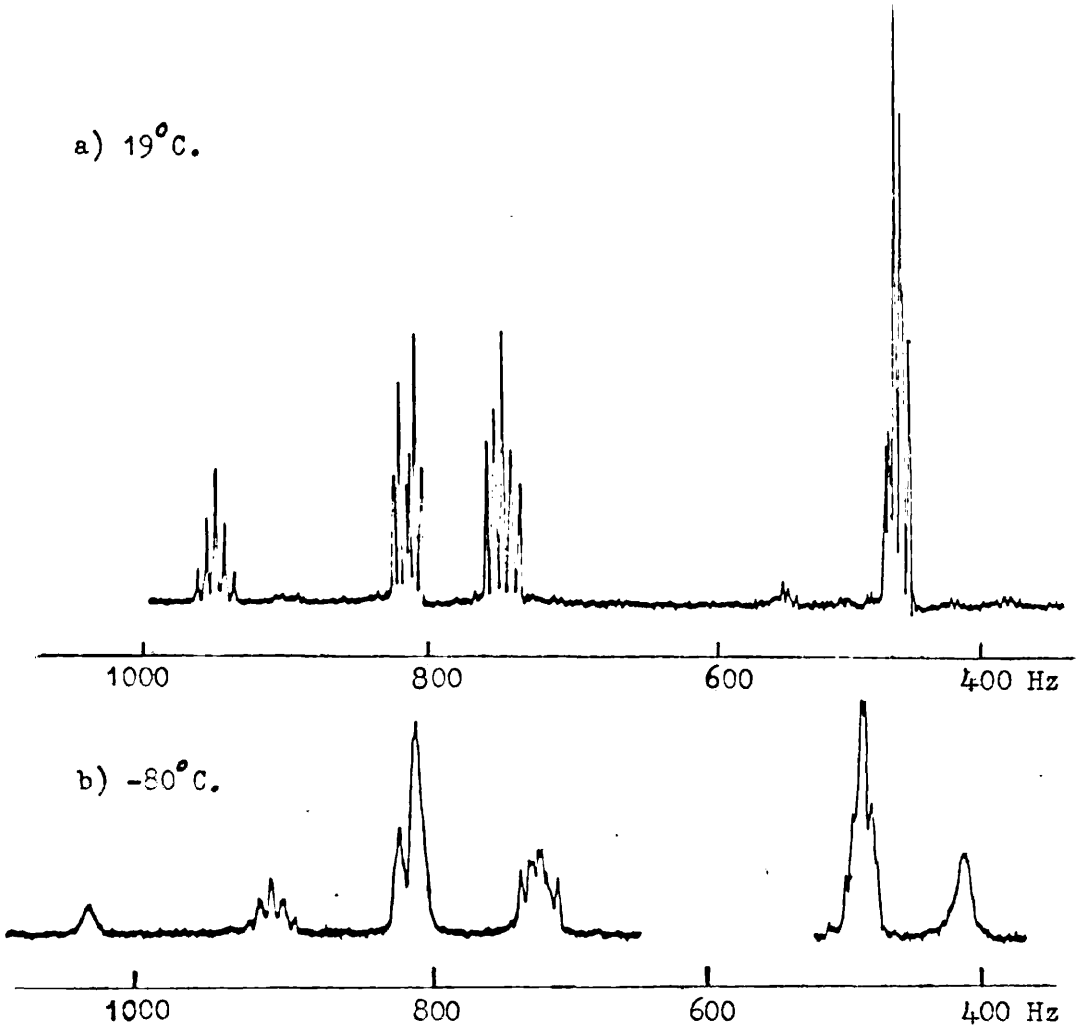

Fig. 2.3.

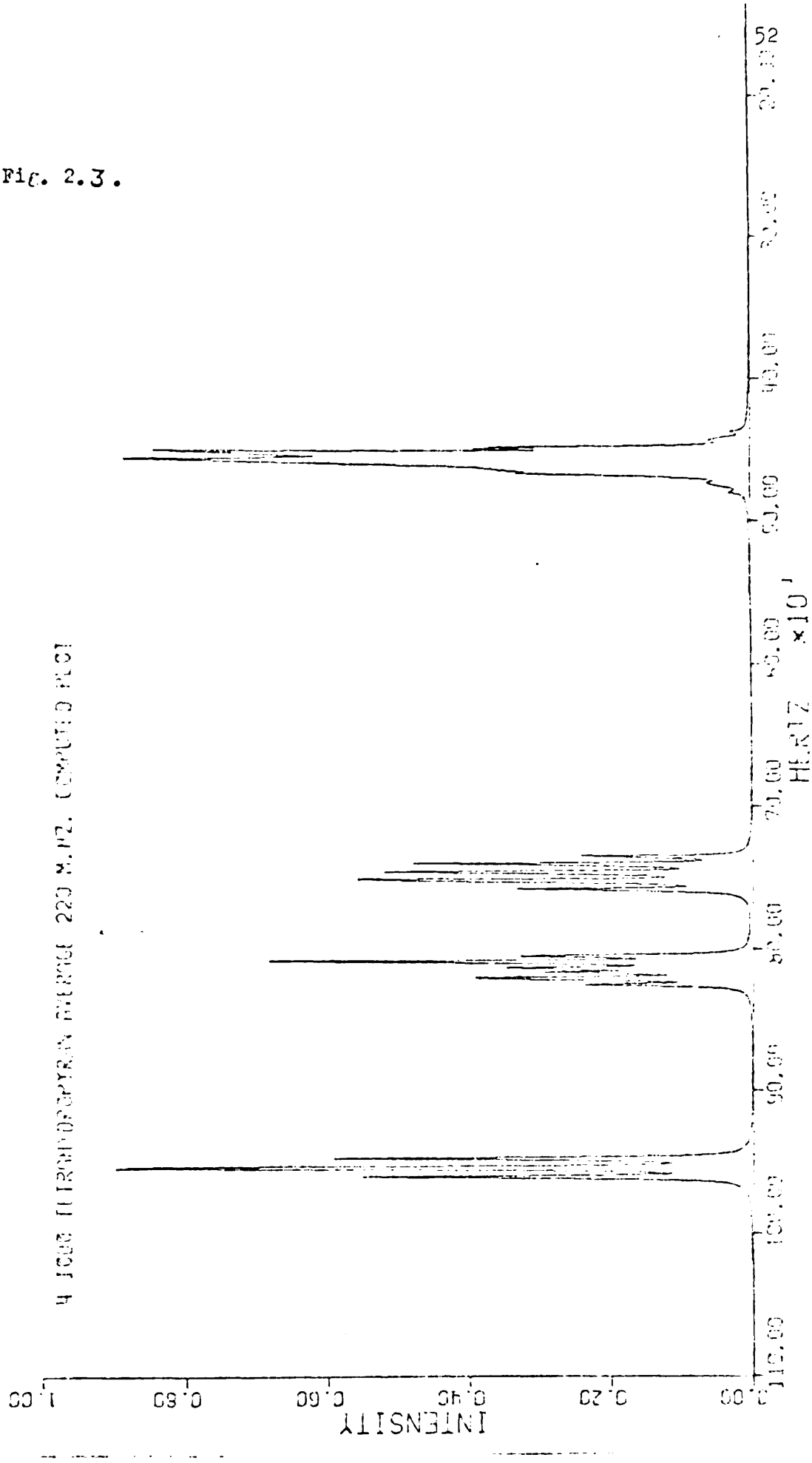

Fig. 2.4 .

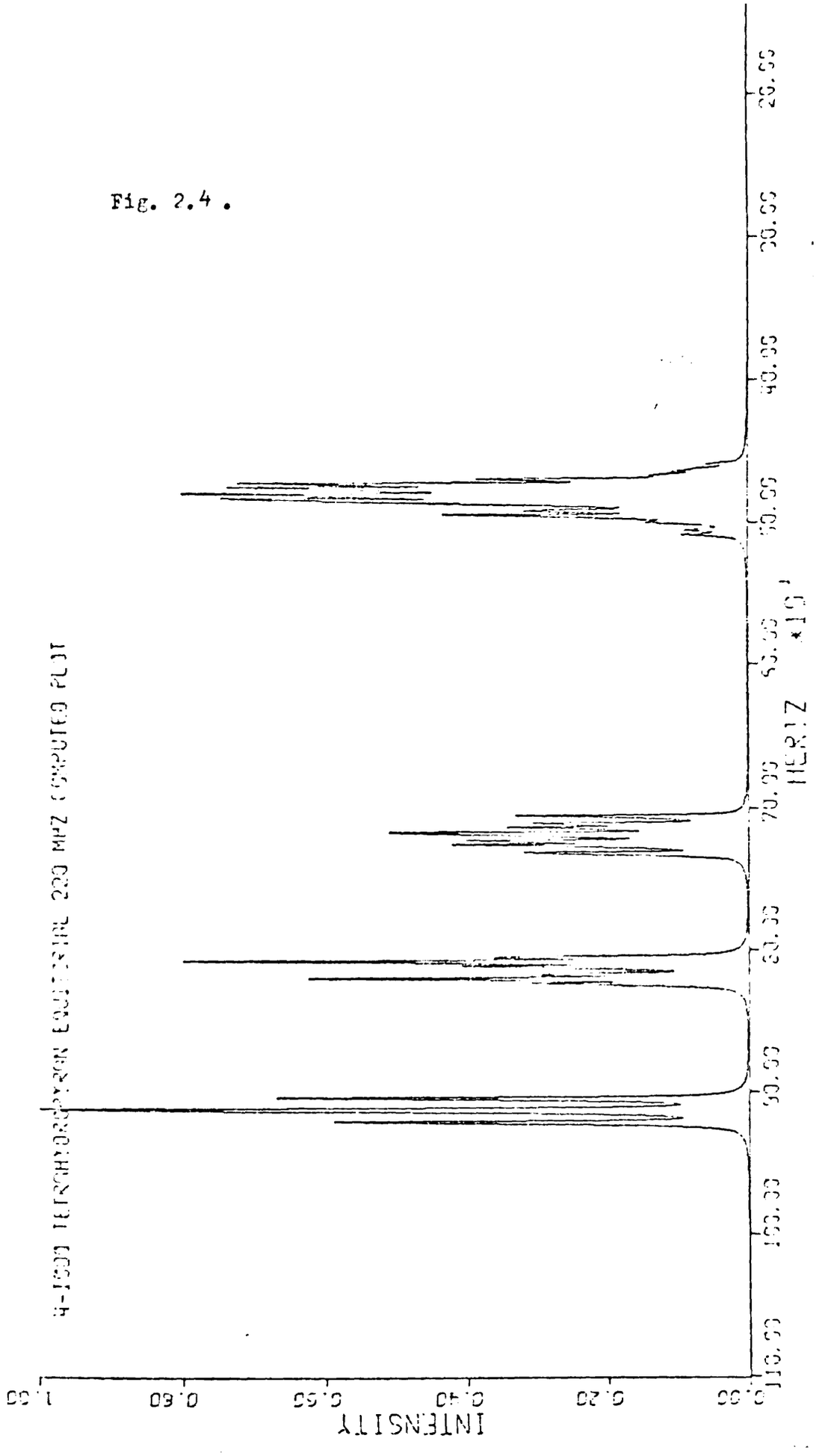

Fig. 2.5 .

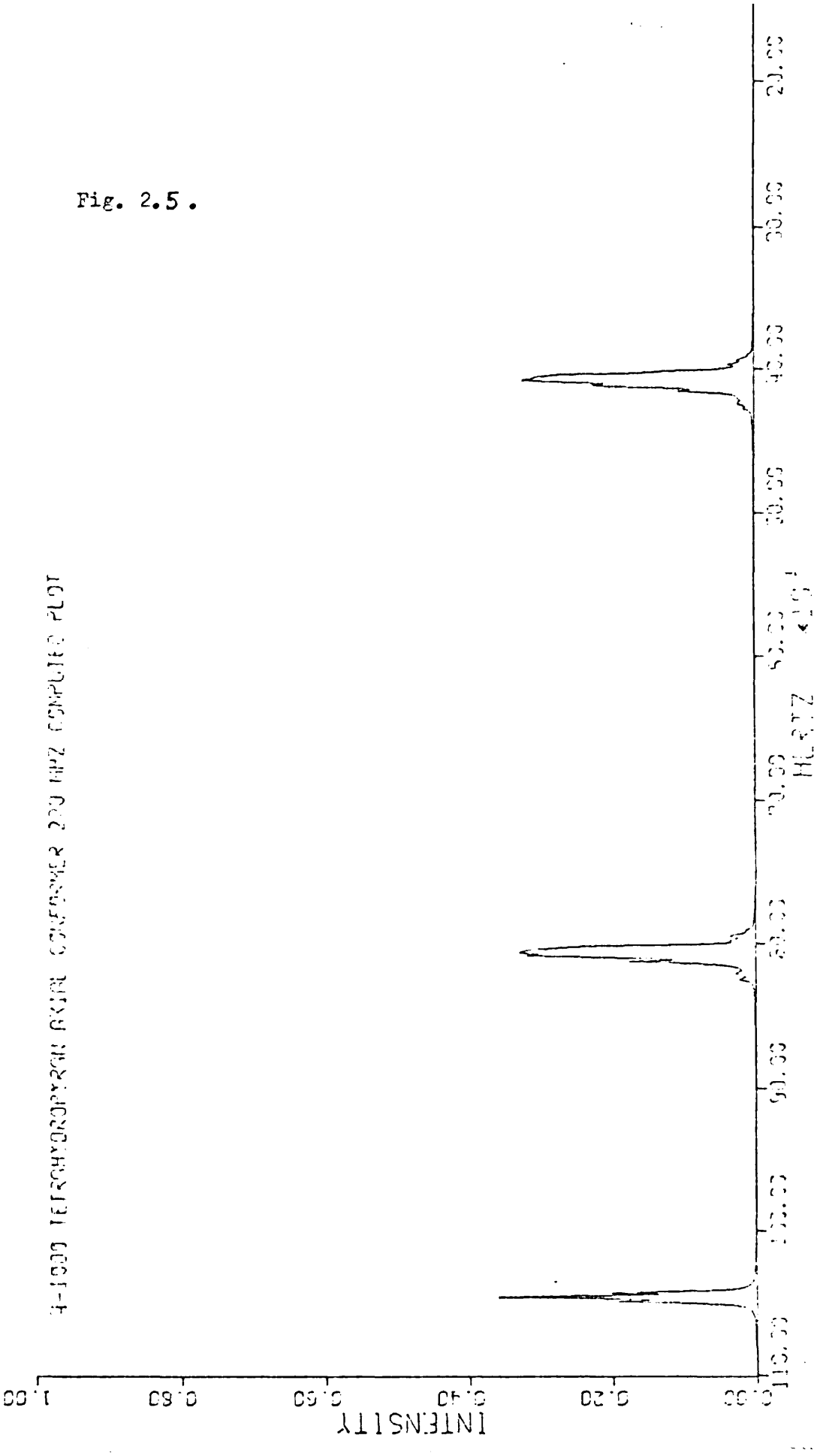

Fig. 2.6. 100 MHz spectrum of 4 - iodo T.H.P. at 30° C and -30° C.

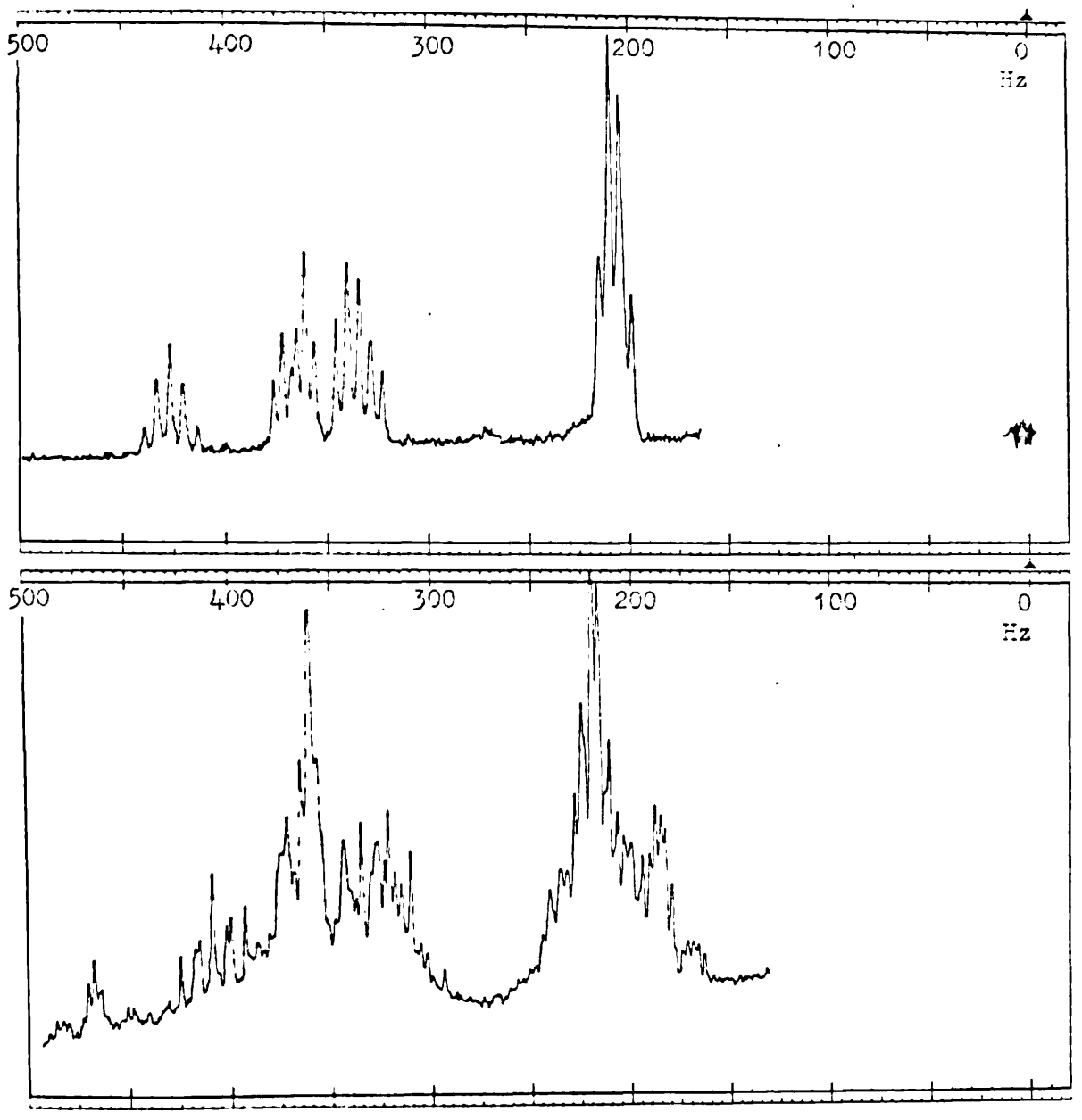

Fig. 2.7.

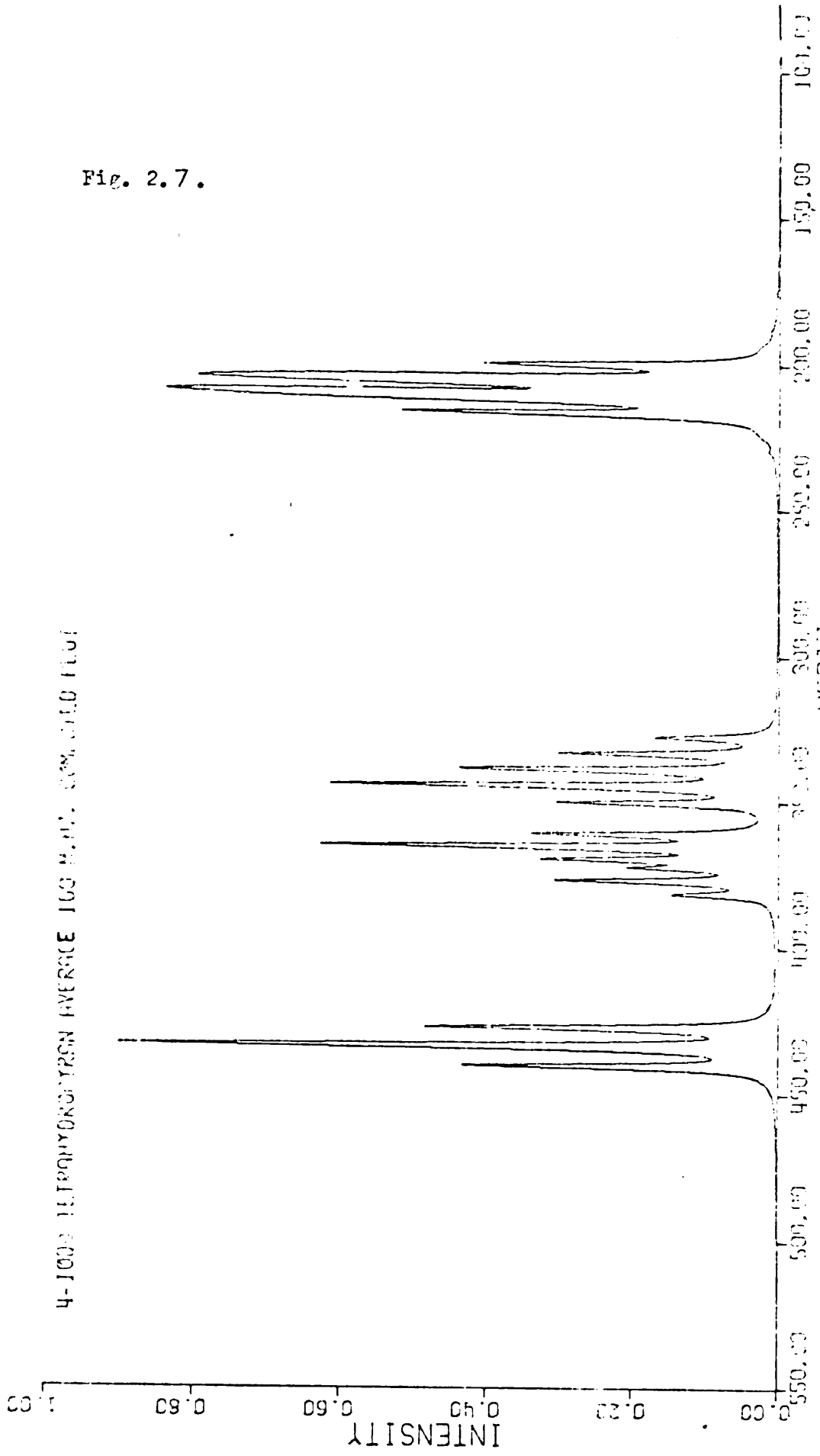

Fig. 2.8 .

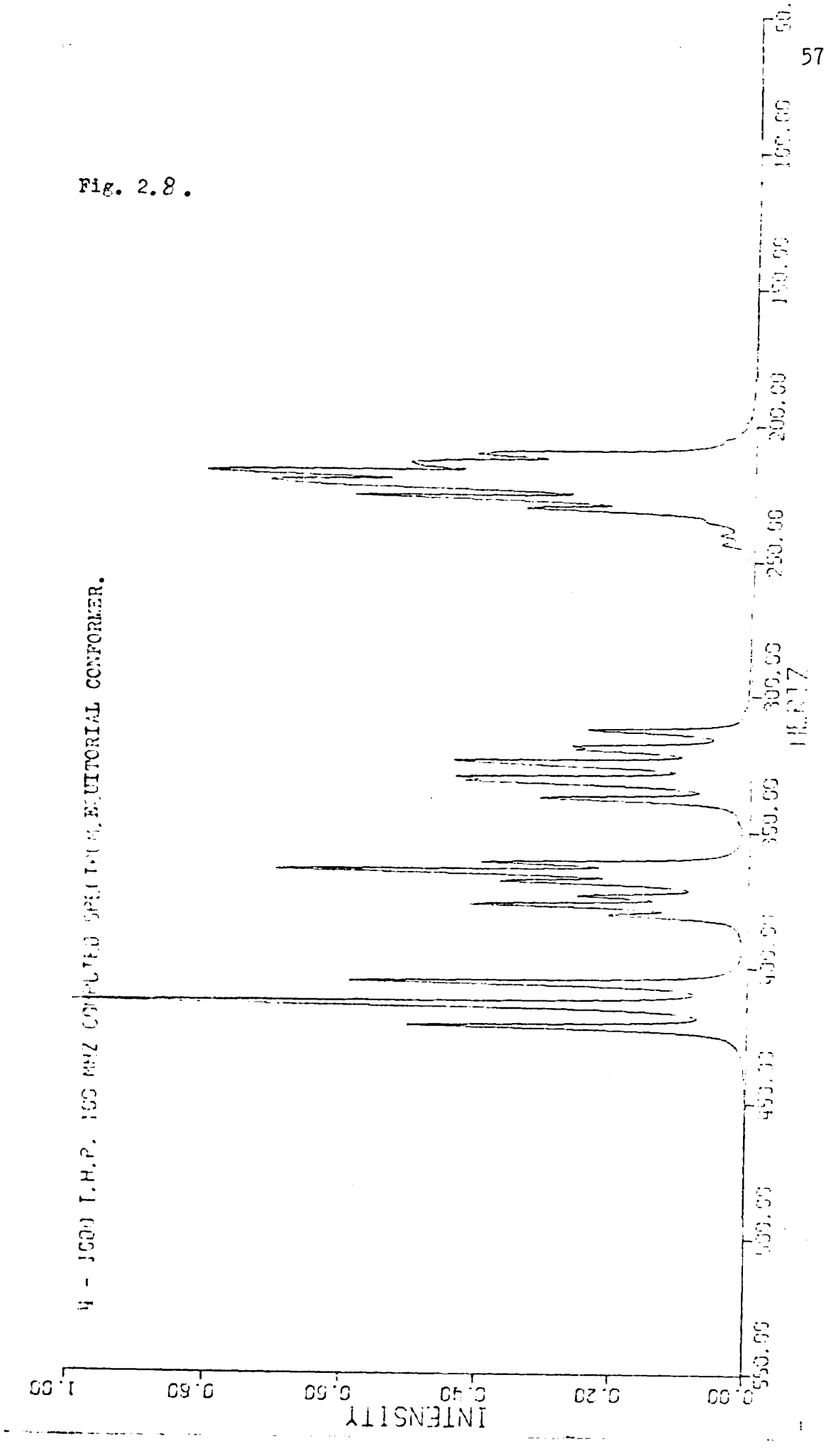
INTENSITY
1.00
0.80
0.60
0.40
0.20
0.00
550.00
500.00
450.00
400.00
350.00
300.00
250.00
200.00
150.00
100.00
50.

Fig. 2.9 .

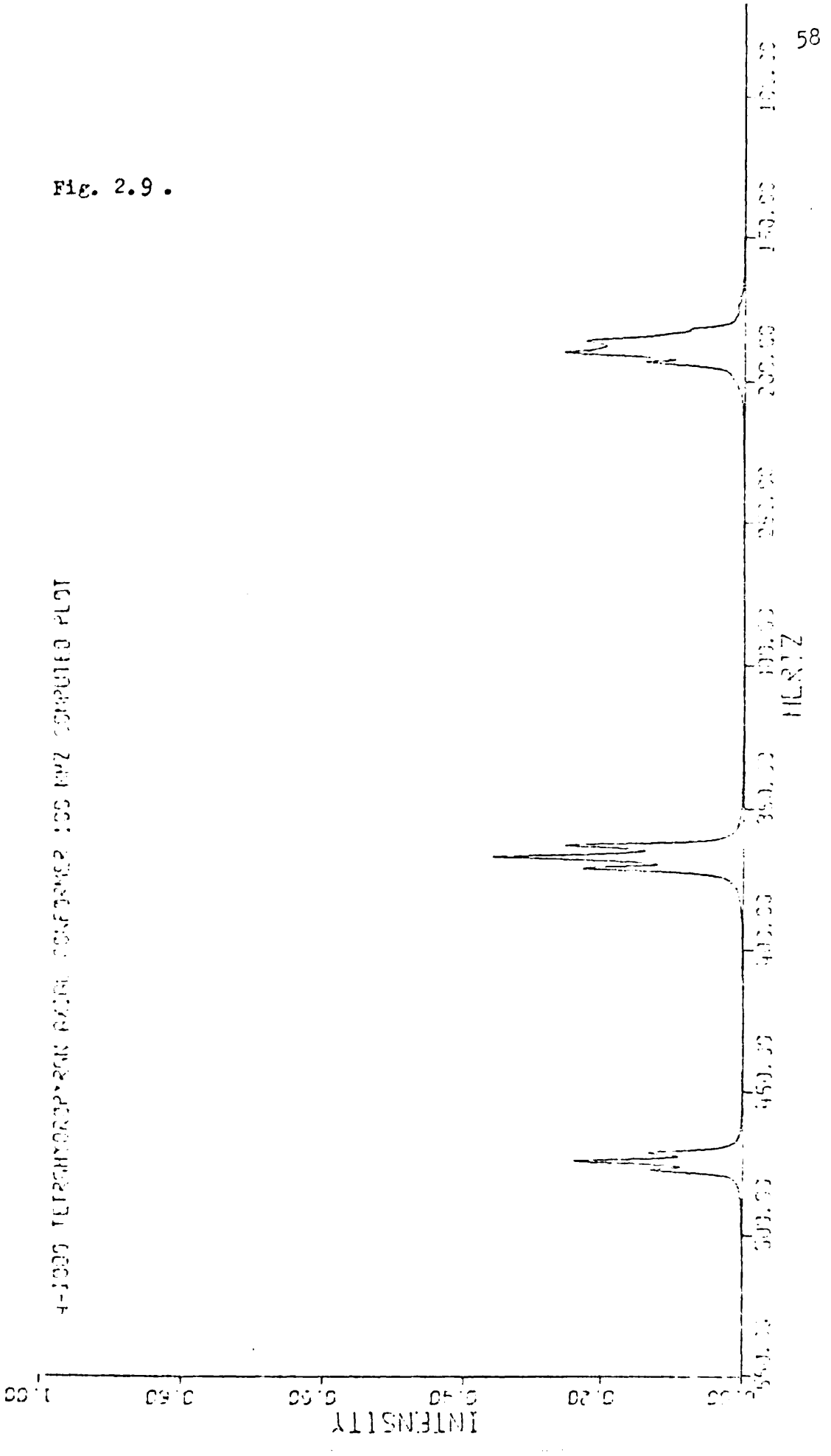

Equatorial (Fig. 2.4)

The shifts for 1, 4 and 5 are good. The coupling constants for 1 are good and those for 4 and 5 are close but not exact. Again it was not possible to analyse in the region of 2 and 3.

Axial (Fig. 2.5)

Although the resonances of 4 and 5 are hidden the use of integration indicates they are in the region of the fourth equatorial proton. The disproportionate areas of this resonance compared with the computed spectrum indicates that the two axial resonances lie under the upfield portion of the resonance. Although resonances 2 and 3, and 4 and 5 are close the shifts are reasonably accurate and both shift and coupling constant values for 1 are accurate.

For this set of spectra the values which are accurately known for all three, axial, equatorial and average, are the shifts for 1, 4 and 5 and the coupling constants for 1.

4 - iodo T.H.P. 100 MHz (Fig. 2.6)

Average (Fig. 2.7)

A very good fit was obtained with this spectrum even in the region of protons 2 and 3. All shifts and coupling constants, with the possible exception of J_{23}, are accurate. Because of the small shifts difference between 2 and 3, J_{23} is not manifest anywhere in the spectrum, but the remainder were established elsewhere.

Equatorial (Fig. 2.8)

As in the case of the 220 MHz spectra the shifts of 1, 4 and 5 and the coupling constants of 1 are good and the coupling constants for 4 and 5 are close but not exact.

Axial (Fig. 2.9)

Again we can accurately measure the coupling constants and shift of 1 and the shifts of 4 and 5 are sufficiently well known to be used in the calcuations.

4 - chloro T.H.P. 220 MHz spectra (Fig. 2.10)

These spectra were recorded and compared with the 100 MHz spectra produced by Dr. Barrett in order to yield the results obtained here.

Average (Fig. 2.11)

In thise case 2 and 3 are separated and it is possible to obtain reasonable values for all the constants. However, under high resolution, it is possible to detect a small additional splitting of about 1 Hz. This could be caused by long range coupling through four bonds in one of the conformers. Long range coupling of this type is most likely to occur when the protons are both equatorially disposed and therefore in the axially substituted conformer. Unfortunately it was not possible to analyse the axial spectrum sufficiently accurately in this region to say whether this was true or not.

Fig. 2.10. 220 MHz spectrum of 4-chloro tetrahydropyran in CS_2.

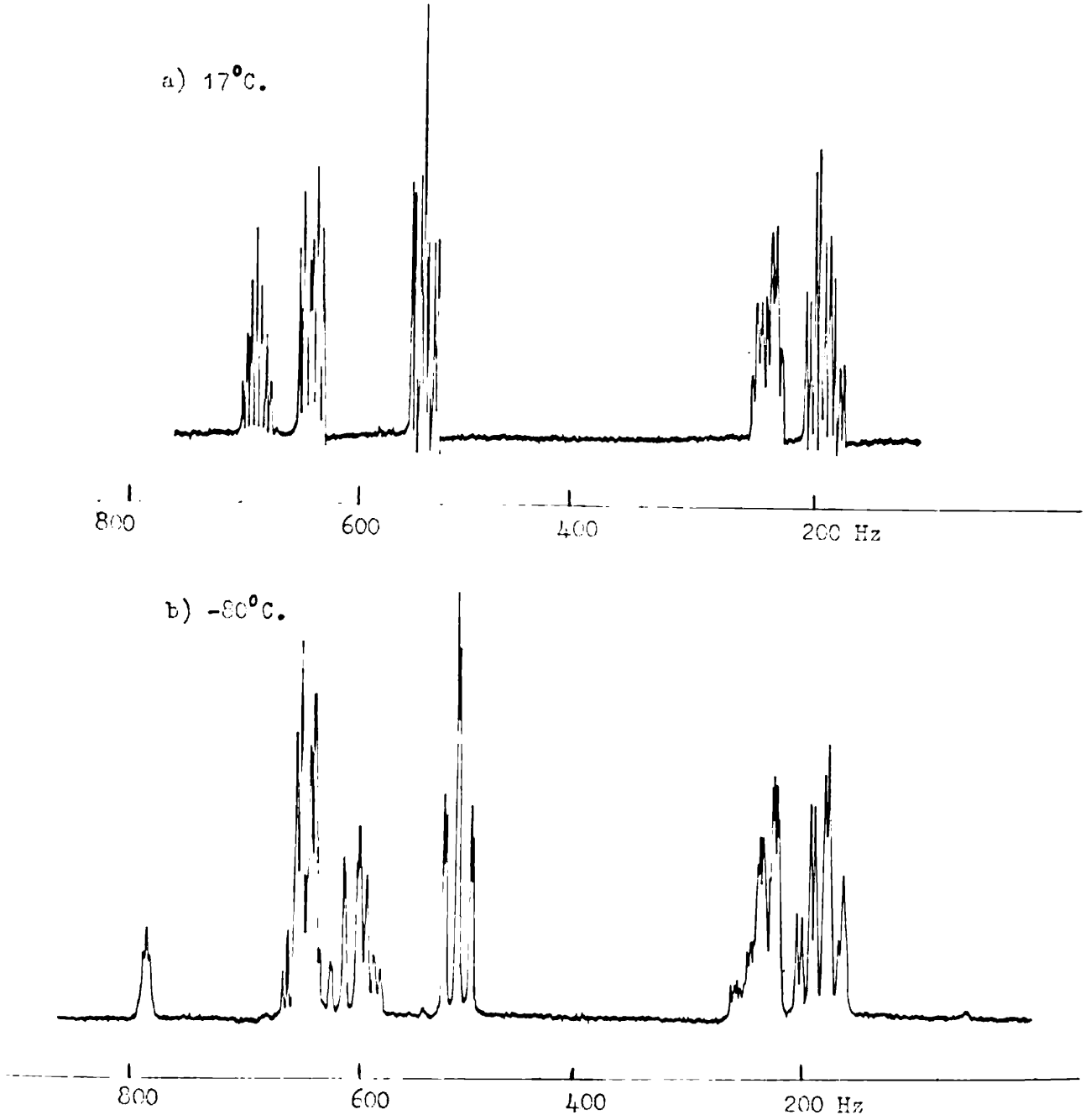

Fig. 2.11 .

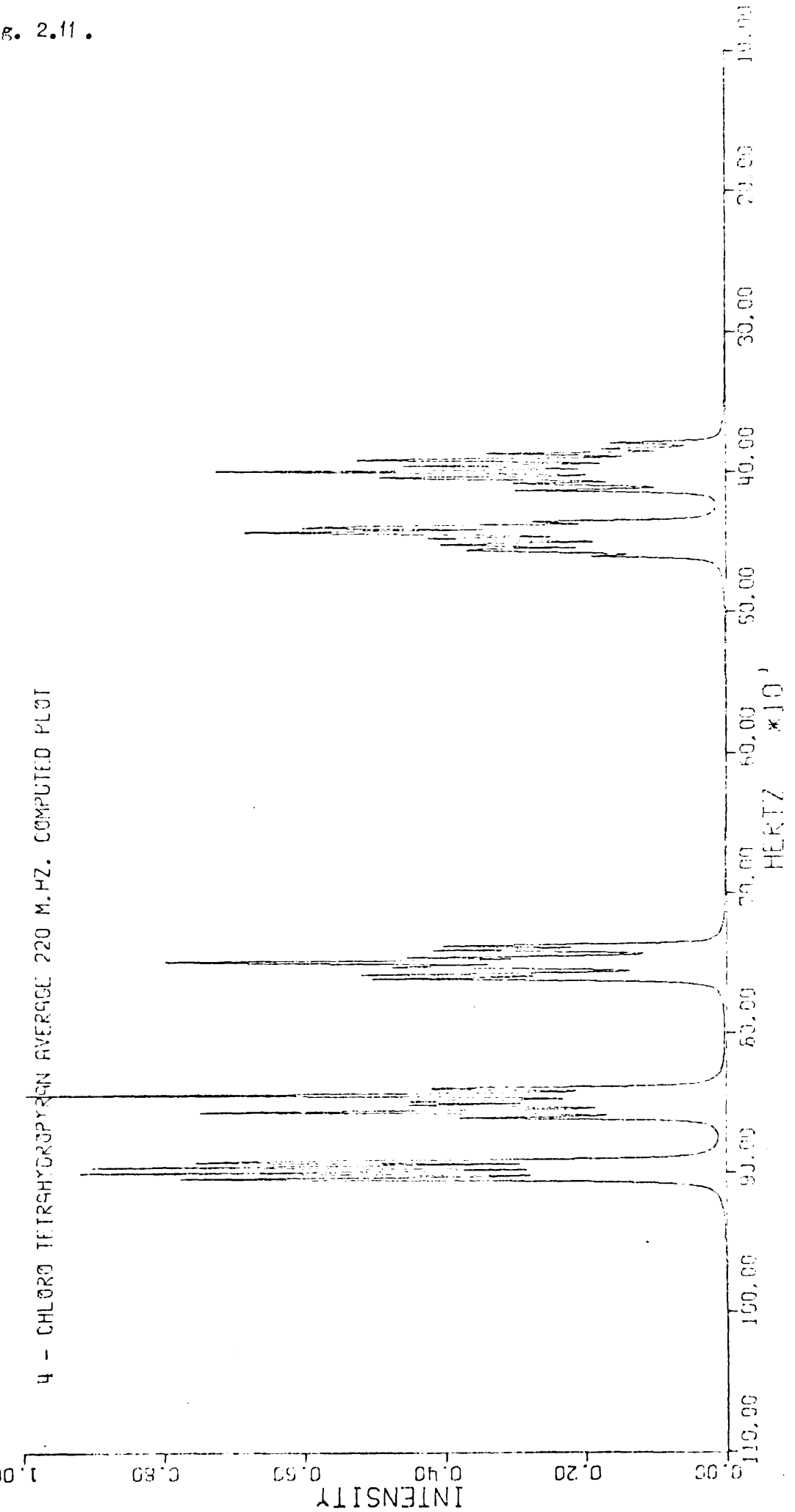
4 - CHLORO TETRAHYDROPYRAN AVERAGE 220 M.HZ. COMPUTED PLOT
INTENSITY
0.00
0.20
0.40
0.60
0.80
1.00
HERTZ *10'
110.00
100.00
90.00
80.00
70.00
60.00
50.00
40.00
30.00
20.00
10.00

Fig. 2.12.

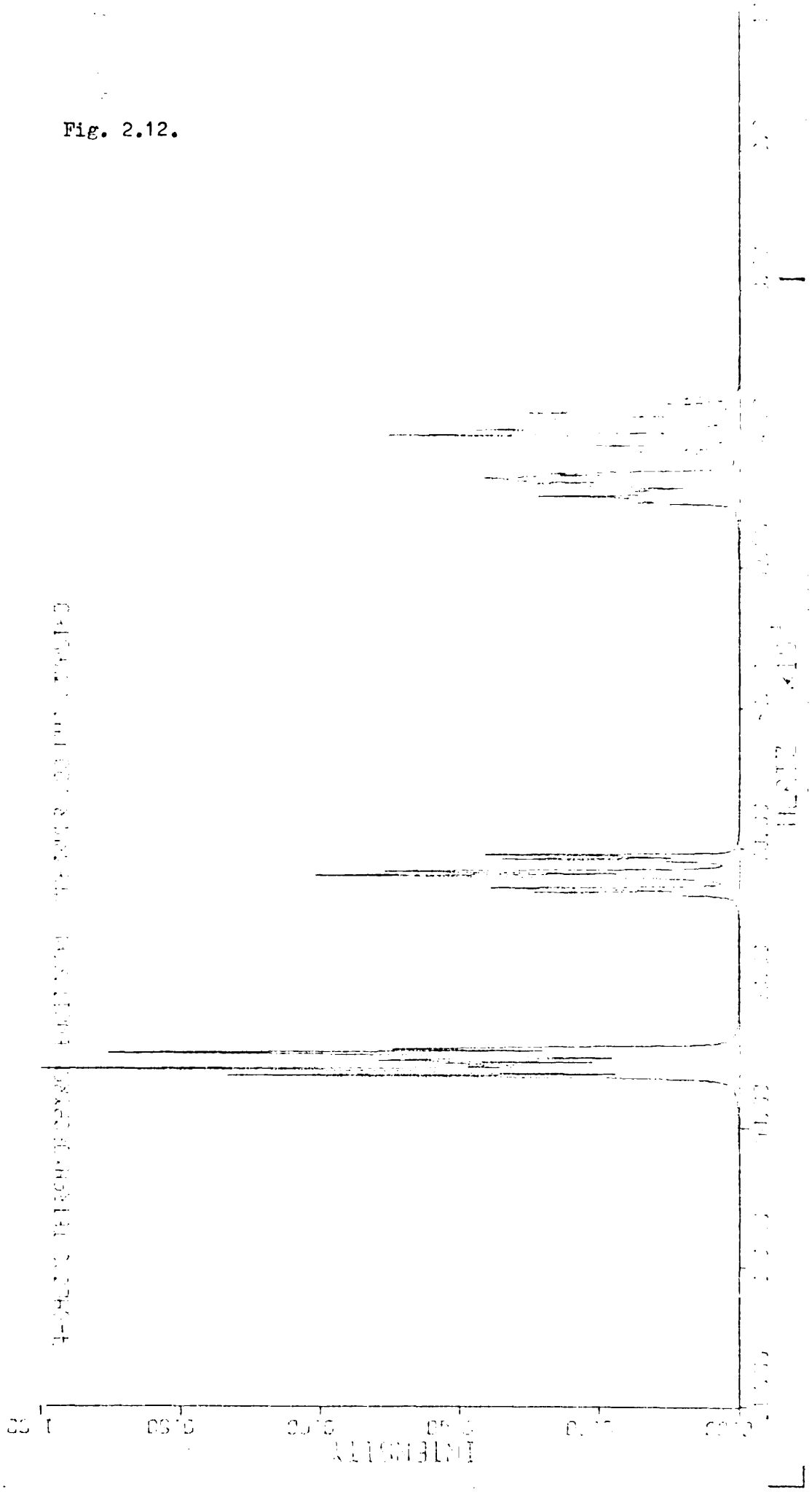

Fig. 2.13.

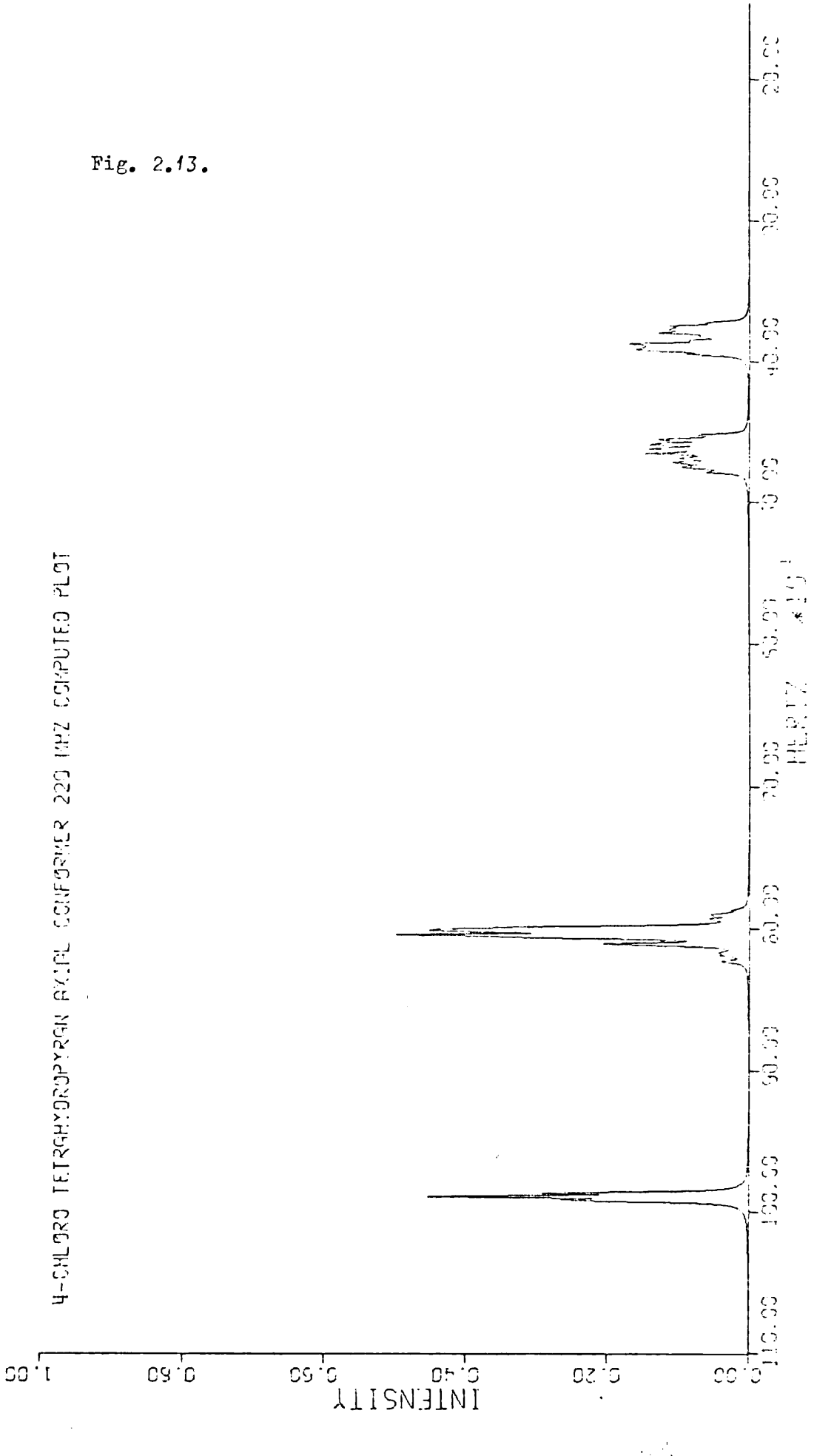
4-CHLORO TETRAHYDROPYRAN AXIAL CONFORMER 220 MHZ COMPUTED PLOT
INTENSITY
HERTZ

Fig. 2.14.

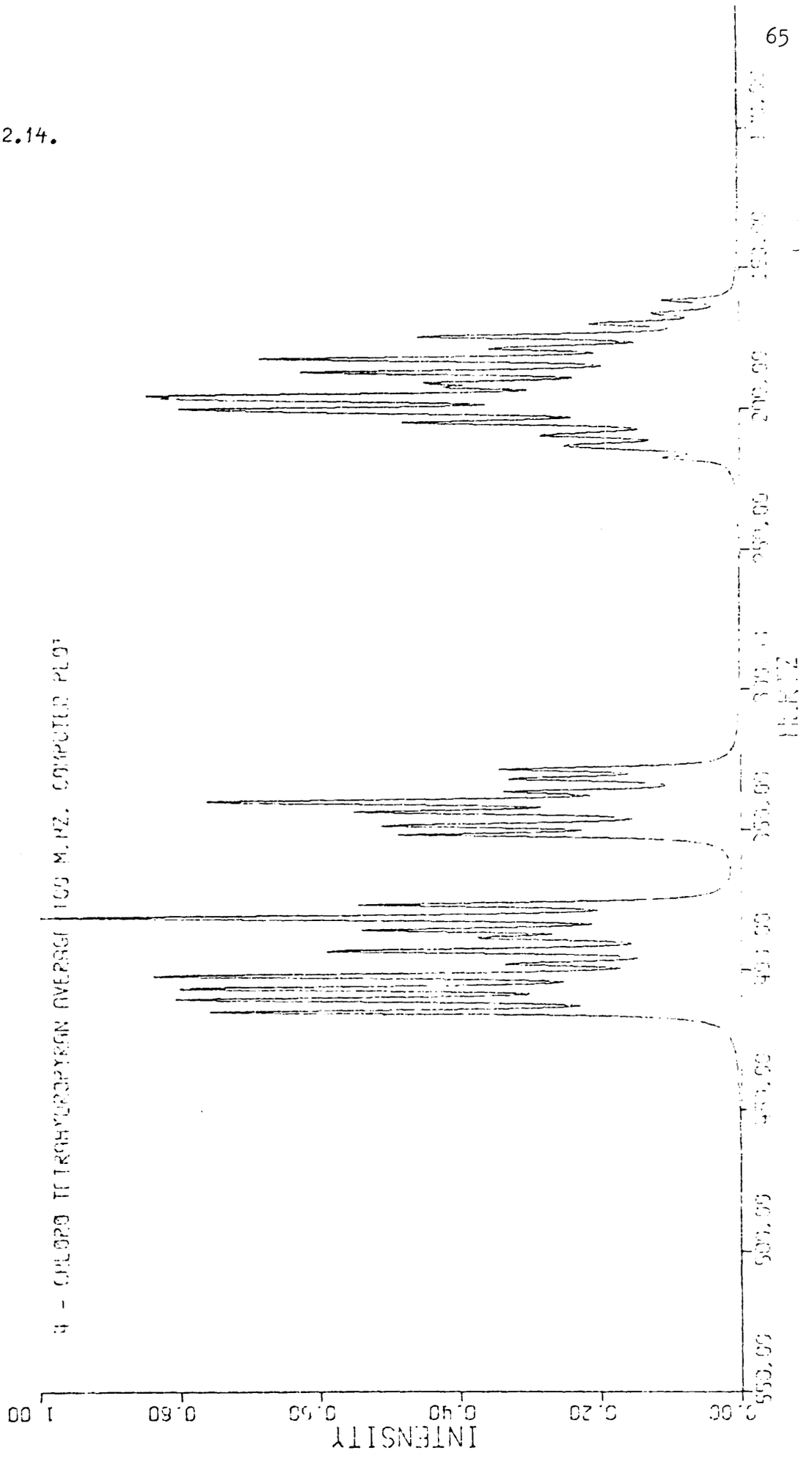

Fig. 2.15.

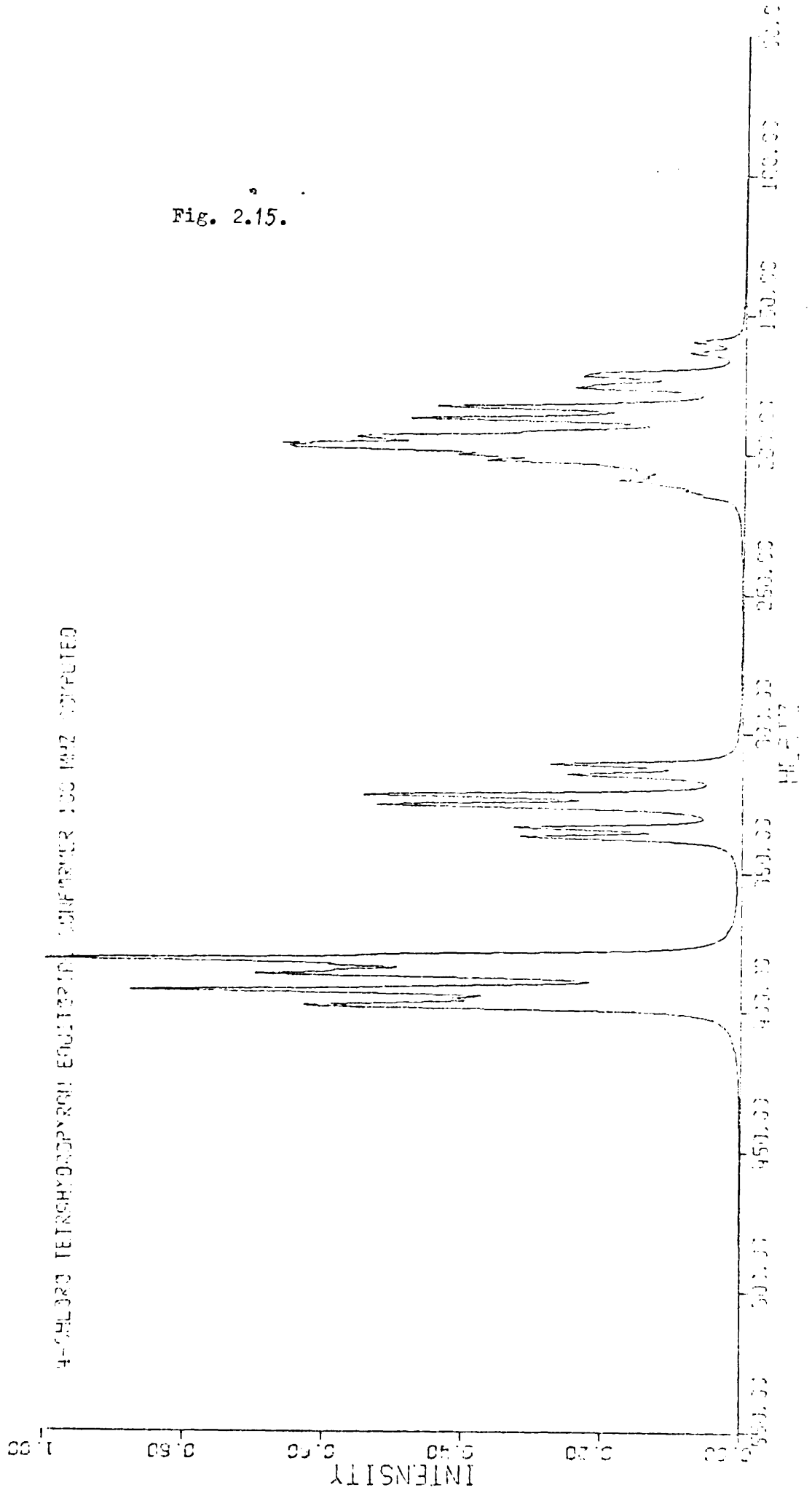

Fig. 2.16.

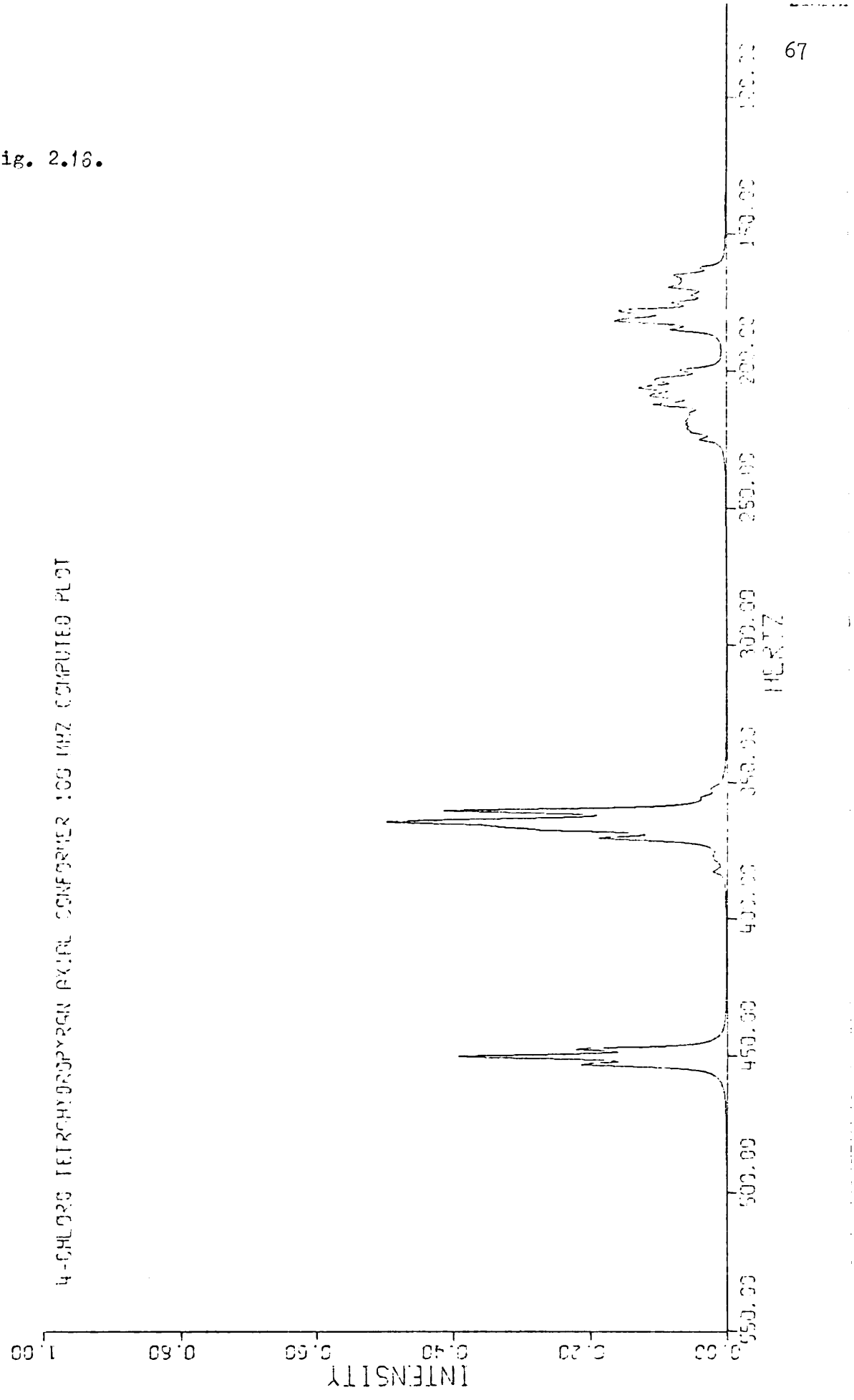
4-CHLORO TETRAHYDROPYRAN AXIAL CONFORMER 100 MHZ COMPUTED PLOT
INTENSITY
1.00
0.80
0.60
0.40
0.20
0.00
550.00
500.00
450.00
400.00
350.00
300.00
250.00
200.00
150.00
HERTZ

Equatorial (Fig. 2.12)

Proton 1 is partially obscured by proton 4 but the splittings which are visible together with the total width of the resonance allows a reasonably accurate estimate to be made. All the shifts are accurate and the coupling constants give a moderately good fit. The results are consistent with the spectrum obtained at 100 MHz.

Axial (Fig. 2.13)

The resonances of 2 and 3 are both partially obscured by the equatorial conformer and the resonances of 4 and 5 interact with each other. The shift and coupling constants concerning proton 1 are well established and the remaining shifts are reasonably well established. The above values were used in the calculation of conformational populations.

Figures 2.14 - 2.16 show the computed 100 MHz spectra.

Standard free energy difference values derived from chemical shifts and coupling constant values.

4 - chloro T.H.P.

If an average of all the calculations using shifts and coupling constants shown in table 2.3 is taken the value for the mole fraction of the equatorial conformer is found to be 0.769 giving a standard free energy difference value of 721.4 cal mol $^{-1}$ (3018 J mol $^{-1}$).

A more realistic value may be obtained by averaging the values obtained from the chemical shifts and coupling constants for proton 1.

Table 2.3. Mole fraction of equatorial conformer present in carbon disulphide solution at room temperature.

Parameter	220 MHz	100 MHz
4-chloro T.H.P.		
Shift 1	0.677	0.715
Shift 2	0.936	0.938
Shift 3	0.783	0.784
Shift 4	0.965	0.936
Shift 5	0.607	0.559
Coupling 1,2	0.659	0.659
Coupling 1,3	0.667	0.667
4-iodo T.H.P.		
Shift 1	0.686	0.672
Shift 5	0.664	0.672
Coupling 1,2	0.655	0.655
Coupling 1,3	0.791	0.791

The mole fraction of the equatorial conformer is found to be 0.680 which is equivalent to a free energy difference value of 451.2 cal mol $^{-1}$ (1888 J mol $^{-1}$). This result is similar to the values obtained by the use of areas which are described later.

4 - iodo T.H.P.

With the exception of the value derived from the coupling constants J_{13} the values are fairly consistent. Their average is 0.670 which gives a standard free energy difference value of 424.3 cal mol $^{-1}$ (1760 J mol $^{-1}$).

Clearly a certain amount of inaccuracy must arise in the methods just described. No account is taken of the possible dependence of the shifts and coupling constants on temperature simply because it is not possible to determine this. The proton evidence examined here gives no indication of such a dependence nor does it rule one out. Another approach was to use ^{13}C proton decoupled spectra which are much more straightforward to interpret.

It was also possible to integrate the areas of the proton peaks. Although it is usual to measure the areas of the peaks attributed to the methine proton in the two conformers this was not found possible in the cases considered here. However the problem was solved by integrating the axial peak, which was always isolated and comparing it with the combined area attributed to the equatorial proton and to protons 4 and 5 in both conformers or by drawing in a background where slight overlap occurs.

Standard free energy difference values derived using peak areas.

The spectra were recorded at -80°C.

4 - iodo T.H.P.

220 MHz spectrum. The areas of the peaks corresponding to proton 1 in the two conformers were measured and compared to give a standard free energy difference value of 303.1 cal mol $^{-1}$ (1268 J mol $^{-1}$).

100 MHz spectrum. Although proton 1 in the equatorial conformer was not completely isolated it was sufficiently clear for a background to be estimated. The good accuracy of the method was indicated by the fact that the left half of the band was a good approximation to half of the total band. An average of these gave a value of ΔG^{o} = 395.0 cal mol $^{-1}$ (1653 J mol $^{-1}$).

4 - chloro T.H.P.

220 MHz spectrum. The area of proton 1 in the axial conformer was compared with the combined areas of protons 4, 5 and equatorial proton 1 to give the value ΔG^{o} = 355.4 cal mol $^{-1}$ (1487 J mol $^{-1}$).

100 MHz spectrum. The same method was used to give a value of ΔG^{o} = 413.0 cal mol $^{-1}$ (1728 J mol $^{-1}$).

b) ^{13} Carbon nuclear magnetic resonance.

Initial ^{13}C variable temperature studies on 4 - chloro T.H.P. showed clearly a temperature dependence of the chemical shifts to the extent that the room temperature shift of the single carbon was outside the region in which the individual peaks were found at low temperature.

Fig.2.17 ^{13}C spectra of 4 - chloro T.H.P. at 30°C and -80°C.

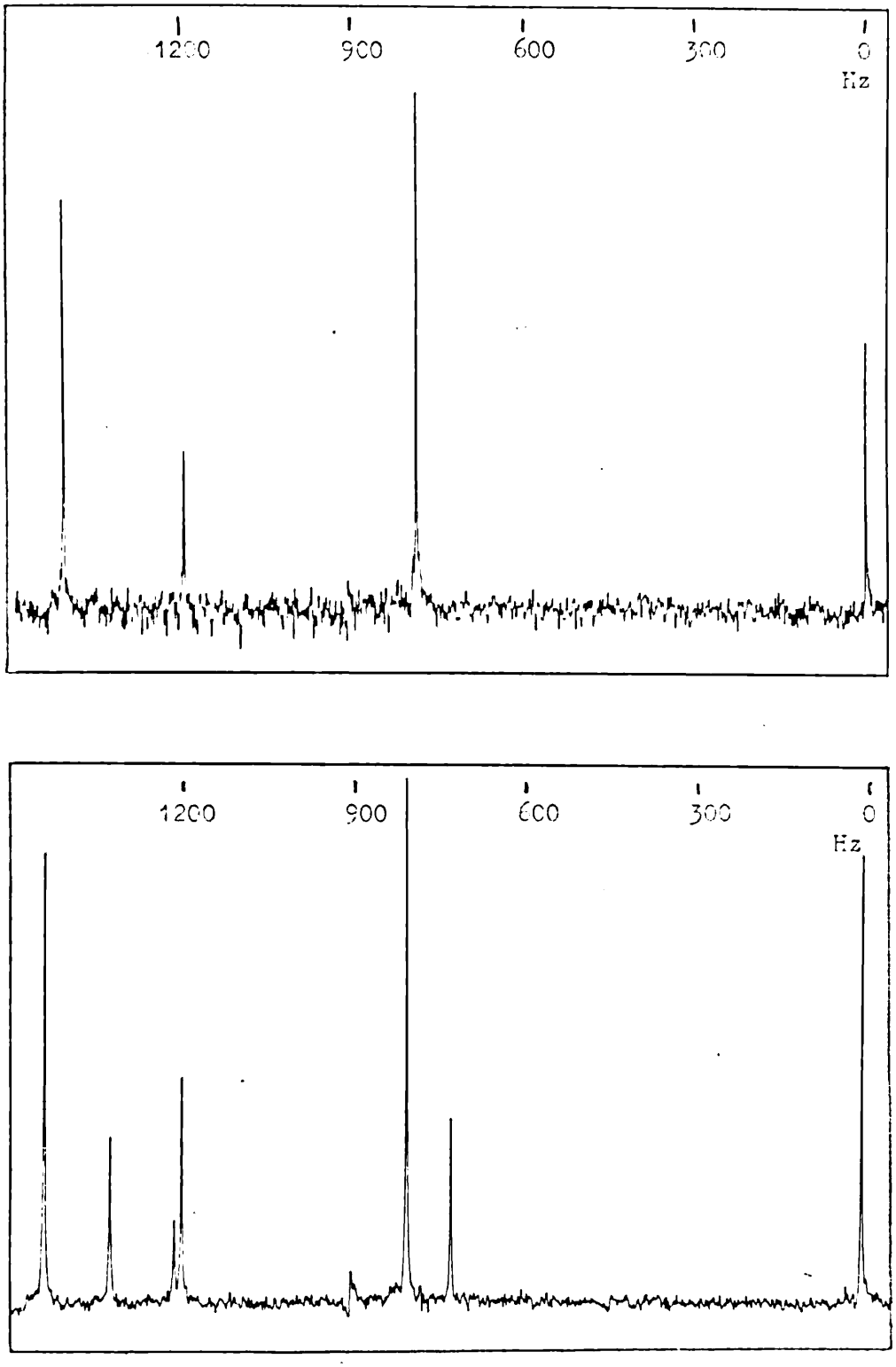

Table 2.4. Effect of temperature on chemical shift in the ^{13}C spectrum of 4 - chloro T.H.P.

Shifts in Hz relative to T.M.S.

Temp. °C	Carbons 4 & 5	Carbon 1	Carbons 2 & 3
	av	av	av
40	1308.4	1114.4	733.7
30	1308.4	1114.6	733.7
10	1307.1	1114.7	730.2
0	1307.2	1114.7	729.5
-20		1114.9	
-30		1115.2	

	eq	ax	ax	eq	eq	ax
-70		1230.0	1113.9		747.8	674.7
-80	1337.8	1230.6	1126.2	1114.6	746.7	673.6
-90	1337.9	1230.6	1127.7	1115.0	746.4	673.1

This required only a small temperature dependence because of the relatively small shift differences of this carbon in the two conformers but the rest of the spectrum showed similar effects.

Fig. 2.17 shows typical spectra at both ends of the temperature scale, the out of phase peak around 900 Hz being attributed to carbon disulphide. Table 2.4 lists chemical shift values, broadening occuring in the regions where no values are quoted.

Table 2. 5. Effect of temperature on chemical shift in the ^{13}C spectrum of tetrahydropyran.

Temperature ^{o}C	Carbons 4 & 5	Carbons 2 & 3	Carbon 1
20	1368.2	543.7	483.0
-50	1364.0	540.7	481.0
-70	1362.1	539.7	480.1

The evidence of this effect means that an attempt must be made to compensate for this effect. There are two alternatives; extrapolation of the shifts of the conformers from low to room temperature or extrapolating the averaged shift down to low temperature. Both methods present problems. Firstly a reasonable temperature range must be available in which the spectrum exhibits shifts of the individual isomers and secondly we must consider the possibility that the temperature dependence of shift may not necessarily be linear. This latter problem arises in the case of T.H.P. (Table 2.5).

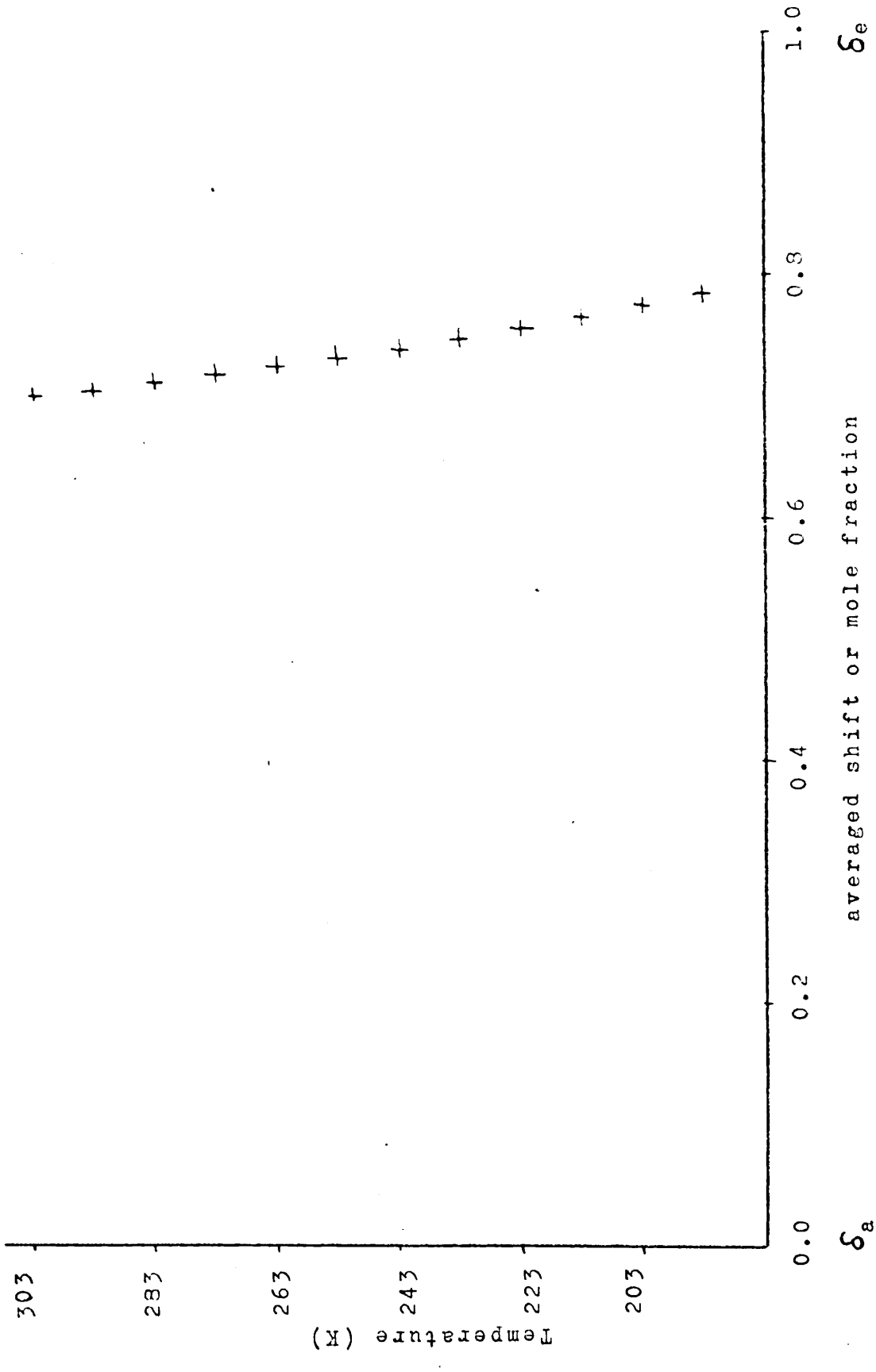

Fig. 2.18. Effect of conformer population on the averaged shift.

Fig. 2.19. Labelling of carbon atoms.

(a) Cyclohexyl derivatives

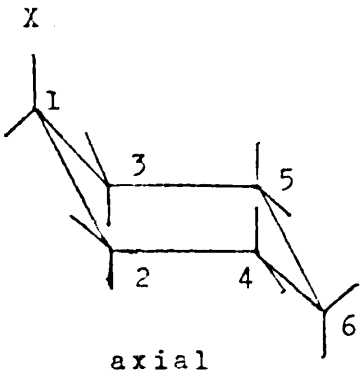

axial

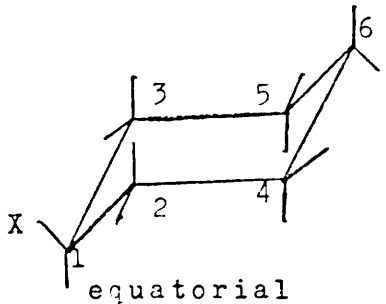

equatorial

(b) Tetrahydropyran derivatives

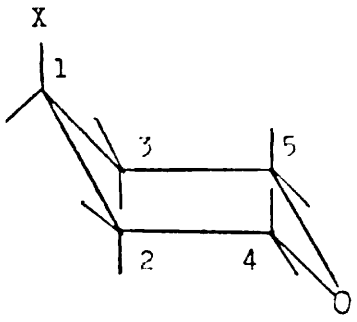

axial

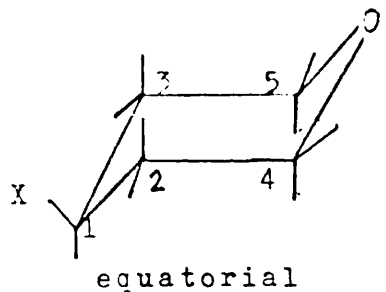

equatorial

Table 2.6. Calculations of ΔG° values for 4 - chloro T.H.P.

a) Carbons 4 and 5

Method	Temp. K	δ_{eq}	δ_{av}	δ_{ax}	ΔG° cal mol $^{-1}$
1	313	1337.9	1308.4	1230.6	607.2
2	313	1336.6	1308.4	1228.0	655.8
3	183	1337.9	1303.2	1230.6	271.6
4	183	1337.9	1305.2	1230.6	278.2

b) Carbons 2 and 3

Method	Temp. K	δ_{eq}	δ_{av}	δ_{ax}	ΔG° cal mol $^{-1}$
1	313	746.4	733.7	673.1	978.0
2	313	754.8	733.7	683.5	542.8
3	183	746.4	720.0	673.1	210.3
4	183	746.4	720.6	673.1	223.2

Methods.

1 - No allowance for effect of temperature on shifts.

2 - Extrapolation of low temperature shifts.

3 - Extrapolation of averaged shift.

4 - As 3 but allowing for effect of change in populations.

Chemical shifts in Hz.

In the case of the other molecules a lower temperature would be a great help, especially in the case of cyclohexyl chloride where even at the lowest temperature some lines are still broad.

When extrapolating the averaged shift it is necessary to remember its dependence on conformer population. Fig. 2.18 indicates this effect in the absence of intrinsic shifts for a standard free energy difference value of 500 cal mol $^{-1}$ (2092 J mol $^{-1}$). Clearly an idea of the size of the standard free energy difference must be assumed before this correction can be applied. The scheme of numbering the carbon atoms for this section is given in Fig. 2.19.

Despite the fact that evidence is limited it is possible to draw certain conclusions from the results obtained. In the case of 4 - chloro T.H.P. (Table 2.6) it is clear that allowance must be made for the effect of temperature on chemical shift but the effect of population on the extrapolation of the averaged spectrum is small when the free energy difference is about 500 cal mol $^{-1}$ (2092 J mol $^{-1}$) or less. The wide difference in results obtained by the different methods of extrapolation are caused by the inaccuracy in the shift data caused particularly by the effect of noise and also by the narrow range of temperature from which extrapolation must be made.

In the case of cyclohexyl chloride particularly there are two factors working in opposition.

Table 2.7. Standard free energy difference values derived by areas for 4 - chloro T.H.P. at 193 K.

Overhauser not suppressed

Carbon	ΔG° cal mol $^{-1}$	ΔG° J mol $^{-1}$
4, 5	332.6	1392
1	319.7	1338
2, 3	387.9	1623

Overhauser suppressed

Carbon	ΔG° cal mol $^{-1}$	ΔG° J mol $^{-1}$
4, 5	353.1	1477
1	362.6	1517
2, 3	393.8	1648

Fig.2.20 Spin - lattice relaxation of 4 - chloro tetrahydropyran.

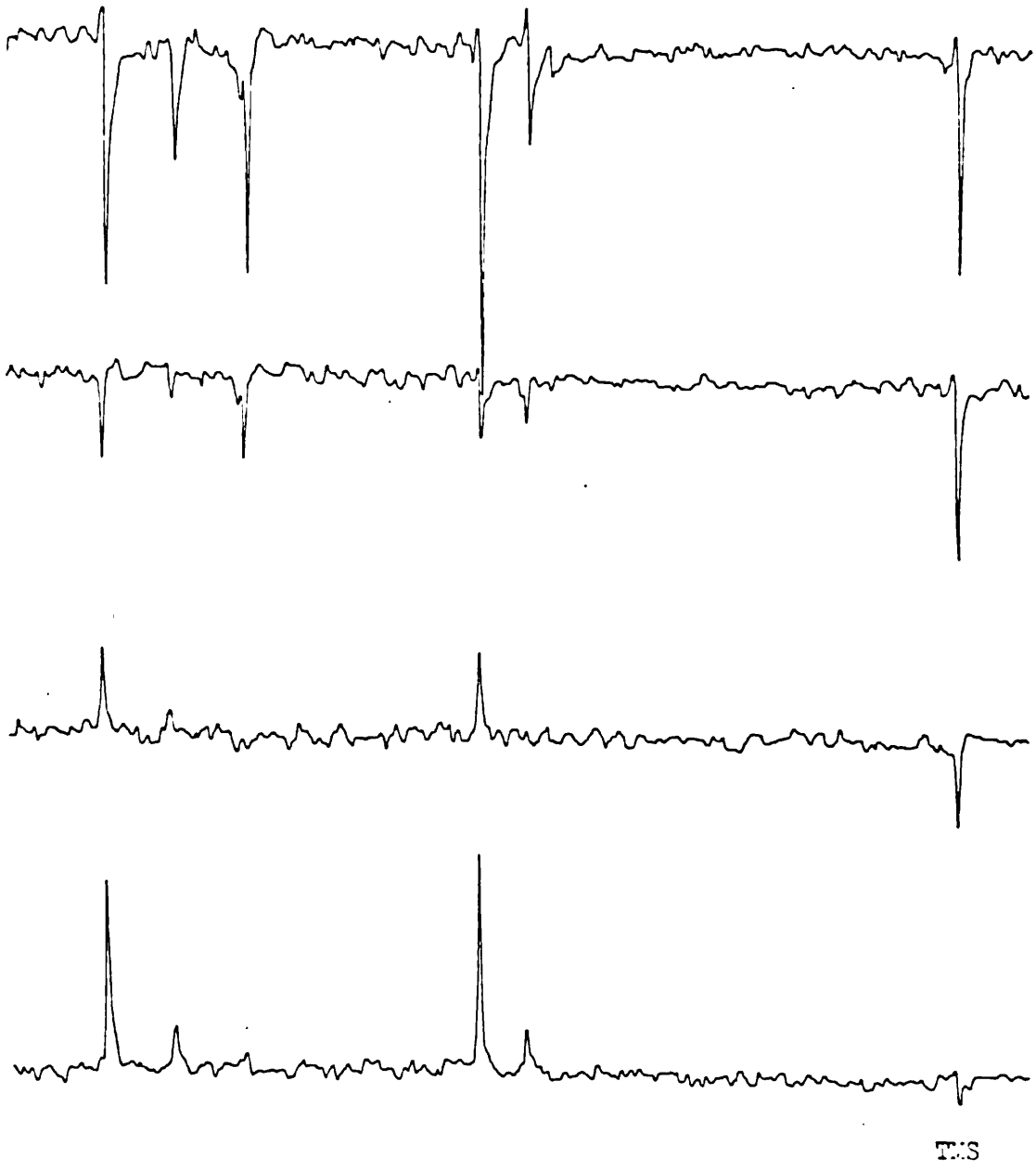

If the shift difference is small, we have a wide range of temperature over which the averaged shift can be measured but the small difference in shift at low temperature enhances the inaccuracy of measurement. If on the other hand the shift difference is large there is only a small temperature range over which the averaged shift can be measured, the upper temperature being limited by the vapour pressure of carbon disulphide.

As has already been mentioned the Nuclear Overhauser effect caused by proton decoupling may be a function of the position of the carbon in the molecule or of the conformer or of both. The measurements on 4 - chloro T.H.P. indicated that areas at room temperature suffered differential enhancement but at low temperature this appeared to be independent of conformer and consistent standard free energy values were obtained for each pair (Table 2.7). An attempt was made to assess the degree of enhancement by suppressing the Overhauser effect. This made little difference and the consistency of the standard free energy differences was not greatly affected. This differential effect could have been due to different rates of relaxation for the different carbons. A set of relaxation studies were carried out at low temperature (Fig. 2.20) which lead to the conclusion that the relaxation rates of all the carbons in both isomers had roughly the same relaxation times.

In the case of cyclohexyl chloride, the standard free energy difference between the conformers has been determined a number of times and this is a good compound to use in order to study the accuracy of the technique.

Fig. 2.21. ^{13}C spectrum of T.H.F. in CS_2 at 20 C.

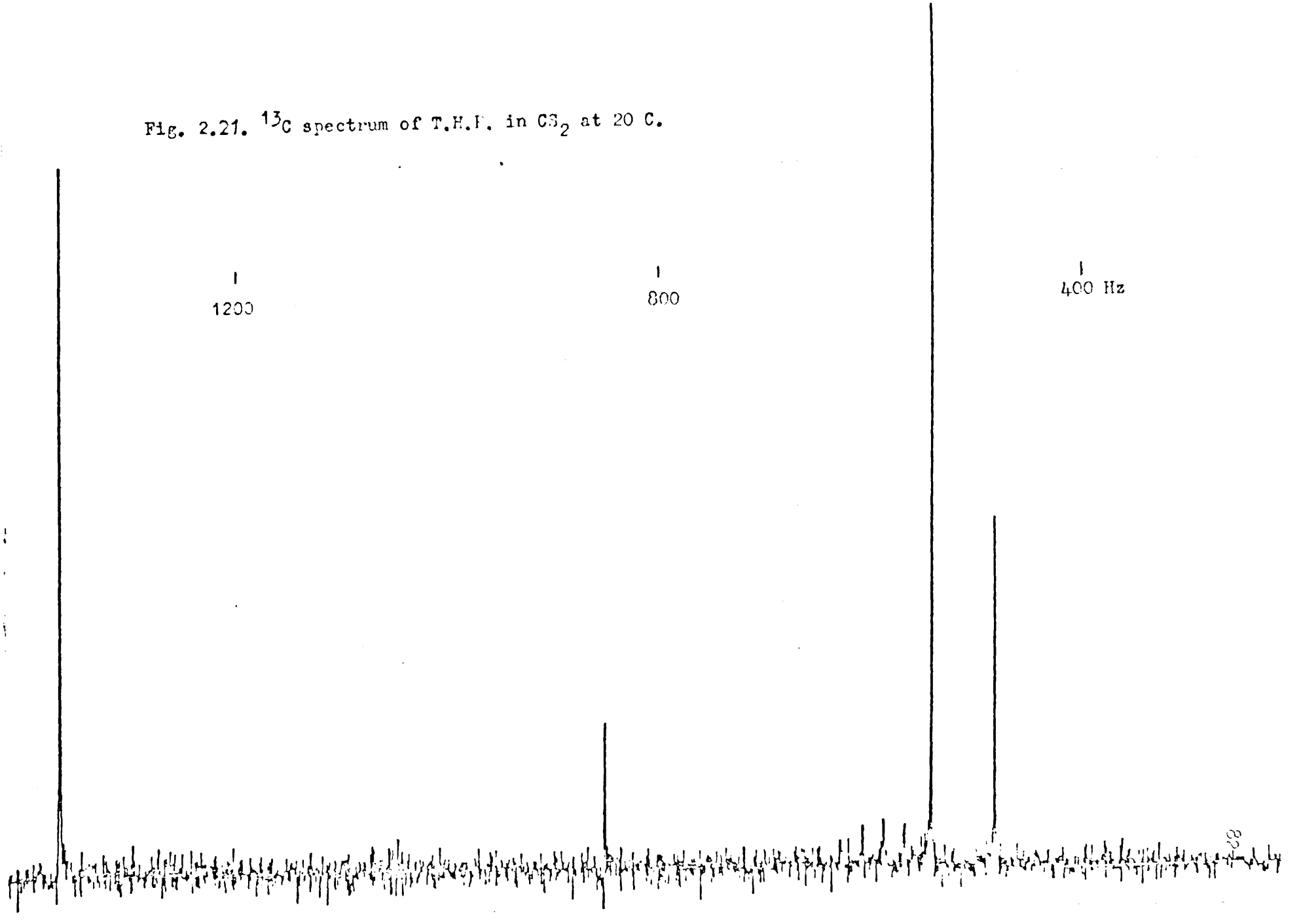

Table 2.8. Effect of temperature on chemical shift in the ^{13}C spectrum of cyclohexyl chloride.

Temp ^{o}C	Carbon 1	Carbons 2 & 3	Carbons 4 & 5	Carbon 6
20	1197.1	739.4	511.4	505.0
10	1197.7	739.5	511.3	505.2
0	1198.2	739.2	(505.8)	510.9
-10	1198.6	(738.7)		510.7
-20	1198.5			509.8
-30	1199.3			509.7
-40	1199.2	(751.2) -		509.3
-50	1199.6	(754.3) -		(507.1)
-60	1200.0	755.8 -	537.4 -	505.6 -
-80	1199.3	754.9 (679.0)	536.9 408.8	504.4 (519.6)
-95	1200.3 (1210.4)	754.1 (677.5)	536.3 408.0	503.4 (530.5)

Bracketed values indicate uncertainty due to broadening.

Chemical shifts in Hz.

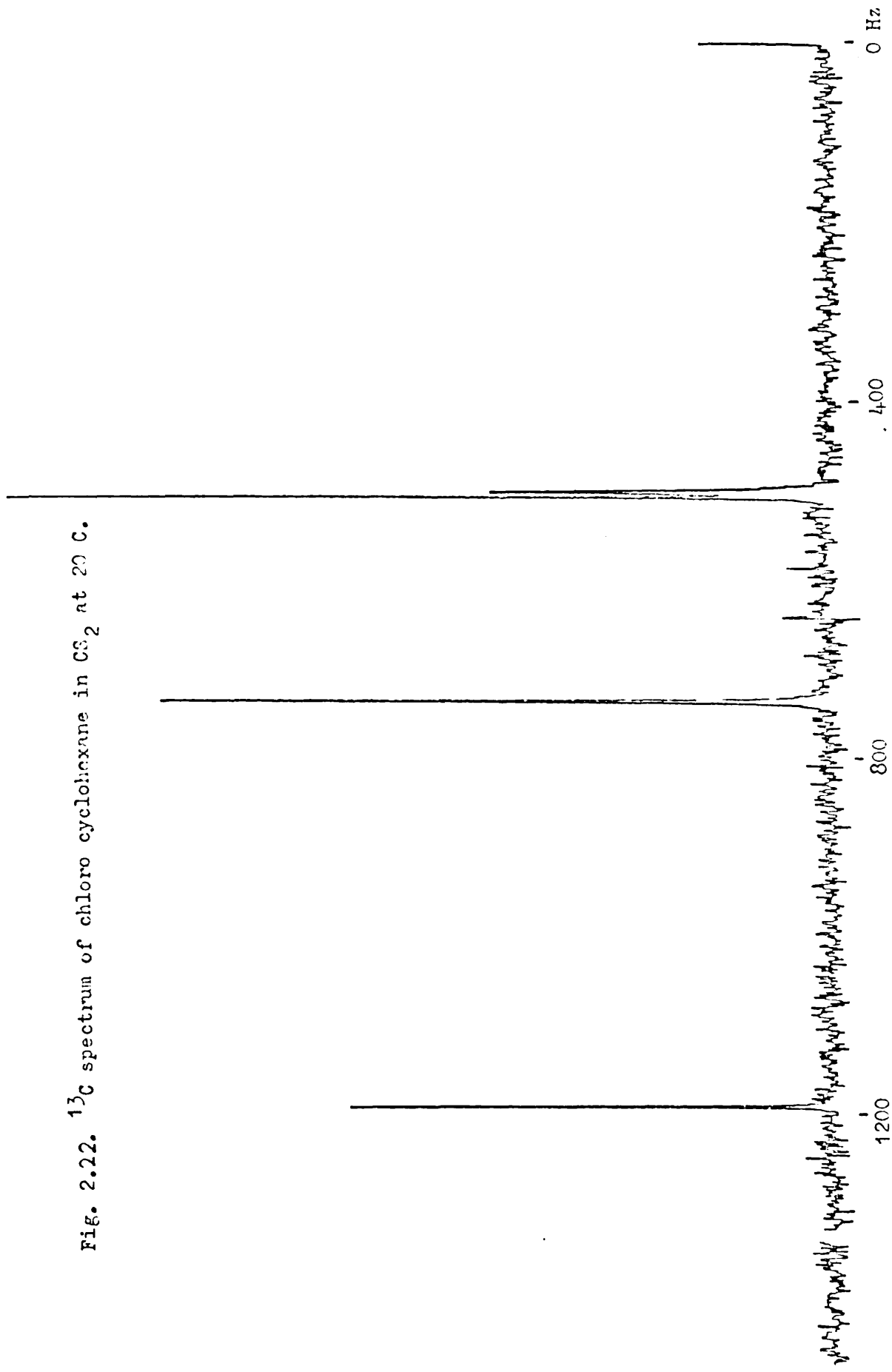

Fig. 2.22. ^{13}C spectrum of chloro cyclohexane in CS_2 at 20 C.

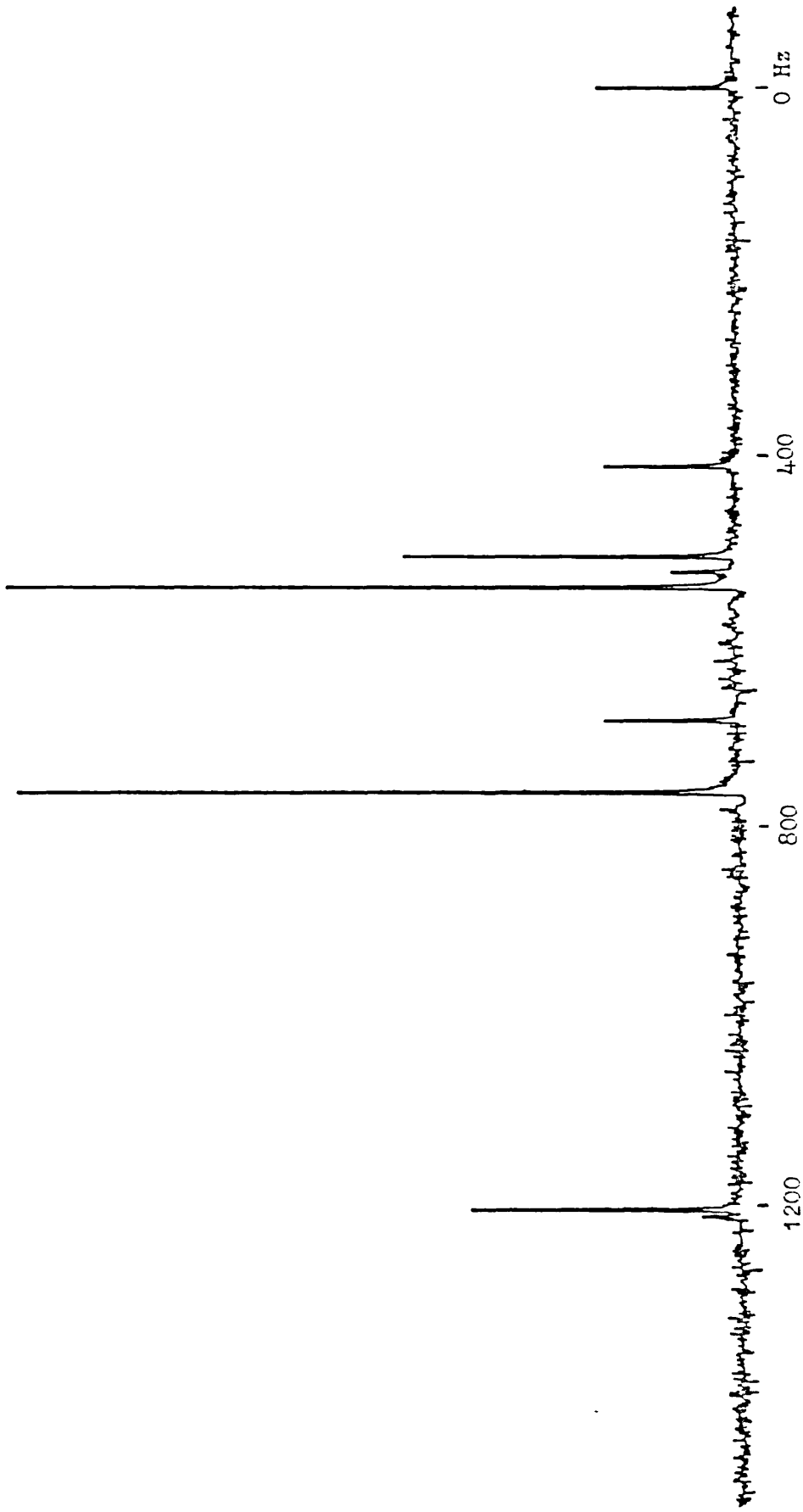

Fig 2.23. ^{13}C spectrum of chloro cyclohexane in CS_2 at -95 C.

Table 2.9 Calcuation of ΔG^{o} values for cyclohexyl chloride.

	Standard free energy value	
Carbon(s)	Cal mol $^{-1}$	J mol $^{-1}$
1	-	-
2	842.5	3525
3	834.2	3490
4	1330.2	5566

Unfortunately it was not possible to reach a low enough temperature for the bands to be no longer broad. However the shift values at the lowest temperature obtainable were used to calculate free energy difference values. The chemical shifts are given in Table 2.8 the standard free energy differences are given in Table 2.9 and spectra of cyclohexyl chloride as shown in Figures 2.22 and 2.23. No attempt was made to assess the intrinsic effect of temperature on the shifts and the inaccuracy of the results suggests that a temperature dependence does exist. Further evidence is given by the fact that the averaged shift of Carbon 1 is outside the range of the low temperature shifts.

Despite the incompleteness of the data certain conclusions can still be drawn.

The tetrahydropyran derivatives so far studied have standard free energy difference values similar to those of their cyclohexyl analogues.

In the cases studied the ^{13}C chemical shifts studied are all temperature dependent. In the case of tetrahydropyran, this dependence is not linear with respect to temperature. Although the dependence is relatively small it significantly affects the calculation of standard free energy differences. Further data are required at lower temperatures using a greater number of transients to improve the signal to noise before accurate assessment of the temperature dependence can be made.

In the absence of overlap or second order effects it is possible to calculate the proton shifts and coupling constants to good accuracy. The standard free energy difference values calculated using these were less accurate but the possibility of this being caused by temperature dependence could not be confirmed or denied.

2.7 Conformational anaylsis by vibrational spectroscopy

It is possible to perform conformational anaylsis using variable temperature vibrational analysis. In this case the spectra of both conformers are observed throughout the temperature range but the intensities vary with concentration.

Firstly, it is necessary to compute expected frequencies using a reasonably accurate force field. It is usual to study the C-X stretch and some earlier work has used an empirical approach to assign these bands. Because of this there are papers in the literature with conflicting assignments. For example Larnaudie (31) and Chiurdoglu and Reisse (32) both assign the equatorial C-I stretch in cyclohexyl iodide as the band at 654cm $^{-1}$ and the axial C-I stretch at 638cm $^{-1}$. However, a comprehensive solvent and temperature study (33) has shown that the band at 652cm $^{-1}$ is in fact the overlap of a band from each isomer, the bands showing a variable intensity relationship at different temperatures and in different solvents. A more recent paper (34) claims that the 639 and 655cm^{-1} bands can "safely" be assigned to the C-I stretching vibrations because the band at 639cm $^{-1}$ persists in the solid but makes no reference to the previous paper.

The equatorial C-Y stretch, where Y is any substituent is generally at a higher frequency than the corresponding axial stretch. It has been suggested (35) that the reason for this consistent difference is that when the C-Y bond is stretched there is a small restoring force acting on the carbon when Y is axial and the vibration is essentially

perpendicular to the plane of the ring but when Y is equatorial the motion of the carbon forces a ring expansion, the restoring force is greater and the frequency therefore higher.

Once the assignments are considered to be correct the optical densities of the bands are recorded at various temperatures. Because of the small energy difference between the conformers, the optical densities must be measured accurately over a wide temperature range, preferably allowing for the fact that the cell itself radiates as a function of temperature.

The optical density equals the path length of the cell multiplied by the concentration of the isomer and the extinction coefficient.

$$\log (I_o/I) = O.D. = E \times C \times l$$

$$\frac{O.D._e}{O.D._a} = \frac{E_e}{E_a} \times \frac{C_e}{C_a} = \propto K$$

In order to find the standard free energy difference it is necessary to know the extinction coefficients of the bands in each isomer. This can be achieved by measuring the coefficients of locked conformer derivatives and assuming they are the same as in the original compounds.

However it is possible to obtain a ΔE value by observing the change of $\propto K$ with temperature (36).

$$\frac{d \ln \propto K}{dT} = \frac{\Delta E}{RT^2}$$

Table 2.10. Force field of tetrahydropyran derivatives.

Stretch constants in N m^{-1}.

Stretch - bend interaction constants in N m^{-1} rad^{-1}

Bending constants in N m^{-1} rad^{-2}

Force constant	Group	Atoms common to interacting co-ordinates	Value
	STRETCH		
$f(CH)^2$	$C-CH_2-O$	-	462.6
$f(CH)^2$	$C-CH_2-C$	-	455.4
$f(CO)^2$	C-O	-	509.0
$f(CC)^2$	C-C	-	426.1
	STRETCH - STRETCH		
f(CH/CH)	$C-CH_2-O$	C	-4.6
f(CH/CH)	$C-CH_2-C$	C	0.6
f(CO/CO)	C-O-C	O	28.8
f(CC/CO)	C-C-O	C	10.1
f(CC/CC)	C-C-C	C	10.1
	BEND		
$f(HCH)^2$	$C-CH_2-O$	-	47.1
$f(HCC)^2$	$C-CH_2-O$	-	75.2
$f(HCO)^2$	$C-CH_2-O$	-	90.1
$f(HCH)^2$	$C-CH_2-C$	-	55.0
$f(HCC)^2$	$C-CH_2-C$	-	65.6
$f(COC)^2$	C-O-C	-	131.3

Force constant	Group	Atoms common to interacting co-ordinates	Value
$f(CCO)^2$	C-C-O	-	118.2
$f(CCC)^2$	C-C-C	-	107.1
	STRETCH - BEND		
f(CO/HCO)	C-CH_2-O	C-O	38.7
f(CC/HCC)	C-CH_2-O	C-C	47.8
f(CC/HCC)	C-CH_2-C	C-C	32.8
f(CC/HCC)	C-CH_2-C	C	7.9
f(CO/COC)	C-O-C	C-O	48.3
f(CO/CCO)	C-C-O	C-O	61.8
f(CC/CCO)	C-C-O	C-C	40.3
f(CC/CCC)	C-C-C	C-C	41.7
	BEND - BEND		
f(HCO/HCO)	C-CH_2-O	C-O	-0.5
f(HCC/HCC)	C-CH_2-O	C-C	10.5
f(HCO/HCC)	C-CH_2-O	C-H	11.5
f(HCC/HCC)	C-CH_2-C	C-C	-2.1
f(HCC/HCC)	C-CH_2-C	C-H	1.2
$f(H_aCC/H_bCC)$	(H or C)-CH_2-CH_2-C	H_aC-CH_b (G)	-0.5
$f(H_aCC/H_bCC)$	(H or C)-CH_2-CH_2-C	H_aC-CH_b (T)	12.7
$f(H_aCC^1/H_bC^1C^2)$	(H or C)-CH_2-C^1H_2-C^2	* (G)	0.9
$f(H_aCC^1/H_bC^1C^2)$	(H or C)-CH_2-C^1H_2-C^2	* (T)	0.2

* If the plane formed by atoms H_aCC^1 bisects the angle formed by atoms $H_bC^1C^2$ then f is designated as gauche; otherwise it is trans.

Force constant	Group	Atoms common to interacting co-ordinates	Values
f(HCO/CCO)	C-CH_2-O	C-O	-3.1
f(HCC/CCO)	C-CH_2-O	C-C	-3.1
f(HCC/CCC)	C-CH_2-C	C-C	-3.1
f(HCO/COC)	CH-O-C	H-C-O-C (G)	0.4
f(HCO/COC)	CH-O-C	H-C-O-C (T)	-11.2
f(HCC/CCO)	CH-C-O	H-C-C-O (G)	-11.3
f(HCC/CCO)	CH-C-O	H-C-C-O (T)	2.8
f(HCC/CCC)	(O or C)-CH-C-C	H-C-C-H (G)	-5.2
f(HCC/CCC)	(O or C)-CH-C-C	H-C-C-H (T)	4.9
f(COC/OCC)	C-O-C-C	C-O-C-C (G)	1.1
f(CCC/CCO)	C-C-C-O	C-C-C-O (G)	1.1
f(CCC/CCC)	C-C-C-C	C-C-C-C (G)	1.1
f(COC/OCC)	C-O-C-C	C-O-C-C (T)	-1.1
f(CCC/CCO)	C-C-C-O	C-C-C-O (T)	-1.1
f(CCC/CCC)	C-C-C-C	C-C-C-C (T)	-1.1

G - gauche T - trans

Constants relevant for $\begin{matrix} C \\ C \end{matrix}\!\!>\!\!CHX$ group.

Force constant	X = F	X = I
$f(CX)^2$	579.0	208.1
$f(CH)^2$	500.0	458.8
$f(HCX)^2$	75.4	66.3
$f(XCC)^2$	105.9	94.8
$f(CCH)^2$	65.6	65.6

Table 2.11 Calculated frequencies for 4 - fluoro T.H.P.

A′		A"	
axial	equitorial	axial	equitorial
3031	3032	2967	2967
2968	2968	2927	2927
2929	2929	2861	2861
2862	2862	2855	2855
2855	2856	1465	1464
1480	1488	1454	1454
1463	1460	1385	1390
1449	1453	1324	1336
1387	1373	1271	1250
1272	1270	1241	1239
1243	1242	1211	1183
1214	1228	1132	1154
1145	1129	1096	1099
1068	1095	1005	957
1007	1044	879	934
970	979	826	818
879	876	492	453
808	828	366	354
651	594	163	180
520	419		
350	392		
281	299		
113	130		

Table 2.12 Calculated frequencies for 4 - iodo T.H.P.

A′		A"	
axial	equitorial	axial	equitorial
2968	2968	2967	2967
2929	2930	2926	2927
2902	2902	2861	2861
2862	2862	2855	2855
2855	2856	1464	1464
1463	1463	1454	1454
1459	1459	1385	1389
1395	1395	1312	1328
1320	1327	1267	1249
1267	1264	1239	1237
1236	1232	1211	1174
1202	1218	1122	1146
1094	1092	1096	1097
1045	1045	1003	956
991	994	876	920
896	891	826	818
807	824	465	454
711	745	268	209
546	552	134	173
471	384		
308	291		
213	205		
65	96		

Table 2.13 Experimental frequencies for 4 - iodo T.H.P.

infrared	raman	infrared	raman
2960 s	2964	1107 w	
2925 w	2926	1083 m sh	1083
2903 w	2898	1064 w	
2855 sh	2853	1020 m	1023
2842 s		1014 m	
1461 m	1470	995 m	999
1451 w	1462	978 w	
1440 m	1436	870 w	881
1427 w		825 m	828
1412 w		821 w sh	
1379 s		683 w	689
1345 w		672 w	
1335 w	1338	649 w	657
1324 w		532 m	537
1298 w sh	1298	515 vw	520
1291 s		452 w	455
1281 w sh		431 w	436
1257 m	1265	378 vw	384
1242 m	1250	344 w	
1230 m		249 w	254
1215 m		222 w	229
1196 w sh			200
1175 s	1180		144
1167 m sh			116
1135 m	1140		

sh - shoulder all raman bands polarised.

Because it is necessary to measure the optical densities accurately, allowance should be made for the variation in emission from the cell caused by varying its temperature.

2.8 Calculation of vibrational frequencies

Most of the force constants used in these calculations were taken from a force field derived for ten simple alphatic ethers (including tetrahydropyran) by Snyder and Zerbi (37), the force constants for the halogeno part being taken from a paper on methyl halides by Aldous and Mills (38). The force constants are listed in Table 2.10. Both molecules in both conformations belong to the C_s point group having only a plane of symmetry. The 42 normal modes symmetrise into two blocks as 23 A' and 19 A".

All bond angles were assumed to be tetrahedral and the C-O bond length was assumed to be the same as the C-C bond length of 1.54×10^{-10}m. Other bond lengths were taken as follows C-H 1.093, C-F 1.381, and C-I 2.16 all x 10^{-10}m.

The calculated frequencies are listed in tables 2.11 and 2.12 and the experimental results in table 2.13. It is not possible to assign the bands with any certainty with the information available but the C-I stretch has been assigned to the 673cm $^{-1}$ band for equatorial and 649cm $^{-1}$ for axial. However, no variable temperature work was carried out on this molecule.

2.9 A review of vibrational studies.

The initial work on the sterochemistry of halogeno - cyclohexanes was carried out by Hassel (39) but the first conformational analysis on the individual conformers was performed using vibrational spectroscopy. The assignment of bands to each conformer was aided by the fact that by slowly crystallizing these compounds (40) it is possible to convert all the molecules to their more stable state (equatorial). In the case of cyclohexyl fluoride this procedure does not result in any bands vanishing. Nuclear magnetic resonance clearly indicates the presence of two conformers in the liquid and we can assume that the small size of the fluorine atom allows both conformers to align readily in the crystal.

The integrated intensities of the C-Cl stretching modes were measured for chlorocyclohexane (41) in the gas state over a temperature range of 83 K and a ΔE value of about 340 cal mol $^{-1}$ (1423 J mol $^{-1}$) was obtained. A similar paper (36) confirms this value in solution and gives a value of 200 cal mol $^{-1}$ (837 J mol $^{-1}$) for bromocyclohexane.

Neither of these papers measured the ratio between the extinction coefficients of the two bands measured. The value of 1.85 measured for bromocyclohexane (42) clearly shows that this factor cannot be ignored. However this paper calculated a very high free energy difference of 610 cal mol $^{-1}$ (2552 J mol $^{-1}$). The value for the extinction coefficient ratio was determined using locked conformers and therefore could be inaccurate. There is one paper which appears to support this value (34) but on examination the two measurements were made at temperatures differing by 25 K and can hardly be considered accurate.

A value for iodocyclohexane is also quoted as 730 cal mol $^{-1}$ (3054 J mol $^{-1}$). This is based on measurements of the 639 and 655cm $^{-1}$ bands and ignores the more likely assignment proposed in reference 33. A further paper (43) has recently been published using this assignment which quotes ΔE = 400 cal mol $^{-1}$ (1674 J mol $^{-1}$) and extinction coefficients for axial of 70 and for equatorial of 108 l mol $^{-1}$ cm $^{-1}$.

The activation energy of chlorocyclohexane has been determined (44) as $\Delta G^{+}_{eq \rightarrow ax}$ = 10.6 k cal mol $^{-1}$ (4.44 x 10^4 J mol $^{-1}$) and $\Delta G^{+}_{ax \rightarrow eq}$ = 10.2 k cal mol $^{-1}$ (4.27 x 10^4 J mol $^{-1}$) by studying its kinetics in solution at temperatures below its melting point.

The relative intensities of rotational transitions of the axial and equatorial conformers of cyclohexyl fluoride have been measured (45) to give a free energy difference of 298 $\pm$ 28 cal mol $^{-1}$ (1247 $\pm$ 117 J mol $^{-1}$) at 187 K.

The only previous vibrational study on halogeno - tetrahydropyrans was carried out by Dr. Barrett on 4 - chloro T.H.P. (4). He was unable to preferentially crystallize the more stable isomer and integrated areas at low temperature were within experimental error the same at room temperature.

A more comprehensive review of various sizes of ring system studied by vibrational spectroscopy is available (46) as well as reviews on cyclohexyl systems (47, 48, 49) and a general review of conformational analysis in the last twenty five years (50).

CHAPTER THREE

CONFORMATIONAL ANALYSIS OF BIPHENYL AND SOME OF ITS DERIVATIVES

3.1 Introduction

Biphenyl has been shown to be planar in the solid state[50] but non-planar in solution or the vapour phase.[51]

Although there is no doubt about the structure of biphenyl in the solid state the various methods used to determine the dihedral angle in solution have given a variety of results between 0° and 60°.

U.V. spectroscopy has given a value of $18^{\circ} - 23^{\circ}$,[52-55] e.s.r. gave an angle of 38°,[56] dipole moments gave $30^{\circ} - 40^{\circ}$ [57] and the depolarisation of Rayleigh scattered light gave $24^{\circ} - 31^{\circ}$.[58,59] A number of techniques have suggested a planar structure despite the fact that this is theoretically unlikely. Measurement of molar Kerr constants,[60] light scattering and magnetic anisotropy investigations[61] as well as other U.V. and e.s.r.[62] investigations gave this result and there is no satisfactory way of correlating the divergence of results.

Theoretical studies using molecular mechanics gave a value of 35°.[63]

A n.m.r. investigation of 3,3', 5,5'-tetrachlorobiphenyl in a liquid crystal solution[64] gave a dihedral angle of 34° and the authors suggested that biphenyl was likely to have a similar value in a normal solution.

A value of $32 \pm 2^{\circ}$ has been obtained using vibrational spectroscopy[65] which is in good agreement. However, in the calculations certain invalid assumptions were made. Two of these assumptions were removed in the course of the current work, and the improved model was used to

Fig. 3.1. The possible symmetries of the biphenyl molecule.

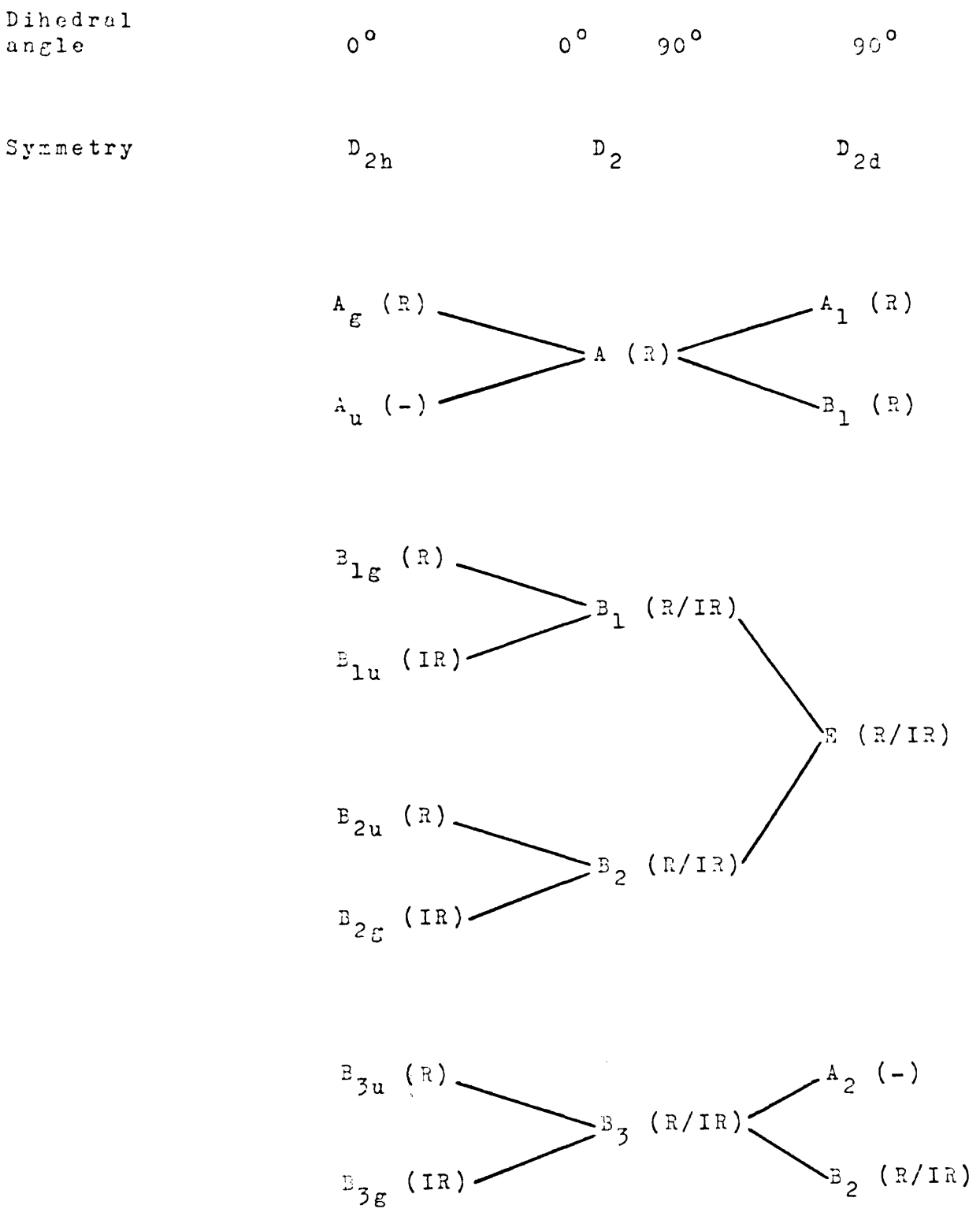

R - Raman active IR - Infrared active

compute the force field and dihedral angle of 4,4' difluoro biphenyl d^8, a previously unreported compound.

This is another method whereby spectroscopy can be used as a method of conformational analysis.

3.2 Theoretical Considerations

Biphenyl consists of two six-membered aromatic rings joined by a carbon-carbon bond. The angle between the planes of the rings is called the dihedral angle. This angle determines the symmetry of the molecule and hence the symmetry of the vibrational frequencies.

Biphenyl can belong to one of three symmetry groups depending on whether the dihedral angle is 0°, 90° or something in between. The symmetry of the frequencies may best be described in a diagram (Fig. 3.1).

It can be seen that if the molecule changes from planar to non-planar the symmetry is lowered and each in plane group combines with an out of plane group to form four new symmetry groups. Force field changes caused by a change in dihedral angle may arise in two ways.

a) Steric interactions

It is expected that there will be repulsions between the ortho hydrogens in planar biphenyl. As in the a_g motions both pairs of ortho hydrogens are bouncing against one another, those fundamentals involving strong β deformations will be most affected on change of dihedral angle. However the observed frequency shifts are small suggested that steric interactions are small unless other effects are being observed.

It has been suggested that steric hindrance is reduced by distortion of the C-C-H angle, and this can be seen to be true (Fig. 3.2).

Fig. 3.2. Geometry used for biphenyl calculations.
Bond lengths in 10^{-10} m and angles in degrees.

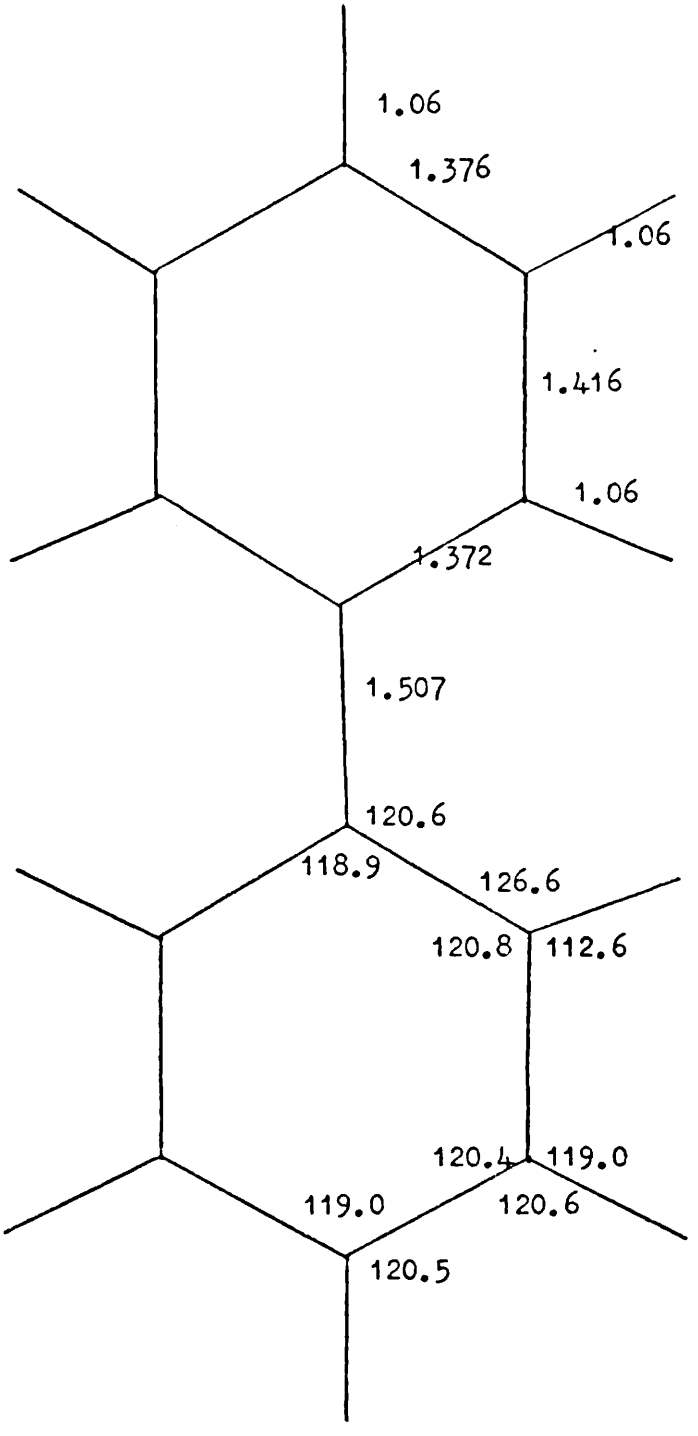

b) Resonance interaction between the two rings

Biphenyl may be regarded as a resonance hybrid of several canonical structures[66] one of which involves the inter-ring double bond. This structure is thought to have little contribution because the inter-ring bond length in the solid (1.51×10^{-10}m) is almost as large as that of a single C-C bond (1.54×10^{-10}m). The double bond structure will contribute even less on twisting and this would be reflected in a force constant change. There is evidence[65] that there is a slight weakening of the inter-ring bond but it was not possible to estimate the magnitude of the change.

If biphenyl is considered as two mono-substituted benzene molecules (C_{2v} symmetry), each of the C_{2v} motions of biphenyl gives rise to a splitting of the original degenerate levels, A_1 modes (C_{2v}) split into a_g (in-phase) and b_{3u} (out-of-phase) parallel modes and B_2 modes split into b_{1g} (in phase) and b_{2u} (out-of-phase) perpendicular modes.

The amount of splitting and the eventual frequency shifts will depend on the strength of the inter-ring C-C bond, on possible steric interactions and on the extent of kinetic coupling between the two rings.

Because steric interactions and inter-ring π-bonding are small, a change in geometry will have little effect on the force field. The most important change in frequencies is caused by the merging of the symmetry groups.

Combining the groups causes interactions which force the frequencies apart. From first order perturbation theory the interaction is inversely proportional to the differences in the energy levels which

are being mixed. Because out-of-plane modes only occur below 1000 cm^{-1} it follows that this is the region where the most important interactions are likely to occur. By symmetry considerations it can be shown that the vibrational wavefunctions of the a_g and a_u and also of the b_{3g} and b_{3u} modes remain orthogonal on going from the planar D_{2h} structure to the non-planar D_2 structure. For example, since a_u vibrations are antisymmetric to all planes, the inter-ring bond atoms cannot move. It follows that the in-plane and out-of-plane distortions remain orthogonal on twisting the ring. Thus only B_1 or B_2 modes below 1000 cm^{-1} are able to show any interaction through effects not related to force constant changes.

Frequency shifts caused by symmetry groups merging

If it is assumed that the molecular force field is independent of the dihedral angle, then the frequency shifts are due to changes in the G (inverse kinetic energy) matrix.[67] Thus if we take a realistic force field and calculate the vibrational frequencies for a number of different dihedral angles it becomes apparent that certain of the B_1 and B_2 modes are a function of the angle. By measuring the change in frequency of these modes on going from the solid to the liquid state we can get an estimate for the dihedral angle.

Coupling can only occur through those modes which span the ring. Since interaction cannot occur in the A species, this precludes any interactions through the C-C stretch. Other internal deformations which span the ring and may lead to coupling are γ_c, β_c and ϕ. The natural frequency of the γ_{CH} deformation lies well above that of the only in-plane deformation coordinate to span the ring, β_c, being

about 900 cm^{-1} compared to 300 cm^{-1}, thus the interaction is expected to be small. The primary perturbations arise from ϕ, β_c interactions.

In order to accurately calculate the dihedral angle it is necessary to calculate the frequencies to a high level of accuracy. Clearly the frequency shift with dihedral angle will depend on the original separation of the interacting species. In an attempt to further improve the force field two of the assumptions previously used were removed.

In order to fully appreciate the improvements made it is necessary first to consider the theory behind the calculations.

It is well known that the vibrations of non-linear molecules can be resolved into 3N-6 normal modes where N is the number of nuclei in the molecule.

Under ideal conditions it is possible for the molecule to absorb energy. If subjected to infrared radiation of a frequency equal to the frequency of one of the normal modes the molecule may absorb some of this energy. If subjected to a high frequency monochromatic source the molecule may scatter radiation such that the component frequencies of the scattered radiation are lower than the source frequency by the frequency of one of the normal modes (Raman effect).

Whether infrared absorbtions or Raman emissions take place will depend on the symmetry of the vibration, and on the transition probability. It is unlikely that all the frequencies can be deduced from the infrared and Raman spectra. Thus 3N-6 is the maximum number of independent observable frequencies (combination or overtone bands may be present).

The frequencies of the normal modes are related to the strength of the bonds in the molecule and the way in which they deform. These are measured in terms of force constants. It is possible to calculate the vibrational frequencies if the force constants are known but a number of approximations and assumptions are necessary.

The way in which the biphenyl molecule vibrates can be described in terms of five types of internal coordinates. These are,

1) Bond stretching (R)
2) Angle bending (α)
3) In-plane wag (β)
4) Out-of-plane wag (γ)
5) Special torsion (ϕ)

Not only are there force constants for the 71 internal coordinates used to describe biphenyl but there are interaction constants between each internal coordinate and every other internal coordinate. Thus we can form a 71 x 71 matrix to show all these force constants (the F matrix).

Even though many of the F elements are not independent on symmetry considerations, there are clearly far more unknowns than pieces of information and various devices must be used to reduce the number of unknowns.

It is well known that there will be no interaction between a large number of pairs of internal coordinates and these can be set to zero. For example, there will be no interaction between the in-plane internal coordinates and the out-of-plane internal coordinates when the molecule is planar.

The remaining force constants are then grouped together by type and are given the same force constant value. There are 36 of these groups in the case of biphenyl and they are listed in table 3.4.

The internal coordinates are given the following symbols

r	CH stretch.
r (c)	inter-ring CC' stretch.
R	intra-ring CC stretch.
α	ring angle bend.
β	anti-clockwise movement of CH bond with respect to the bisector of the adjacent ring angle.
β(c)	as β, but of extra-ring CC' bond.
γ	out-of-plane angular movement of CH bond.
γ (c)	out-of-plane angular movement of CC' bond.
ϕ	Bell type twisting coordinate (special torsion).

If we attempt to calculate the 60 frequencies by selecting random values for the 36 force constants it is highly unlikely that the calculated frequencies would bear much resemblance to the experimental ones. Even if they did there is no guarantee that the force constants would have realistic values.

There are two principal problems. The first is that the experimental data may be insensitive to the force constant parameters. Vibrational frequencies can be very insensitive to force constant coupling distortions which naturally have very different frequencies. This follows from a consideration of the well known relation

$$\lambda_i = \sum_{j,k} l_{ji}\, l_{ki}\, f_{jk} = 4\pi^2 \nu_i^2$$

The l_{ji} are the elements of the transformation matrix L between internal valence and normal coordinates

$$R = LQ$$

If the frequencies which would be associated with the isolated j^{th} and k^{th} internal coordinates are far apart then there will be little mixing of their motions. This implies that if l_{ji} is large, then l_{ki} is small and vice versa. The λ_i are therefore insensitive to the f_{jk}. For this reason it is usually very difficult to establish interaction force constants coupling C-H stretching motions and other types of deformations. Other types of data, such as Coriolis constants, where they are known, may be much more sensitive to these interaction constants.

The second problem arises from inter-relationships amongst the internal coordinates. Thus the ring C-C stretching coordinates are not independent of the ring angles. A number of so called redundancy relations exist amongst them. For example, for a regular hexagonal ring we have

$$\sum_{i=1}^{b} \alpha_i = 0$$

Using these relations the potential energy expression can be reduced to a smaller number of variables, implying that not all the quadratic force constants are derivable.

There is another fact which helps us to choose values for the force constants. It is well established that values of force constants in different molecules but in similar environments bear a close resemblance to each other. Thus in the case of biphenyl the original force field was based on the force field of benzene.

The values of the force constants are chosen using information from related molecules and they are used to calculate the frequencies.

Selected force constants can then be changed in small steps until the best fit between the observed and calculated frequencies is achieved.

The number of observables can be increased without increasing the number of variables by using isotopic substitution. In the previous paper the frequencies were recorded for three molecules, biphenyl, 4,4'-($^2H_2$) biphenyl and ($^2H_{10}$) biphenyl. It may be assumed that the differences in frequencies between the three molecules is due solely to the isotope effect and that there are no differences in geometry or force field between the three molecules. This method therefore increases the number of observables by about three times without increasing the number of variables.

In fact the number of independent observables may be rather less than the total number of observables as a result of frequency product rules as first shown by Redlich and Teller (see section 3.7).[68, 69]

$$\frac{\prod_i \nu_i^a}{\prod_i \nu_i^b} = \frac{\prod_A \left(\mu_A^a\right)^{1/2}}{\prod_A \left(\mu_A^b\right)^{1/2}} \left(\frac{M_a}{M_b}\right)^{T/2} \prod_{q=x,y,z} \left(\frac{I_q^a}{I_q^b}\right)^{\delta_q/2}$$

$\prod$ is the product operator, M_a and M_b refer to the masses of the two molecular species, T is the number of translations in the symmetry species over which the product is taken, δ_q = 1 or 0 depending on whether a rotation about the q axis belongs to the species, and I_q is the moment of inertia about the q axis. The μ_A are the reciprocal masses.

When the best fit is obtained between the observed and calculated frequencies the force field is then used to calculate the frequencies for different dihedral angles.

3.3 The computer programs

Two computer programs are used for these calculations, GZEVAL and MLTPRB and full details of these are already available.[70] They were used with only minor modifications.

GZEVAL

This program is used firstly to help assign the experimental frequencies using the initial force constants. It is used to produce the punch cards needed for the MLTPRB program. Finally it is used to calculate the frequencies for different dihedral angles using the refined force constants.

The input data is as follows,

TEXT (8A10)	Name of program.
NP, NOAT, NR, NIST (4I3)	Number of problems, Number of atoms in molecule, Number of internal coordinates, Number of isotopes.
X(3,NOAT) (9F 8.5)	Cartesian coordinates.
NINT, NDEF, NA1.....6(8I3)	Number of internal coordinate, Type of deformation, Atoms involved.
AM (8F 10.6)	Mass of atoms.
NF, NZ(2I3)	Number of force constants, Number of non-zero Z matrix elements.
FF (8F 10.6)	Values of force constants.
NRA, NCA, NFA, ZA (3I3, F 5.0 (I2, 2I3, F5.0))	Row and column of Z matrix, Number of force constant, Scaling factor.

NSYMB, NS (2I3)	Number of symmetry coordinates, Number of symmetry blocks.
ID, NC (2I3)	Number of rows of block, Number of cards of imput for block.
IX, JX, UX 8(2I3, F 4.0)	Row, Column, Value of U matrix element.

It may be noted that no F matrix is read in; the Z matrix is used instead. The Z matrix is the same as the F matrix with the exception that instead of numerical values for the force constants being read in a number between 1 and 36 and a scaling factor is read in. The numerical values for the force constants are read in as the FF matrix. This technique allows the values of all the elements corresponding to one type of force constant to be changed at once, the value is simply changed in the FF column matrix. The value of the corresponding F matrix element is the force constant value multiplied by the scaling factor.

The program is also able to produce punch cards for the MLTPRB program. These are,

TEXT
NSYMB, NS
ID
F(I, J)
NZS
NRSA, NCSA, NFSA, ZSA

F(I,J) is the G matrix, NRSA etc. describes the symmetrised. Z matrix and the remaining terms have already been defined.

MLTPRB

The program is used to refine the force constants. A set of force constants is used to calculate the frequencies which are compared with the experimental frequencies. The force constants are then changed in four stages to improve the fit.

The input data is as follows,

CARRIE (8A10)	Title of whole calculation.
NMOLS, NPERT, NF, NFR (2I3/2I3)	Number of molecules, Number of perturbations, Number of force constants, Number of perturbed constants.
FF(N) (8F 10.6)	Values of force constants.
PP(N) (40I2)	PP = 1 if constant perturbed.
IFAC, FAC, NV (I3/F4.0/I4)	Weighting percentage or absolute, Scaling factor, Number of variables.

* CARRIEA = TEXT

* N SYMB, NS
  X(I), W(I) — Experimental frequency, Scaling factor.

* JD = ID

* G(I,J) = F (I,J)

* JZ = NZS

* NROW, NCOL, NOFC, Z = NRSA, NCSA NFSA ZSA.

NT — Number of cycles

* This input obtained from GZEVAL program.

Percentage weighting was used for all perturbations allowing for the fact that higher frequencies are liable to have larger errors than lower frequencies.

Table 3.1. Calculation of ring C-C stretch force constants.

Position	Bond length (10^{-10} m)	Force constant (N m^{-1})	New F.C./ Old F.C.
Ortho	1.372	765.6	1.11
Meta	1.416	651.9	0.94
Para	1.376	754.4	1.09

3.4 The improvement of the model

The previous work on biphenyl and its derivatives has used the assumption that all the intra-ring C-C bond lengths and force constants are the same and that all the angles between the bonds are 120°. This has been shown to be untrue.[71] This improved geometry (Fig. 3.2) was used to compute a new cartesian coordinate matrix and the vibrational frequencies were calculated using this (Table 3.2). When calculating the frequencies for the fluorinated biphenyls a value of 1.327×10^{-10} m was used for the C-F bond length.

In the case of the intra-ring C-C bonds, it is illogical to use the same force constant for C-C bonds which have different bond lengths. The force constants were related to the bond lengths by the relationship,

$$f = Ae^{-xr}$$

where A and x are parameters.[72] The value used in the paper for x was 3.65 when the bond lengths were in 10^{-10} m. and this value was used in this work. Substituting the bond length and force constant used in the previous biphenyl work a value of 1.144×10^{5} was obtained for A. The new bond lengths were then used to calculate the new force constants. These were introduced into the Z matrix as a ratio of the old force constant and so the ratio between the three constants remained the same but their actual values could vary during perturbation. The values are given in Table 3.1.

Table 3.2 compares the experimental frequencies of biphenyl with four sets of calculated frequencies.

1 - calculated using the original hexagonal geometry.

2 - calculated using the new geometry but using the same force constant for all the intra-ring C-C stretches.

Table 3.2 Comparison between experimental and calculated frequencies of planar biphenyl.

	Experimental frequencies	Initial calculation		New geometry		N.G. and C-C scaling		After perturbation	
A_g	-	3073		3074		3074		3073	
	-	3072		3072		3073		3071	
	-	3069		3069		3069		3069	
	1610	1593	-17	1600	-10	1606	-4	1583	-27
	1513	1505	-8	1496	-17	1521	+8	1513	0
	1276	1285	+9	1290	+14	1293	+17	1286	+10
	1208	1196	-12	1201	-7	1203	-5	1200	-8
	1036	1027	-9	1032	-4	1056	+20	1049	+13
	1002	987	-15	988	-14	992	-10	984	-18
	739	736	-3	731	-8	738	-1	736	-3
	331	322	-9	324	-7	325	-6	323	-8
A_u	-	959		956		956		947	
	-	847		857		857		851	
	-	428		434		434		425	

Table 3.2 (continued)

	Experimental frequencies	Initial calculation		New geometry		N.G. and C-C scaling		After perturbation	
B_{1g}	–	3070		3070		3071		3070	
	–	3069		3069		3069		3067	
	1592	1626	+34	1620	+28	1691	+99	1624	+32
	1462	1466	+4	1471	+9	1490	+28	1451	−11
	1333	1355	+22	1353	+20	1363	+30	1329	−4
	1263	1285	+22	1285	+22	1300	+37	1289	+26
	1165	1160	−5	1161	−4	1168	+3	1161	−4
	1097	1082	−15	1074	−23	1069	−28	1069	−28
	610	611	+1	612	+2	613	+3	607	−3
	–	407		410		412		426	
B_{1u}	968	982	+14	983	+15	983	+15	980	+12
	903	899	−4	900	−3	900	−3	896	−7
	729	726	−3	722	−7	722	−7	725	−4
	695	705	+10	709	+14	709	+14	698	+3
	458	456	−2	449	−9	449	−9	442	−16
	73	78	+5	77	+4	77	+4	79	+6

Table 3.2 (continued)

	Experimental frequencies	Initial calculation		New geometry		N.C. and C–C scaling		After perturbation	
B_{2u}	–	3069		3070		3071		3070	
	–	3069		3068		3069		3067	
	1568	1599	+31	1590	+22	1661	+93	1629	+61
	1428	1434	+6	1436	+8	1449	+21	1435	+7
	1344	1325	−19	1326	−18	1354	+10	1339	−5
	1268	1293	+25	1294	+26	1299	+31	1290	+22
	–	1165		1167		1172		1168	
	–	1055		1045		1044		1036	
	626	629	+3	631	+5	631	+5	630	+4
	118	120	+2	123	+5	123	+5	120	+2
B_{2g}	978	985	+7	987	+9	987	+9	985	+7
	–	903		905		905		916	
	–	732		735		735		785	
	–	708		710		710		700	
	546	532	−14	529	−17	529	−17	554	+8
	251	233	−18	226	−25	226	−25	230	−21

Table 3.2 (continued)

	Experimental frequencies	Initial calculation		New geometry		N.G. and C-C scaling		After perturbation	
B_{3u}	-	3073		3073		3074		3073	
	-	3072		3072		3073		3071	
	-	3069		3069		3069		3068	
	1597	1592	-5	1599	+2	1597	0	1575	-22
	1480	1478	-2	1470	-10	1492	+10	1487	+7
	1181	1198	+17	1200	+19	1201	+20	1198	+17
	1041	1032	-9	1036	-5	1067	+26	1060	+19
	1006	1016	+10	1022	+16	1028	+22	1027	+21
	985	974	-11	974	-11	992	+6	966	-19
	610	615	+5	614	+4	614	+4	609	-1
B_{3g}	-	959		956		956		947	
	846	847	+1	857	+11	857	+11	851	+5
	409	428	+17	434	+25	434	+25	425	+16

3 - calculated using the new geometry and scaling the C–C stretch force constants to the C–C bond lengths.

4 - calculated from the force constants after perturbation.

Only 59 normal modes were computed. The missing fundamental is attributed to the lowest a_u mode, and is known as the "butterfly" torsion. This deformation was omitted because the nature of the torsion in solution is uncertain. Because the frequency of this mode is low, the approximation is justified as there is little mixing with other normal coordinates.

It is helpful to consider the calculated frequencies both before and after perturbation. After perturbation analysis has been carried out the frequency fit is expected to be the best possible one under the circumstances. Therefore, if adjustments are made to the model after a perturbation the frequency fit is expected to worsen. This is found to be true in this case.

The effect of the new geometry can be seen in both the in-plane and out-of-plane modes. However the effect is very slight, the largest change in frequency being 9 cm^{-1} but for the most groups there is a slight worsening in the frequency fit.

The effect of scaling the C–C force constants to the bond lengths is only seen in the in-plane modes. A worsening in the fit is noticeable particularly for the highest ring mode in the B_{1g} and B_{2g} groups. Both calculated frequencies go up by about 70 cm^{-1}. Apart from these two the overall worsening is not great and is similar to that caused by the introduction of the new geometry. It is interesting to note that the changes caused by the scaling of the force constants,

Table 3.3 Comparison between experimental and calculated frequencies of planar biphenyl d^{10} as calculated after perturbation of the force constants.

	Experimental frequencies	Initial calculated frequencies		Final calculated frequencies	
A_g	2287	2288	+1	2291	+4
	2285	2285	0	2284	−1
	2280	2280	0	2278	−2
	1563	1576	+13	1566	+3
	1411	1387	−24	1405	−6
	1186	1191	+5	1189	+3
	965	947	−18	949	−16
	880	864	−16	868	−12
	846	838	−8	847	+1
	690	692	+2	692	+2
	312	309	−3	309	−3
A_u	-	777		761	
	-	659		663	
	-	374		375	
B_{1g}	2281	2283	+2	2287	+6
	2279	2279	0	2274	−5
	1583	1601	+18	1592	+9
	1347	1333	−14	1325	−22
	1280	1265	−15	1246	−34
	-	1054		1039	
	850	844	−6	840	−10
	831	827	−4	825	−6
	583	586	+3	584	+1
	-	378		398	

Table 3.3 (continued)

	Experimental frequencies	Initial calculated frequencies		Final calculated frequencies	
B_{1u}	818	815	−3	808	−10
	742	732	−10	730	−12
	620	631	+11	616	−4
	538	527	−11	537	−1
	410	407	−3	393	−17
	83	72	−11	74	−9
B_{2u}	2281	2281	0	2287	+6
	2278	2278	0	2274	−4
	1522	1573	+51	1598	+76
	1317	1284	−33	1329	+12
	1260	1262	+2	1231	−29
	1024	1023	−1	1014	−10
	844	845	+1	843	−1
	818	825	+7	819	+1
	594	603	+9	604	+10
	112	110	−2	111	−1
B_{2g}	816	813	−3	824	+8
	-	759		807	
	651	640	−11	647	−4
	539	541	+2	546	+7
	459	459	0	467	+8
	225	217	−8	214	−11

Table 3.3 (continued)

	Experimental frequencies	Initial calculated frequencies		Final calculated frequencies	
B_{3u}	2287	2286	−1	2288	+1
	2285	2284	−1	2284	−1
	2280	2279	−1	2277	−3
	1566	1571	+5	1557	−9
	1343	1301	−42	1326	−17
	981	991	+10	988	+7
	950	933	−17	929	−21
	854	859	+5	858	+4
	813	818	+5	839	+26
	588	594	+6	587	−1
B_{3g}		777		761	
	655	659	+4	663	+8
	354	374	+20	375	+21

with only two exceptions, result in an increase in the calculated frequency. This is because the average of the ortho meta and para C-C bond lengths is less than the 1.40×10^{-10}m used in the previous calculation. Thus in the present calculation the average of the force constants is larger than the one previously used.

A perturbation was carried out on the force constants in a number of stages. The frequency fit is not very different from that reported in the previous work but of course the force constants are different.

The highest ring modes in the B_{1g} and B_{2g} groups have improved but in the case of the B_{1g} mode it is no better than after the previous work and in the case of the B_{2g} mode it is considerably worse. These improvements are at the expense of the fit of the highest ring modes in the other two in-plane groups.

The effects caused directly by perturbing the force constants were a general improvement in the fit for groups B_{1g}, B_{2u}, B_{2g} and B_{3g}, although no better than after the previous perturbation and the fit for the remaining groups was similar.

The fit of those frequencies previously used to calculate the dihedral angle was no better and consequently the angle was not recalculated.

The frequencies of biphenyl d^{10} were also calculated using the same force constants. The fit for the A_g frequencies was noticeably improved whereas the fit for the B_{1u} and B_{3u} frequencies was similar. The fit for the B_{2g} frequencies was worse and that for the B_{1g} and B_{2u} frequencies was much worse. The large error in the third highest B_{2u} frequency of 76 cm^{-1} which is an increase from the previous error of 51 cm^{-1} suggests that the assignment is wrong. The frequencies are listed in Table 3.3.

Table 3.4 Force constants used for biphenyl calculation, before and and after perturbation.

		Before	After			Before	After
1	R	691.3	657.4	21	$\alpha_i r_i$	- 1.0	- 1.0*
2	r(c)	639.2	653.9	22	$\alpha_i \beta_{i+1}$	4.2	4.2*
3	$R_i R_{i+1}$	52.8	48.1	23	$\alpha_i \beta(c)_{i+1}$	3.1	3.8
4	$r(c)_i R_i$	30.1	34.0	24	γ	26.6	25.9
5	$R_i R'_{i+1}$	25.6	26.3	25	γ (c)	12.7	14.8
6	$r(c)_i \alpha_i$	- 88.7	- 90.0	26	$\gamma_i \gamma_{i+1}$	0.9	0.8
7	r	512.5	512.3	27	$\gamma_i \gamma_{i+2}$	- 1.4	- 0.8
8	α	57.1	57.2	28	$\gamma_i \gamma_{i+3}$	- 1.7	- 1.4
9	$\alpha_i \alpha_{i+1}$	- 5.0	- 5.0*	29	$\gamma_i(c) \gamma_{i+1}$	1.5	0.9
10	β	89.1	89.0	30	$\gamma_i(c) \gamma_{i+2}$	- 1.8	- 2.2
11	$\beta(c)$	73.3	73.6	31	$\gamma_i(c) \gamma_{i+3}$	1.0	1.0
12	$\beta_i \beta_{i+1}$	2.4	2.5	32	$\gamma(c) \gamma'(c)$	- 1.0	- 3.1
13	$\beta_i \beta_{i+2}$	- 1.9	- 1.9*	33	ϕ	4.0	4.1
14	$\beta_i \beta_{i+3}$	- 2.7	- 2.7*	34	$\phi_i \phi_{i+1}$	- 0.6	- 0.4
15	$\beta(c)_i \beta_{i+1}$	1.8	- 3.1	35	$\gamma_i \phi_i$	1.5	1.4
16	$\beta(c)_i \beta_{i+2}$	- 1.4	- 1.4*	36	$\gamma_i(c) \phi_i$	1.9	1.6
17	$\beta(c)_i \beta_{i+3}$	- 2.0	- 2.0*				
18	$\alpha_i R_i$	31.6	23.5				
19	$\beta_i R_i$	33.6	33.6*				
20	$\beta_i(c) R_i$	24.6	48.6				

* - Force constants not perturbed.

$R_i R_{i+1} = -R_i R_{i+2} = R_i R_{i+3}$

C-C stretch values after perturbation

ortho	729.7
meta	618.0
para	716.6
average	688.1

All values in units of Nm^{-1}, Nm^{-1} rad^{-1} or Nm^{-1} rad^{-2} as appropriate.

The force constants before and after perturbation are given in Table 3.4.

The value for the intra-ring C-C stretch is lowered as expected because of the adjustment in the bond length made during the calculation. However the average of new values is close to the old value. The inter-ring force constant increased even higher than before and is greater than would be expected from the bond length. It is thought that this discrepancy is due to the steric repulsions between the ortho hydrogens.

The interaction constant $\gamma(c)\ \gamma'(c)$ became increasingly negative. As will be explained later this constant is only valid for the planar molecule.

The remaining constants show no untoward changes.

There are two further improvements which could be made to the force field. The restriction,

$$R_i\ R_{i+1} = -R_i\ R_{i+2} = R_i\ R_{i+3}$$

could be lifted, and some allowance could be made for the steric interaction between the ortho hydrogens in the planar molecule. It would be useful if this interaction could be expressed in terms of the force constants already used to describe the molecule.

Earlier work on substituted benzenes[73] suggested that

$$R_i\ R_{i+1} > |R_i\ R_{i+2}| \sim R_i\ R_{i+3}$$

but the results were unstable.

3.5 Preparation of 4-4' difluorobiphenyl d[8]

The preparation was carried out starting with biphenyl d[10].

Dinitro biphenyl

A mixture of fuming nitric acid (37 ml) and concentrated nitric acid (183 ml) was heated to about 40°C and biphenyl d^{10} (10 g) was added in six portions at 15 minute intervals. The mixture was slowly cooled to about 20°C, filtered and the solid washed with concentrated nitric acid, water and finally with methanol. The product was dried to yield 3.65 g 4-4' dinitro biphenyl d^8.

4-4' diamino biphenyl d^8

4-4' dinitro biphenyl d^8 (3.65 g), tin (4 g), hydrochloric acid (25 ml) and ethanol (200 ml) were refluxed for three hours during which time the colour changes from pale yellow to orange yellow to yellow. The mixture was cooled in an ice-bath and the solution of product decanted off the excess tin.

4-4' difluoro biphenyl

Benzidine d^8 (3.3 g), concentrated hydrochloric acid (10 ml) and water (10 ml) was cooled in a freezing mixture. Sodium nitrite (2.1 g) in water (4 ml) was added dropwise. Sodium borofluoride (5 g) in water (10 ml) was then added and a cream precipitate of bisdiazonium borofluoride was formed. This was dried and heated to 150°C to convert the product to 4-4' difluoro biphenyl d^8. This was recrystallised from ethanol and further purified by sublimation. The yield for the fluorination was between 80 and 90 per cent.

3.6 Frequency assignment of 4-4' difluoro biphenyl d^8.

The infrared and Raman spectra were run on the 4-4' difluoro-biphenyl prepared as above. A Raman spectrum was run of the solid in a capillary tube and of solutions in carbon disulphide, carbon

tetrachloride and in benzene. Infrared spectra were run as a CsI disc, a solidified melt and as solutions in carbon disulphide and cyclohexane. The range 3000 - 200 cm^{-1} were scanned for all spectra.

In addition to the information obtained on the frequency shifts on going from solid to solution information is obtained which helps in the assignment of the bands.

A group

The A_g group appears in the Raman spectrum and both A_g and A_u appear in the Raman in solution and the bands are polarised. There is little frequency shift on changing from solid to solution.

B_1 group

The B_{1g} group appears in the Raman and the B_{1u} appears in the infrared. Both appear in the Raman and infrared solution spectra. Frequency shifts are expected on changing from solid to solution for those bands whose frequencies lie below 1000 cm^{-1}.

B_2 group

In solution the selection rules are relaxed so that both B_{2u} and B_{2g} modes become infrared and Raman active. Frequency shifts are expected as above.

B_3 group

As with the B_2 group the selection rules are relaxed in solution. Both groups appear in the Raman and infrared spectra. Little frequency shift is expected here. The solid infrared spectra is interesting because the relative intensity of the B_{3g} group bands depend on whether a disc or solidified melt is run. The B_{3u} modes can be identified by their reduction in intensity on going from the

Fig. 3.3 . Partial infrared spectrum of difluoro biphenyl d^8.

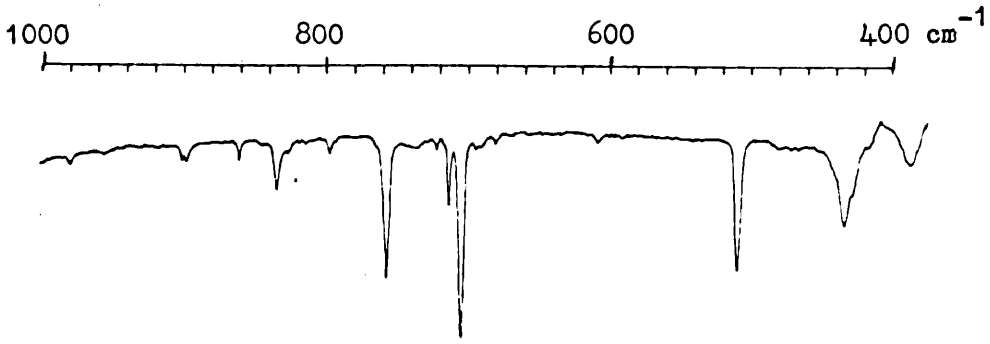

a) Solid (CsI disc).

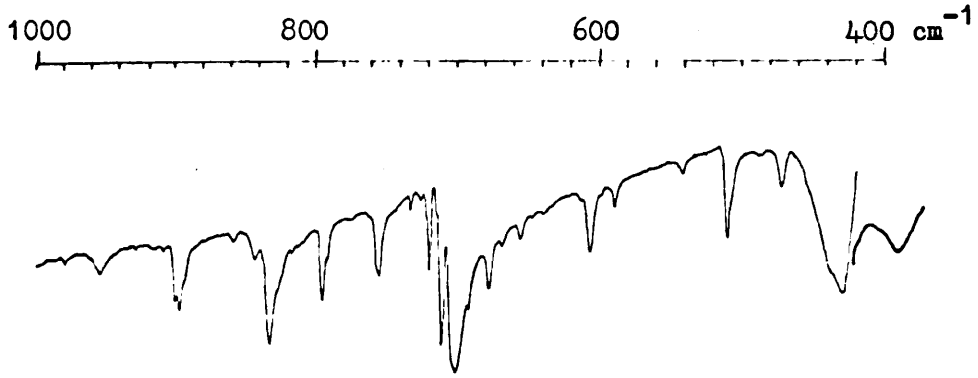

b) Solidified melt.

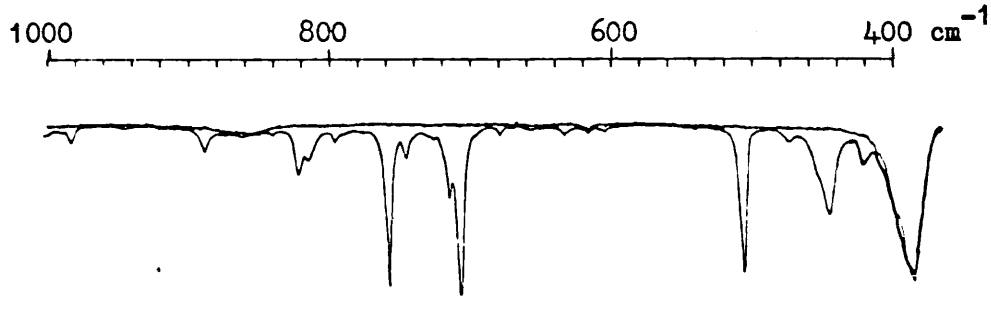

c) Solution in CS_2.

Fig. 3.4. Demonstration of the motions associated with certain interaction force constants.

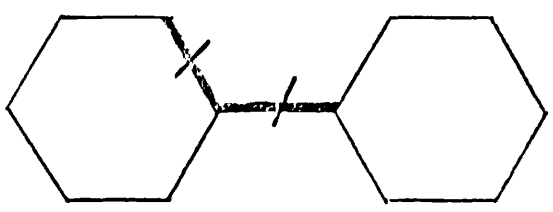

$r(c)_i\ R_i$

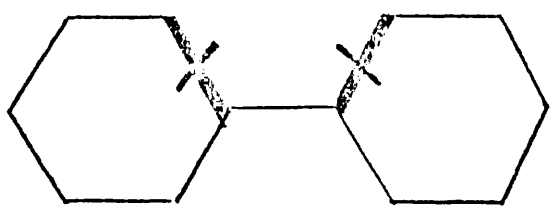

$R_i\ R'_{i+1}$

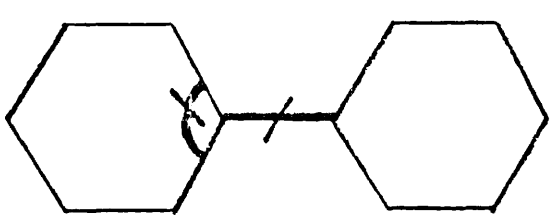

$r(c)_i \propto_i$

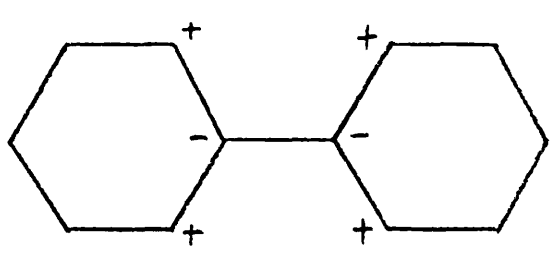

$\gamma_i(c)\ \gamma'_i(c)$

disc to the solidified melt. This is because in the disc the orientation of the biphenyl molecules is random whereas in the solidified melt the molecules crystallise with the long axis perpendicular to the plane of major crystal growth.

Fig. 3.3 shows a partial infrared spectrum of 4-4' difluoro biphenyl run as a CsI disc, solidified melt and as a solution in carbon disulphide.

In order to help assign the bands an initial set of frequencies were calculated for various dihedral angles using the refined set of force constants for biphenyl where appropriate. The force constants peculiar to the fluorine substitution were taken from previous work on fluorobenzenes.[70, 73]

As expected the frequencies of groups A and B_3 were independent of the dihedral angle but the majority of those of groups B_1 and B_2 were dependent. It is expected that when the dihedral angle is 90° and the symmetry is D_{2d} the frequencies for groups B_1 and B_2 are degenerate. This was not found to be so and the error arises from one of the interaction force constants introduced in the previous work on biphenyl.[65] Fig. 3.4 illustrates the four interaction coordinates introduced in the previous work. These are valid in the planar case but when the dihedral angle is non-zero the interaction constant ($\gamma_i(c)\ \gamma'_i(c)$) is not valid. It was therefore necessary to set this constant to zero in the subsequent work. This means the calculations in the previous biphenyl work is inaccurate and consequently so is the present biphenyl work. However, in the work on the fluorinated molecules, the results do not include this constant.

Table 3.5 Assignment of 4-4' difluoro biphenyl frequencies between between 1600 cm^{-1} and 200 cm^{-1}

Raman		Infrared		Assignment
Solid	Liquid	Solid	Liquid	
1585 (w)	1585 (vs)			A_g/B_{1g}
		1576 (vs)	-	B_{3u}
		1555 (m)	-	B_{2u}
1453 (m)	1458 (s)			A_g
		1397 (vs)	1398 (vs)	B_{3u}
		1330 (w)	-	B_{2u}
1284 (w)	1288 (w)			B_{1g}
1255 (s)	1253 (s)			A_g
1241 (m)	1237 (m)			
		1192 (vs)	1196 (m)	B_{2u}
		1156 (vs)	1159 (m)	B_{3u}
1140 (m)	1139 (w)			A_g
		1011 (m)	-	B_{2u}
		980 (w)	983 (w)	B_{3u}
884 (m)	880 (s)			A_g
		862 (m)	-	B_{3u}
850 (m)	848 (m)			A_g
		835 (s)	-	B_{1u}
		827 (m)	823 (m)	B_{3u}
810 (s)	794 (vs)			A_g
		798 (m)	797 (vw)	B_{2u}
	779 (w)			A_u
		757 (vs)		B_{3u}
		705 (vs)	708 (s)	B_{1u}

Table 3.5 (continued)

Raman		Infrared		
Solid	Liquid	Solid	Liquid	Assignment
638 (m)	638 (m)			A_g
626 (m)	621 (m)			B_{1g}
	611 (w)			A_u
		609 (w)	605 (vw)	B_{2u}
		509 (s)	507 (s)	B_{3u}
457				B_{2g}
		436 (s)	447 (s)	B_{1u}
-	402 (m)			A_u
		392 (m)		B_{2u}
			349 (w)	B_{1g}
275 (s)	261 (s)			A_g
		272 (m)	246 (w)	B_{1u}

After the first perturbation it was noted that a few of the calculated frequencies were in poor agreement with the experimental frequencies. The spectra were re-examined and the assignments were adjusted in the light of the new information. The perturbation was repeated using the new assigned frequencies.

A_g modes are recognised by their appearance in the Raman solid and liquid spectra, the bands being polarised in the latter. It was necessary to assign the bands at 1255 and 1241 cm^{-1} as a fermi resonance pair. The fit for this pair was still poor, the calculated band being at 1288 cm^{-1}. Otherwise the calculated bands are in good agreement, the worst showing a difference of 14 cm^{-1}. The intensity of these bands are moderate or strong.

A_u modes are only observable in solution in the Raman spectrum where they are polarised. The fit is good and the intensities are fairly weak.

The B_{1g} modes are difficult to assign because they are not easily identified in the way that A and B_{3u} modes are. Only four frequencies were assigned one of which did not appear in either Raman spectra but appeared in the infrared liquid spectrum. The band at 1585 cm^{-1} was 46 cm^{-1} higher than the calculated frequency, but there is no other band in the Raman spectrum in this region. The band is doubly assigned to the A_g group and this latter assignement is almost certainly correct. However the band has a doublet structure which may be caused by the B_{1g} mode. The corresponding mode in the undeuterated molecule shows a much better fit and so the assignment is in considerable doubt.

B_{1u} modes appear in the infrared spectra. Only two bands were not assigned one of which was below 200 cm^{-1} which was not measured.

Table 3.6 Comparison between observed and calculated frequencies of planar 4-4' difluoro biphenyl

	observed	calculated	
A_g	-	3105	
	-	3094	
	1603	1603	0
	1529	1526	-3
	1323	1314	-9
	1277	1261	-16
	1169	1168	-1
	1017	1036	+19
	846	841	-5
	660	655	-5
	277	273	-4
A_u	-	982	
	-	741	
	-	468	
B_{1g}	-	3101	
	-	3090	
	1554	1563	+9
	-	1377	
	1257	1270	+13
	1245	1241	-4
	1098	1081	-17
	627	638	+11
	464	460	-4
	340	342	+2

Table 3.6 (continued)

	observed	calculated	
B_{1u}	-	970	
	822	827	+5
	702	693	-9
	-	486	
	283	270	-13
	71	70	-1
B_{2u}	-	3101	
	-	3090	
	1585	1597	+12
	1393	1382	-11
	1317	1325	+8
	1286	1264	-22
	-	1053	
	642	638	-4
	414	413	-1
	84	85	+1
B_{2g}	938	963	+25
	-	845	
	722	707	-15
	540	528	-12
	395	389	-6
	180	176	-4

Table 3.6 (continued)

	observed	calculated	
B_{3u}	-	3104	
	-	3093	
	1600	1602	+2
	1495	1495	0
	1235	1266	+31
	1158	1167	+9
	1016	1014	-2
	1007	996	-11
	804	786	-18
	518	523	+5
B_{3g}	966	982	+16
	-	741	
	-	468	

The observed frequencies were given a weighting of 1.0. The remainder were given a weighting of 0.0, which means that the frequency takes no part in the calculation and can be given any value. The final column shows the differences between the observed and calculated frequencies.

Table 3.7 Comparison between the experimental and calculated frequencies of planar 4-4' difluoro biphenyl d^8.

	Experimental frequencies		Calculated frequencies	
A_g	-	0.0	2302	
	-	0.0	2288	
	1585	1.0	1593	+8
	1453	1.0	1439	-14
	1255	1.0	1288	+33
	1140	1.0	1135	-5
	884	1.0	895	+11
	850	1.0	839	-11
	810	1.0	799	-11
	638	0.5	625	-13
	275	1.0	268	-7
A_u	779	1.0	777	-2
	611	1.0	612	+1
	402	1.0	395	-7
B_{1g}	-	0.0	2291	
	-	0.0	2278	
	1585	0.2	1539	-46
	1284	1.0	1276	-8
	-	0.0	1198	
	-	0.0	1010	
	-	0.0	818	
	626	0.2	618	-8
	-	0.0	430	
	349	0.3	335	-14

Table 3.7 (continued)

	Experimental frequencies		Calculated frequencies	
B_{1u}	-	0.0	780	
	705	1.0	705	0
	-	0.0	590	
	436	1.0	431	-5
	272	1.0	270	-2
	-	0.0	69	
B_{2u}	2298	1.0	2291	-7
	2272	1.0	2279	+7
	1555	1.0	1578	+23
	1330	1.0	1333	+3
	1194	0.2	1186	-8
	1011	1.0	1016	+5
	798	1.0	810	+12
	609	1.0	618	+9
	392	1.0	395	+3
	-	0.0	81	
B_{2g}	-	0.0	775	
	-	0.0	716	
	-	0.0	638	
	457	0.3	453	-4
	-	0.0	381	
	-	0.0	173	

Table 3.7 (continued)

	Experimental frequencies		Calculated frequencies	
B_{3u}	-	0.0	2299	
	-	0.0	2285	
	1576	1.0	1589	+13
	1397	1.0	1390	-7
	1156	1.0	1149	-7
	980	0.2	971	-9
	862	1.0	864	+2
	827	1.0	829	+2
	757	1.0	751	-6
	509	1.0	517	+8
B_{3g}	-	0.0	777	
	-	0.0	612	
	-	0.0	395	

The second column shows the weighing factors used for the observed frequencies.

The highest of these frequencies is in poor agreement and may be wrong.

The B_{2u} modes in the region measured were all assigned from the solid infrared although not all these appeared in the infrared liquid spectra. Apart from a disagreement of 23 cm^{-1} the frequencies are in good agreement with the calculated ones.

Only one B_{2g} mode was assigned.

The intensity of B_{3u} modes decreases on going from disc spectra to solidified melt spectra and the bands were assigned on this basis. None of the B_{3g} frequencies were assigned.

The number of spectra which could be run and the number of times the sample could be purified was limited by the small quantity of material available, due to the high cost of preparation.

The frequencies of 4-4' difluoro biphenyl have already been assigned[4] and the experimental frequencies are compared with the calculated frequencies in Table 3.6.

The frequencies compare quite well and only three modes show a difference of more than 20 cm^{-1}. These are the B_{2u} mode at 1286 cm^{-1} (22 cm^{-1}), the B_{2g} mode at 938 cm^{-1} (25 cm^{-1}) and the B_{3u} mode at 1235 cm^{-1} (31 cm^{-1}). Generally the fit has considerably improved during perturbation.

The experimental data is listed in Table 3.5 the experimental and calculated frequencies are listed in Table 3.7 and the force constants before and after perturbation are listed in Table 3.9.

The increase in the inter-ring C-C stretch force constant and of the interaction constant involving the inter-ring stretch and an adjacent C-C stretch $(r(c)_i R_i)$ may indicate that the structure

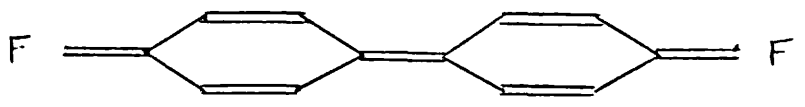

Table 3.8 Comparison between computed and experimental data for 4-4' difluoro biphenyl d^8

A species (A_g and A_u when $\theta = 0^\circ$)

	Frequencies calculated for all θ	Experimental frequencies: Raman Solid	Raman Liquid (ρ)	Infrared Solid	Infrared Liquid
A_g	2302	-	-		
	2288	-	-		
	1593	1585 (w)	1585 (0.41) (vs)		
	1439	1453 (m)	1458 (0.43) (s)		
	1288	1255 (s) 1241 (m)	1253 (0.05) (s) 1237 (0.00) (m)		
	1135	1140 (m)	1139 - (w)		
	895	884 (m)	880 (0.00) (s)		
	839	850 (m)	848 (0.20) (m)		
	799	810 (s)	794 (0.00) (vs)		
	625	638 (m)	638 (0.46) (m)		
	268	275 (s)	261 (0.17) (s)		
A_u	777	-	779 (0.00) (w)		
	612	-	611 (0.60) (w)		
	395	-	402 (0.67) (m)		

Table 3.8 (continued)

B_1 species (B_{1g} and B_{1u} when $\theta = 0^\circ$)

	Frequencies calculated for dihedral angles of					Experimental frequencies			
						Raman		Infrared	
	0°	30°	45°	60°	90°	Solid	Liquid	Solid	Liquid
B_{1g}	2291	2291	2291	2291	2291	-	-		
	2278	2278	2278	2278	2278	-	-		
	1539	1541	1543	1546	1554	1585(w)	1586(s)		
	1276	1279	1283	1288	1302	1284(w)	1288(w)		
	1198	1197	1196	1194	1191	-	-		
	1010	1010	1010	1010	1010	-	-		
	818	818	818	818	816	-	-		
	618	618	618	619	624	626(m)	621(m)		
	430	417	413	409	404	-	-		
	335	347	355	362	372	-	-		349(w)
B_{1u}	780	779	778	777	775			835(s)	-
	705	706	707	709	713			705(vs)	708 (s)
	590	593	597	603	613			-	-
	431	450	460	468	473			436(s)	447(s)
	270	253	239	225	202			272(m)	246(w)
	69	70	70	71	73			-	-

Table 3.8 (continued)

B_2 species (B_{2u} and B_{2g} when $\theta = 0^\circ$)

	Frequencies calculated for dihedral angles of					Experimental frequencies Raman		Infrared	
	0°	30°	45°	60°	90°	Solid	Liquid	Solid	Liquid
B_{2u}	2291	2291	2291	2291	2291			2298(w)	-
	2279	2279	2279	2279	2278			2272(w)	-
	1578	1574	1570	1565	1554			1555(m)	-
	1333	1329	1324	1318	1302			1330(w)	-
	1186	1186	1187	1188	1191			1194(vs)	1196(m)
	1016	1015	1014	1013	1010			1011(m)	
	810	811	812	814	816			798(m)	797(vw)
	618	617	617	616	613			609(w)	605(vw)
	395	397	397	400	404			392(m)	-
	81	80	78	76	73			-	-
B_{2g}	775	774	774	774	775	-	-		
	716	716	716	715	713	-	-		
	638	636	635	632	624	-	-		
	453	457	462	467	473	457	-		
	381	380	379	377	372	-	-		
	173	176	180	186	202	-	-		

Table 3.8 (continued)

B_3 species (B_{3u} and B_{3g} when $\theta = 0^\circ$)

	Frequencies calculated for all θ	Experimental frequencies			
		Raman		Infrared	
		Solid	Liquid	Solid	Liquid
B_{3u}	2299			-	-
	2285			-	-
	1589			1576(vs)	-
	1390			1397(vs)	1398(vs)
	1149			1156(vs)	1159(m)
	971			980(w)	983(w)
	864			862(m)	-
	829			827(m)	823(m)
	751			757(vs)	758(s)
	517			509(s)	507(s)
B_{3g}	777	-	-		
	612	-	-		
	395	-	-		

Table 3.9 Force constants used for 4-4' difluoro biphenyl d^8 calculation before and after perturbation.

		Before	After			Before	After
1	R	657.4	661.3	21	$\alpha_i r_i$	- 1.0	- 15.8
2	r(c)	653.3	716.7	22	$\alpha_i \beta_{i+1}$	4.2	- 2.2
3	$R_i R_{i+1}$	48.1	49.9	23	$\alpha_i \beta(c)_{i+1}$	3.8	- 6.5
4	$r(c)_i R_i$	34.0	70.8	24	γ	25.9	25.9
5	$R_i R'_{i+1}$	26.2	43.5	25	γ (c)	14.8	11.2
6	$r(c)_i \alpha_i$	- 90.1	- 81.3	26	$\gamma_i \gamma_{i+1}$	0.8	- 1.6
7	r	512.3	526.0	27	$\gamma_i \gamma_{i+2}$	- 0.8	- 2.8
8	α	57.2	69.7	28	$\gamma_i \gamma_{i+3}$	- 1.4	0.8
9	$\alpha_i \alpha_{i+1}$	- 5.0	4.5	29	$\gamma_i(c)\gamma_{i+1}$	0.9	3.8
10	β	89.0	89.4	30	$\gamma_i(c) \gamma_{i+2}$	- 2.2	0.8
11	β(c)	73.6	62.6	31	$\gamma_i(c) \gamma_{i+3}$	1.0	1.8
12	$\beta_i \beta_{i+1}$	2.5	6.7	32	γ (c) γ'(c)	- 3.1	0.0
13	$\beta_i \beta_{i+2}$	- 1.9	- 2.0	33	ϕ	4.1	1.7
14	$\beta_i \beta_{i+3}$	- 2.7	- 2.6	34	$\phi_i \phi_{i+1}$	- 0.4	- 2.4
15	$\beta(c)_i \beta_{i+2}$	- 3.1	- 9.2	35	$\gamma_i \phi_i$	1.4	2.7
16	$\beta(c)_i \beta_{i+2}$	- 1.4	0.4	36	$\gamma_i(c) \phi_i$	1.6	- 1.9
17	$\beta(c)_i \beta_{i+3}$	- 2.0	- 8.9	37	r(f)	585.0	509.7
18	$\alpha_i R_i$	23.5	41.5	38	β(f)	110.7	104.2
19	$\beta_i R_i$	33.6	26.8	39	α(f)	68.1	98.4
20	$\beta_i(c) R_i$	48.6	61.9	40	γ(f)	24.8	25.1
				41	ϕ(f)	3.6	10.7

C-C stretch values after perturbation

ortho	734.0
meta	621.6
para	720.8
average	692.1

Units as in Table 3.4.

is more important in the fluorinated molecules. The C-F stretch force constant decreased, however, which is not consistent with the above, but it must be remembered that the force constant has been transferred from a different environment and firm conclusions cannot be drawn from the change. The increase in the inter-ring bond order may explain the increase in constants 4 and 5.

The large negative value of interaction constant $r(c)_i \alpha_i$ may be explained as follows. The change from sp^3 to sp^2 to sp hybridisation results in an opening of the bond angles at the carbon atom. Thus opening the bond angle results in more p character being available in the bond along the angle bisector. An increase in the p character of a bond is accompanied by an increase in bond length. It follows that it is energetically favourable to simultaneously increase both distortions. Therefore the potential energy element $f_{ij} \Delta\alpha_i \Delta R_i$ is negative and hence f_{ij} is negative.

Although there are other force constant differences between the fluorinated and non-fluorinated molecules it is not possible to draw any conclusions from these without further investigation.

3.7 Some relationships between the frequencies of related molecules

Because it is often difficult to assign the frequencies of complex molecules the following relationships may be used if data is available from related molecules. The relationships between the molecules depend on whether they are isotopically related or not. For example, in the current work, biphenyl is isotopically related to biphenyl d^{10} but not to 4-4' difluoro biphenyl.

a) Redlich-Teller Product Rule

This rule relates the product of the frequencies of a given species of a molecule to the product of the corresponding frequencies of some isotopically related molecule. The ratio is a function of the molecular geometry and the nuclear masses. The relationship derived assumes that the force field for the isotopically related molecules is identical but by modifying the expression a relationship between non-isotopically related molecules can be derived. This modification involves the ratio between the R-X and R-Y stretch force constants where X and Y are the non-isotopically related atoms. Agreement between experimental and calculated ratios to within 4 per cent is considered acceptable.

b) The Sum Rule

This relationship involves the sum of the squares of the frequencies of three or more isotopically related molecules. The rule states that if several isotopic systems can be geometrically superimposed with appropriate signs in such a way that the atoms vanish in all positions then the corresponding linear combination of the sums of the squares of the frequencies will vanish in the harmonic approximation. The sums may be taken independently over the frequencies of the symmetry classes of the sub-group arising from the symmetry elements common to all superimpositions of the molecules.

Extending to molecules which are not isotopically related, the rule appears to hold quite well as long as the rates of change of force constants with perturbing influence are uniform throughout the series under consideration.

Table 3.10 List of ratios required to check assignments using the Redlich-Teller Product Rule

		$\frac{F^0d^0}{F^0d^{10}}$	$\frac{F^2d^0}{F^2d^8}$	$\frac{F^0d^0}{F^2d^0}$	$\frac{F^0d^{10}}{F^2d^8}$
A_g	C	5.643	3.995	3.707	2.623
	O	5.729	3.947	3.775	2.601
A_u	C	1.810	1.813	1.006	1.007
	O	1.810	1.780	1.006	0.989
B_{1g}	C	5.332	3.905	3.459	2.533
	O	5.071	3.529	3.516	2.446
B_{1u}	C	2.734	1.960	3.039	2.178
	O	2.149	2.059	2.709	2.595
B_{2u}	C	5.450	3.941	4.164	3.011
	O	5.203	4.188	3.812	3.069
B_{2g}	C	2.571	1.967	2.902	2.221
	O	2.827	2.063	3.067	2.238
B_{3u}	C	5.460	3.918	3.689	2.647
	O	5.334	3.888	3.634	2.649
B_{3g}	C	1.810	1.813	1.006	1.007
	O	1.857	1.783	0.978	0.939

F^0d^0 - biphenyl F^0d^{10} - biphenyl d^{10}

F^2d^0 - 4-4' difluoro biphenyl

F^2d^8 - 4-4' difluoro biphenyl d^8

C - Calculated O - Observed

Table 3.11 List of ratios obtained by dividing the calculated by observed values in the previous table.

	$\frac{F^0d^0}{F^0d^{10}}$	$\frac{F^2d^0}{F^2d^8}$	$\frac{F^0d^0}{F^2d^0}$	$\frac{F^0d^{10}}{F^2d^8}$
A_g	0.985	1.012	0.982	1.008
A_u	1.000	1.019	1.000	1.018
B_{1g}	1.051	1.107	0.984	1.036
B_{1u}	1.272	0.952	1.122	0.839
B_{2u}	1.047	0.941	1.092	0.981
B_{2g}	0.909	0.953	0.946	0.992
B_{3u}	1.024	1.008	1.015	0.999
B_{3g}	0.975	1.017	1.029	1.072

c) Rayleigh's Rule and the Inequality Rule

Rayleigh's rule states that increasing any mass in a periodically vibrating system without changing the force field must decrease all frequencies. Thus the j^{th} highest frequency of any symmetry species of a deuterated molecule must lie below the j^{th} highest frequency of the non-deuterated molecule.

The Inequality rule is an extension of this. Consider two molecules RX and RY, the mass of X being greater than that of Y. Then in any given symmetry class of RX containing "a" modes associated with the RX bond, the j^{th} highest frequency lies between the j^{th} and $(j + a)^{th}$ highest frequencies of the equivalent symmetry class of RY.

In the case of non-isotopically related molecules, experience has shown that the rule holds apart from minor infringements.

The Isotope rule was used when assigning the frequencies of 4-4' difluoro biphenyl d^{10} and the Product rule was used to check the frequencies of the four molecules considered during this work. The ratios required to use the Product rule were not calculated from first principles but were obtained from the calculated frequencies produced by the computer. The experimental ratios were derived from the experimental frequencies where available otherwise the equivalent calculated frequencies were used. The ratios derived from the observed and calculated frequencies are listed in Table 3.10. and the ratios between the observed and calculated values are listed in Table 3.11. The underlined values may be considered to be in poor agreement.

These arise from discrepancies between the products of the calculated and observed frequencies. These do not indicate a generally bad assignment. For biphenyl the B_{2u} and B_{2g} groups show a discrepancy

Fig. 3.5. Plot of frequency shift against dihedral angle for two modes of 4 - 4' difluoro biphenyl d^8.

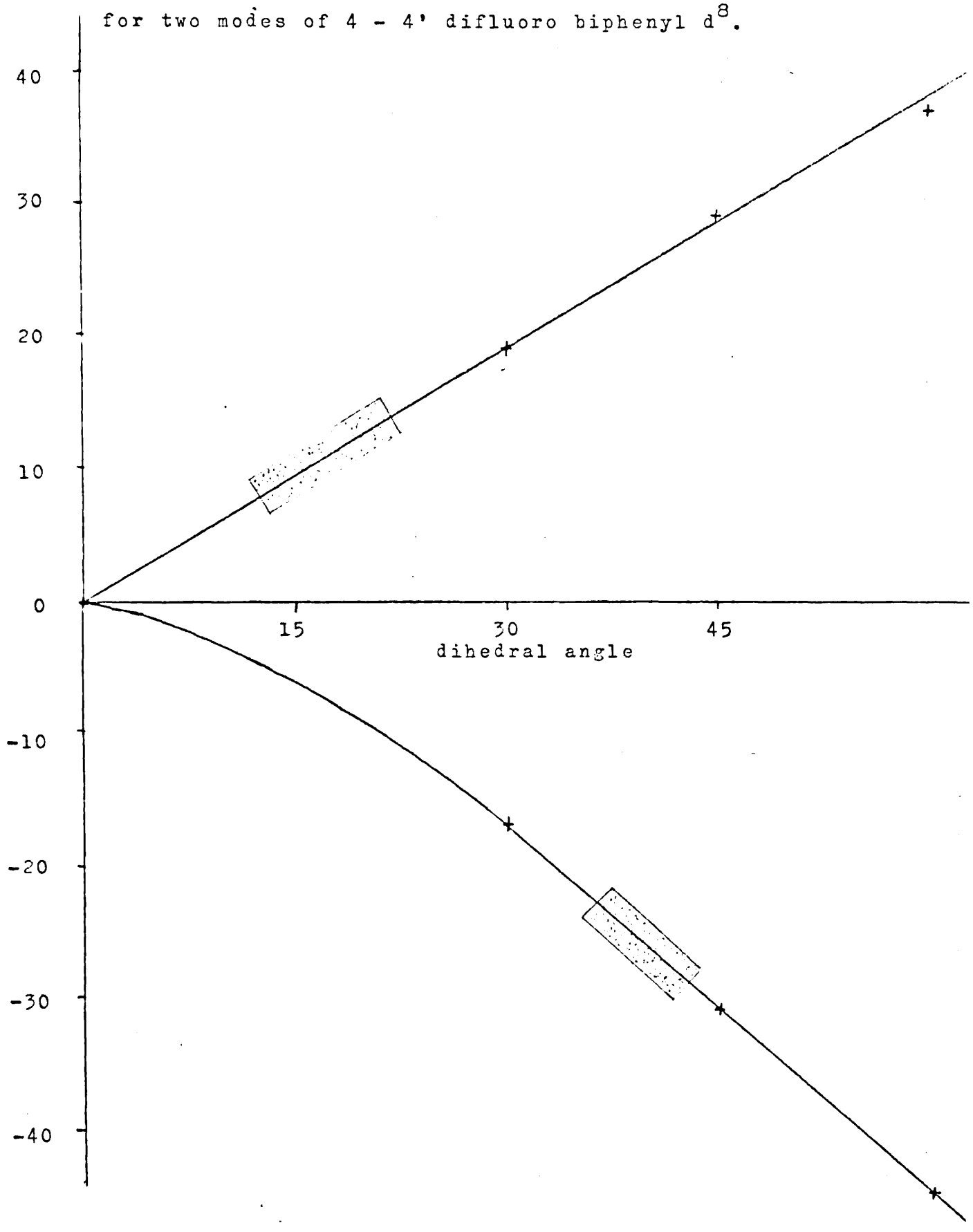

B_{1u} bands calculated at 431 and 270 cm^{-1}.

of greater than 5 per cent. The B_{2u} frequency observed at 1568 cm^{-1} is calculated 61 cm^{-1} away at 1529 cm^{-1}. If the calculated frequency is used instead to calculate the observed product the discrepancy is less than 5 per cent. The error in the B_{2g} products arises from a difference of 21 cm^{-1} between observed and calculated for the lowest frequency in the group. Large errors are exaggerated in low frequency modes using this method and this is the reason for the discrepancy in a number of groups.

The other groups with worse than 5 per cent fit are biphenyl d^{10} (B_{1g}, B_{1u}, B_{3g}) 4-4' difluoro biphenyl (B_{1u}, B_{2g}) and 4-4' difluoro biphenyl d^{8} (B_{1g}, B_{2u}).

3.8 Calculation of the dihedral angle

It was only possible to obtain both solid and liquid frequencies for two of the bands where there is a considerable dihedral angle dependence. The frequencies calculated for different dihedral angles were used to prepare Fig. 3.5 from which the dihedral angles were measured. The two values are not consistent and for a more accurate result data from 4-4' difluoro biphenyl and possibly other deuterated derivatives would be necessary. However the average is similar to that derived for biphenyl and shows that the fluorine atoms have no profound effect on the conformation of the molecule.

Dihedral angle (1)	17.3°
Dihedral angle (2)	39.4°
Average angle	28.4°

CHAPTER FOUR

BAND SHAPE ANALYSIS OF THE γ_{CH} MODE OF p-DIFLUOROBENZENE

4.1 Introduction

Vibrational band shapes are known to be a valuable source of information on molecular dynamics. We study the relaxation of the vibrational-transition moment using the Fourier transform relation

$$\langle \mu(0).\mu(t) \rangle = \frac{9ch}{8\pi^3} \int_{band} \Gamma(\omega) \exp(2\pi i c \bar{\omega} t)\, d\bar{\omega}$$

μ - transition operator

ω - frequency shifts from the pure vibrational-transition frequency ($\bar{\omega}$)

$\Gamma(\omega)$- intensity of absorbtion at frequency ω

By normalising the band intensity to unity, attention is focussed on the time decay of the correlation functions. Such normalised correlation functions, C(t), are directly comparable between different molecular species and different environmental situations of the molecules. For a symmetrical band the above equation may be rewritten

$$C'(t) = \int_{band} \Gamma'(\bar{\omega}) \cos(2\pi \bar{\omega} c t)\, d\bar{\omega}$$

where the primes denote normalised quantities.

The application of correlation functions to vibrational transitions is mainly due to R.G. Gordon.[74-7] Gordon analysed the vibrational rotation band of carbon monoxide as measured in a variety of solvents. For a low pressure gas the correlation function drops sharply from t = 0 passing to negative values followed in some instances by a return to small positive values (rapidly damped oscillation) and then dropping to zero. The physical explanation of the negative correlation function at short times is that the molecule is freely rotating and at a time of the order of half the rotation period the molecules are predominantly

orientated in the opposite direction to their initial state. As the pressure of gas increases intermolecular collisions lead to a steadily decreasing probability of such coherence of the molecular motions. In solution the rotational mechanism of relaxation becomes largely superseded by collisional reorientation.

The finite breadth of an absorption band can arise from radiation damping, doppler broadening and collisional broadening. The first and third of these lead to a Lorentzian band shape. This band shape leads to an exponential relationship between correlation coefficients and time. However two difficulties arise. Firstly, in the limit as $t \rightarrow 0$ all bands may be shown to have the same limiting behaviour

$$\frac{dC(t)}{dt} \longrightarrow 0 \text{ as } t \rightarrow 0.$$

Secondly, the time scale of infrared spectroscopy is so small that relaxation by free rotational motion is significant. Such relaxation leads to a different form of relationship between $C(t)$ and t from collisional relaxation and is incompatible with a Lorentzian band shape.

Hence the vibrational band shape and the shape of the correlation function depend on molecular reorientations and molecular interactions. If we neglect cross terms we can write the corresponding relaxation function for the rotational and vibrational mechanisms.

$$\Phi(t) = \Phi_R(t)\,\Phi_V(t)$$

If the log of the correlation function is plotted against time the curve may be examined in two parts. Between time zero and about 0.5 ps the graph is curved and relates particularly to rotational relaxation and derives its greatest contribution from the wings of the

band. After about 0.5 ps the graph is essentially straight but with oscillations increasing with time. These oscillations arise from practical limitations due to sampling intervals, the limited range from the band centre which can be studied as well as experimental errors. However, between 0.5 and 3.5 ps the graphs arising from the current work were sufficiently straight for a gradient to be determined and the gradients derived were compared to see the effect of the different conditions applied.

When the spectrum of benzene is recorded in certain solvents a broadening of the band arising from the γ_{CH} mode is noted and of those combination bands associated with it. The band is broader if acetonitrile is used rather than cyclohexane as solvent. The fact that we do not see broadening of any other bands suggests that there is something more specific than a simple polar interaction responsible for the relaxation. If the acetonitrile interacts with the π cloud then we may get a structure as shown in Figure 4.5(b) which involves rehybridisation of the carbon atoms towards sp^3.

This can lead to a specific interaction with the γ_{CH} mode which will be clearly modified by this interaction since it has been shown from intensity studies that there is probably a significant rehybridisation moment associated with the γ_{CH} mode of the order of 0.3 D rad^{-1}.[78, 79]

It has been shown[80] that broadening in benzene is generally proportional to the dipole moment of the solute and that the frequency shift is also proportional for furans, thiophens etc. but not for acetylenes where hydrogen bonding is believed to occur.[81]

The purpose of the current work was to examine the effect of solvent and temperature on the γ_{CH} mode of p-difluorobenzene, using two solvents, cyclohexane and acetonitrile. As is discussed later, it was not possible to use differing proportions of these solvents because of solubility problems.

4.2 Experimental work

The infrared γ mode of p-difluorobenzene was recorded in two solvents, cyclohexane and acetonitrile, at various temperatures. The instrument slit width was approximately 0.8 cm^{-1}. The single absorption was recorded on a Perkin Elmer PE 325 using a RIIC variable temperature cell. The low temperature spectra were recorded using crushed ice as a refrigerant and the temperatures were accurate to within $\pm$ 3°C. The spectra were recorded at the lowest speeds consistent with the cell not leaking. On each chart two spectra were recorded. For the spectrum of p-difluorobenzene in the solvent, a variable path length cell was placed in the reference beam containing the solvent only and the cells were balanced to cancel out the absorptions due to the solvent using a suitable solvent band which did not exhibit total absorption at this path length. This spectrum was used to record the values of I. The background (I_o values) was recorded by filling the sample cell with solvent only and balancing the absorption due to cell and contents with a variable path length cell containing solvent.

Because it was difficult to replace the sample cell in the variable temperature unit exactly as it was before, the two spectra often became parallel in the wings but did not meet. It was therefore necessary to adjust the background such that the value of I_o approached the value of

Fig. 4.1 . Effect of background scaling factor.
p difluoro benzene in acetonitrile at 40°C.

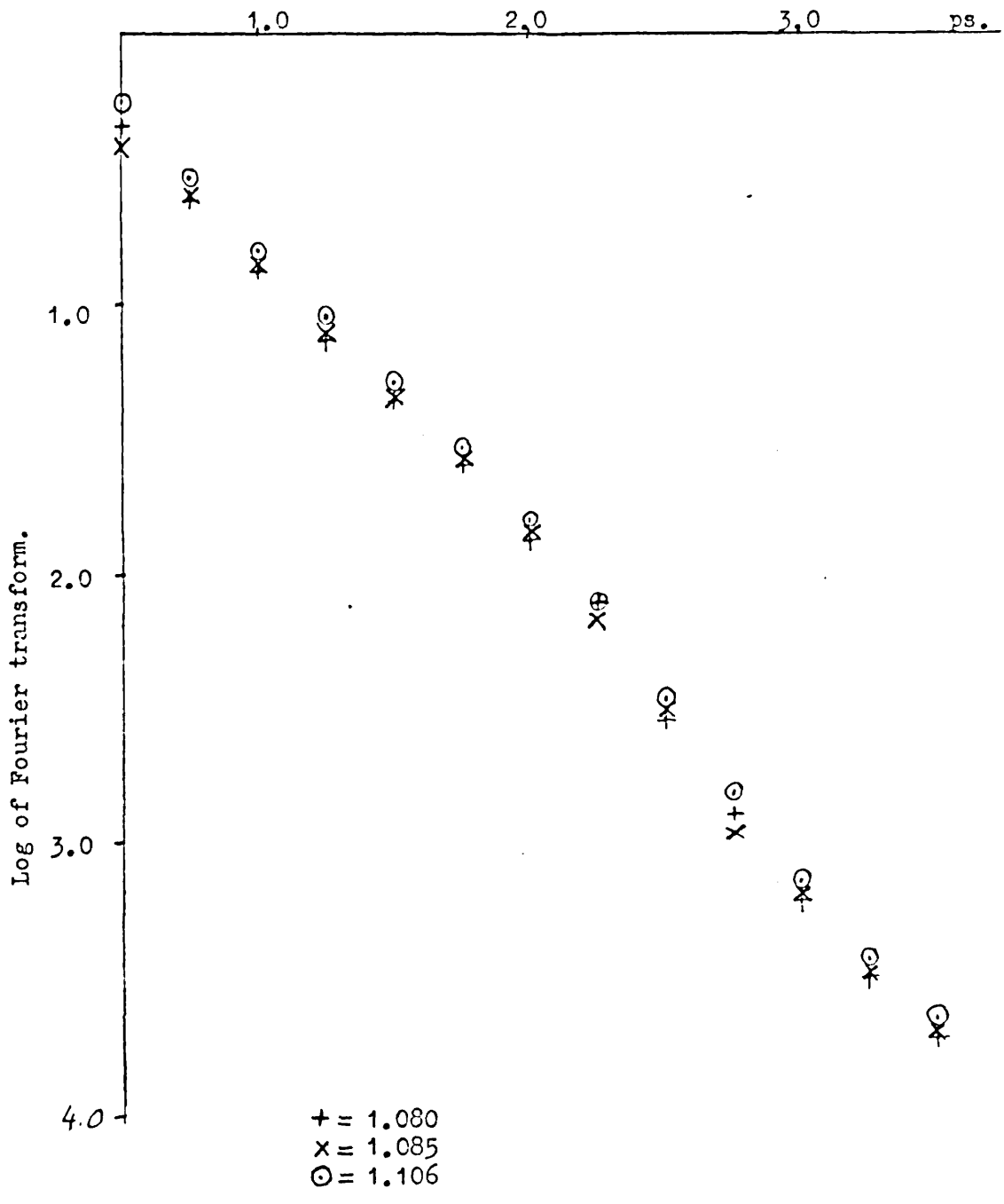

I in the wings. This was done by taking the wing with the closest agreement between I and I_o values and extrapolating the values of I by eye. Where the values of I levelled off to a steady value then the value of I_o/I at this point is used to correct all the other I_o values.

The wings are most affected by inaccuracy in this adjustment and although the wings have relatively little effect on the gradient of the Fourier transform of the band the effect of the error in the background was assessed as follows.

The value of I_o/I was estimated for the band in acetonitrile at 40^oC as 1.085. The Fourier transform was then calculated. Values of 1.080 and 1.106 were also used and the wings extrapolated to zero absorption. If the value of I in the wings was 80.0 per cent the values of I_o would be 86.4 per cent and 88.5 per cent respectively, the original value having been 86.8 per cent. The log of the Fourier transforms against time are compared in Fig. 4.1. As can be seen changing the ratio from 1.080 to 1.106 has little effect on the gradient between 0.5 and 3.5 ps. This is equivalent to changing the background by 2.1 per cent when I is 80 per cent and as the accuracy of I_o will be accurate to within $\pm$ 1 per cent it can be seen that the effect of adjusting the background on the gradient is small.

For all the calculations the values of I and I_o were measured from the chart by hand at 0.4 cm^{-1} intervals. The wings were difficult to measure accurately because of the noise on the spectrum so it was necessary to estimate the extreme parts of these using a relationship derived by I.R. Hill. He has suggested that the parts of the wings furthest from the band centre are exponential. The approximate values for I_o and I were measured and a graph of ln (ln (I_o/I)) against

wavenumber was plotted. The straight part of the graph was extrapolated until ln (ln (I_o/I)) was sufficiently large that I_o/I was less than 1.002. Values of I_o/I were calculated using the straight part of the graph, at 0.4 cm^{-1} intervals and were used instead of the inaccurate experimental values.

Thus the data was subject to the following inaccuracies, in addition to any inaccuracy in measurement caused by noise in the spectrum. Firstly the background was adjusted to match the band in the wings and secondly the wings were adjusted to give an exponential function with respect to wavenumber. The first inaccuracy affects the whole spectrum but particularly the wings and the second only affects the wings. Because the gradient of the log of the Fourier transform between 0.5 and 3.5 ps is mainly affected by the shape of the band near the band centre, these inaccuracies have only a small effect.

Because the intensity of the absorption is high, a short path length was used (2.5×10^{-5}m). It was also necessary to use low concentrations of p-difluorobenzene at which acetonitrile and cyclohexane are immiscible. It was therefore not possible to record the band shape in a mixture of the solvents.

The concentration of p-difluorobenzene was 1.96×10^{-4}M in cyclohexane and 2.75×10^{-4}M in acetonitrile.

In cyclohexane the band centre is at 833.2 cm^{-1} but in acetonitrile the band is broader and the band centre is at 842.8 cm^{-1} at 12°C and at 842.0 cm^{-1} at 50°C. The band in acetonitrile is also unsymmetrical with a small absorption to low wavenumber overlapping with the main band. It is well known that the amount of asymmetry in a band

Fig. 4.2 . p difluoro benzene in acetonitrile at 12°C.

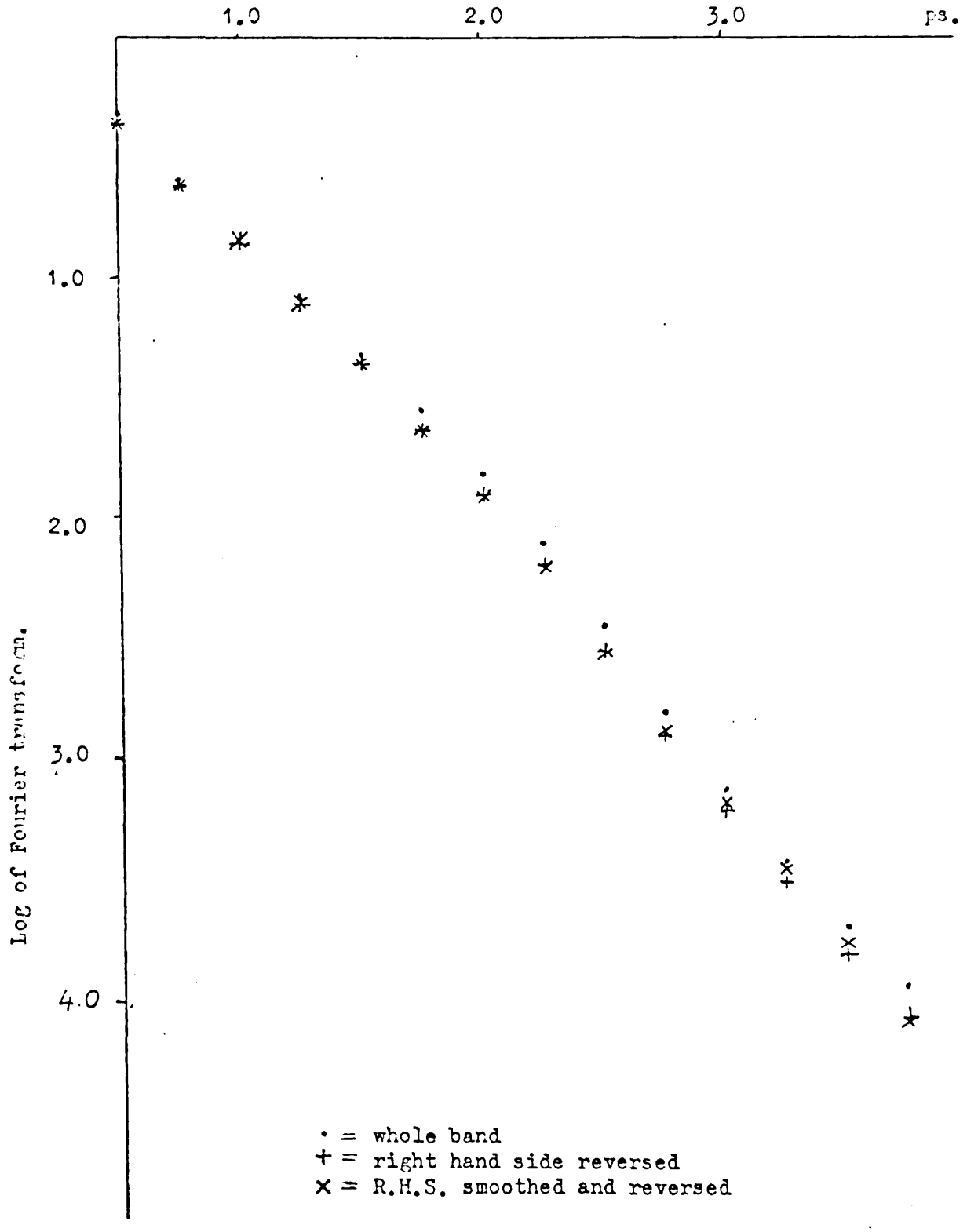

determines the strength of oscillations in the Fourier transform.

In these calculations the complex transform

$$\int \Gamma(\omega) \exp(i\Delta\omega t)\, d\omega$$

was used rather than

$$\int \Gamma(\omega) \cos(\Delta\omega t)\, d\omega$$

which reduces the effect of asymmetry on the two sided transform. For instance, suppose we have an error in the band centre of Δ

$$\int \Gamma(\nu) \exp(-i\, 2\pi(\nu - \nu_0 + \Delta)t)\, d\nu$$

$$\equiv \int \Gamma(\nu) \exp(-i\, 2\pi(\nu - \nu_0)t.\ \exp(-i\, 2\pi\Delta t)\, d\nu$$

If Δ is small then $\exp(-i\, 2\pi\Delta t)$, which is independent of ν, approaches unity and we have the true transform left.

In an attempt to determine the effect of this asymmetry on the Fourier transform the Fourier transform of the band in acetonitrile at 12°C was calculated in three ways. Firstly the whole band was measured up and all the data was used. Secondly the right hand side (lower wavenumber) of the band was reflected about the band centre and this data was used. Thirdly the small band was estimated and was eliminated from the spectrum. The amended right hand side was then reflected about the band centre. Fig. 4.2 shows the effect of these different methods on the log plot of the Fourier transform. As can be seen the improvement achieved by reflection is minimal and the accuracy of measuring the gradient is not improved. There is very little difference between the transform where the small band was eliminated and where it was not. It was therefore decided to use the data from the whole band for the remainder of the calculations.

Table 4.1. Gradient of log of Fourier transform against time in ps^{-1}.

Temp. ^{o}C	in cyclohexane	in acetonitrile
12	-0.405	-1.08
20	-	-1.01
30	-0.438	-1.02
40	-	-1.10
50	-0.504	-1.11

Fig.4.3. p - difluoro benzene in cyclohexane.
Log plot of Fourier transform v. time.

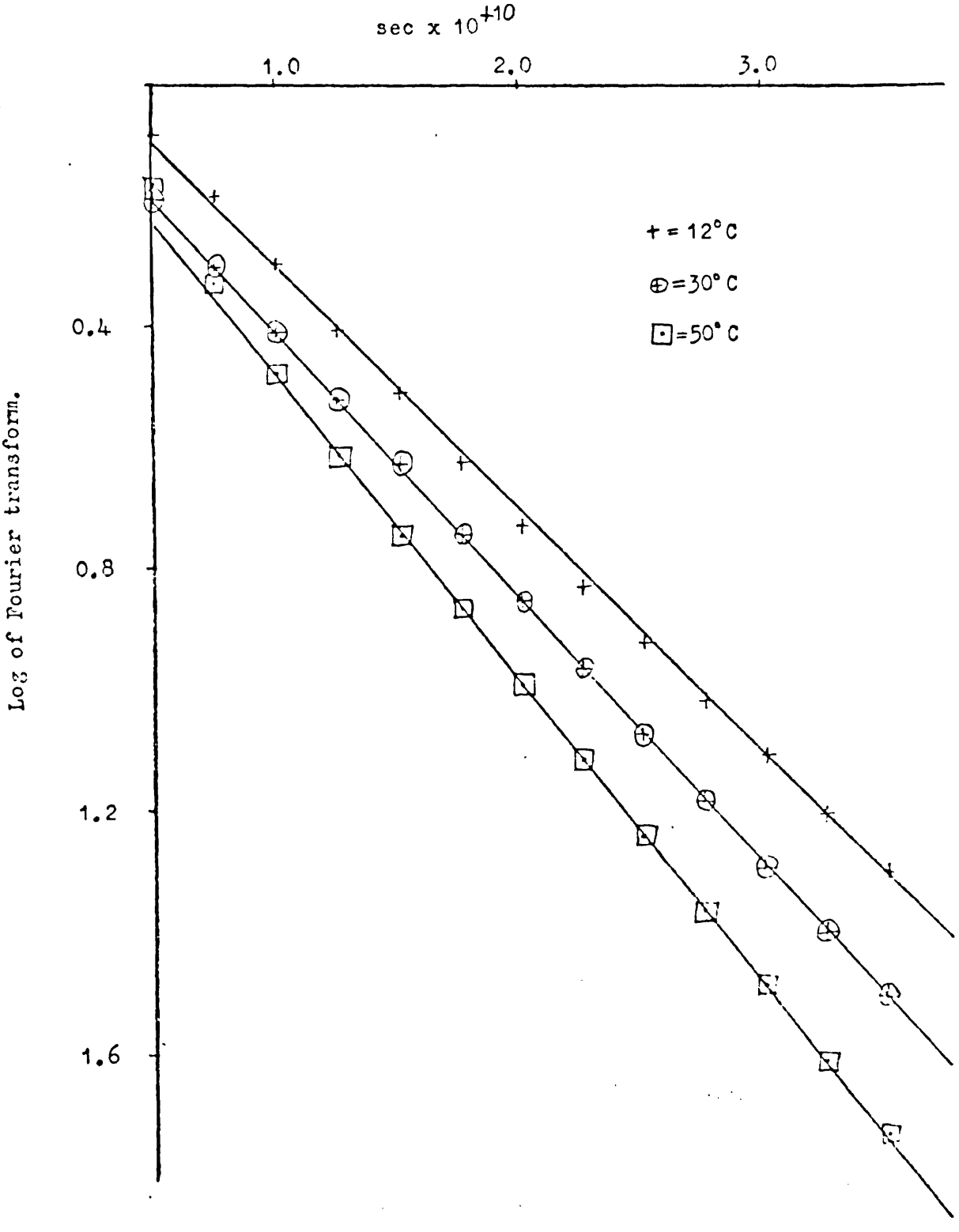

Fig. 4.4. p-difluoro benzene in acetonitrile with gradients of p-difluoro benzene in cyclohexane for comparison.

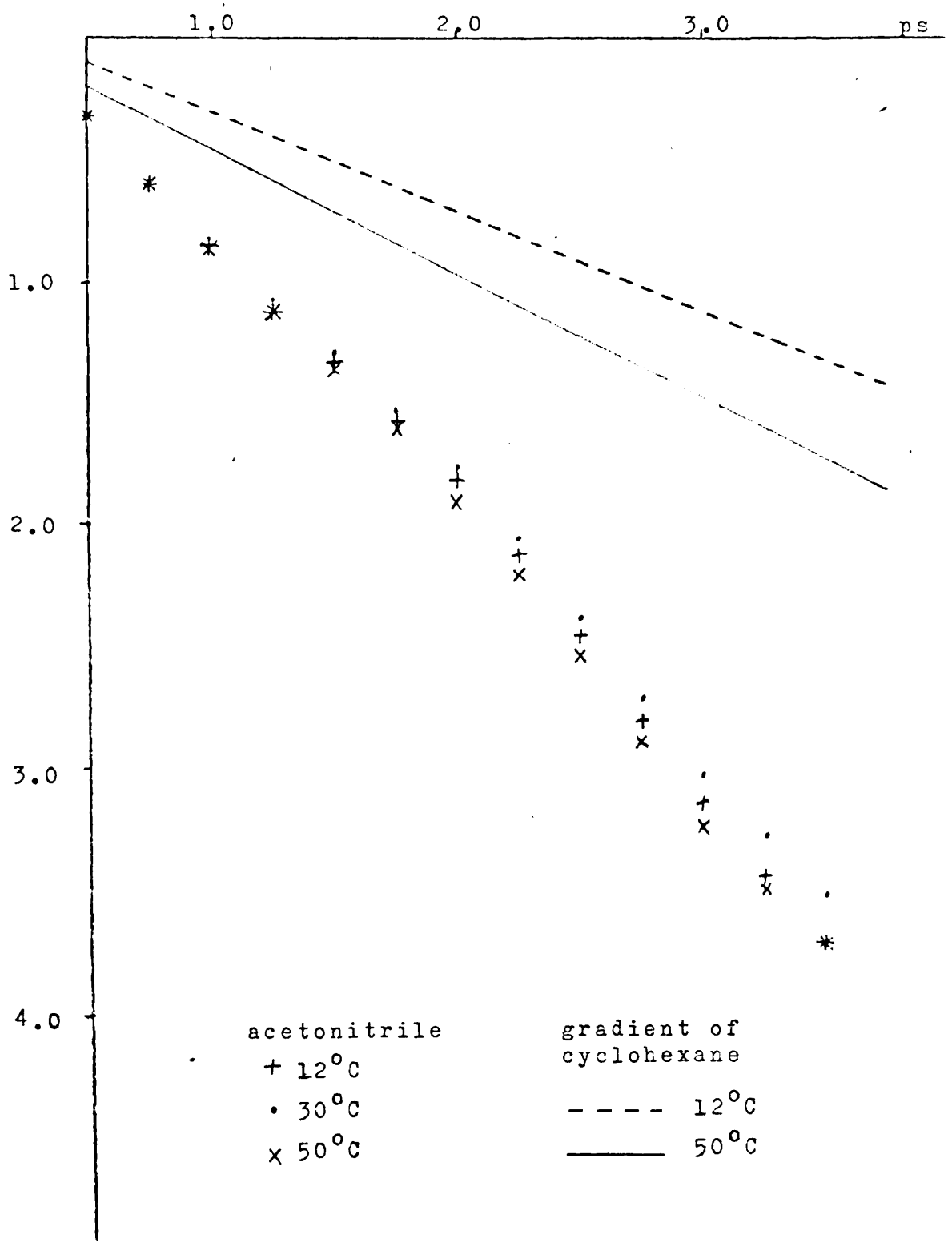

The position of total absorption was marked on the chart by blocking the beam between the source and the sample. This was to compensate for the differences in sample radiation at different temperatures.

The calculation of the Fourier transform was achieved using a computer program VANSA supplied by E.B. Gill. The program incorporates a correction of the band contour which is distorted by the finite slit width of the spectrometer.[82]

4.3 Results

The log of the Fourier transform was plotted against time for each solvent at each temperature and the gradient of the graph between 0.5 and 3.5 ps was recorded. The results are given in Table 4.1. The log of the Fourier transforms against time of the cyclohexane solutions at the three temperatures recorded are shown in Fig. 4.3 but only three of the five temperatures of the acetonitrile solutions are shown in Fig. 4.4. The gradients of the cyclohexane solutions at 12°C and 50°C are also shown on the same scale for easier comparison.

The gradients of the solutions in cyclohexane have a marked temperature dependence, the gradient increasing with an increase in temperature. The gradients of the solutions in acetonitrile are more than double those of the solutions in cyclohexane and show no temperature effect. The plots show more oscillation than those for the cyclohexane solutions. This oscillation makes the gradients more difficult to measure and so a slight temperature dependence cannot be ruled out. It would, however, be much smaller than that of the cyclohexane solutions.

Fig. 4.5. Possible associations between p-difluoro benzene and the solvent.

a) cyclohexane

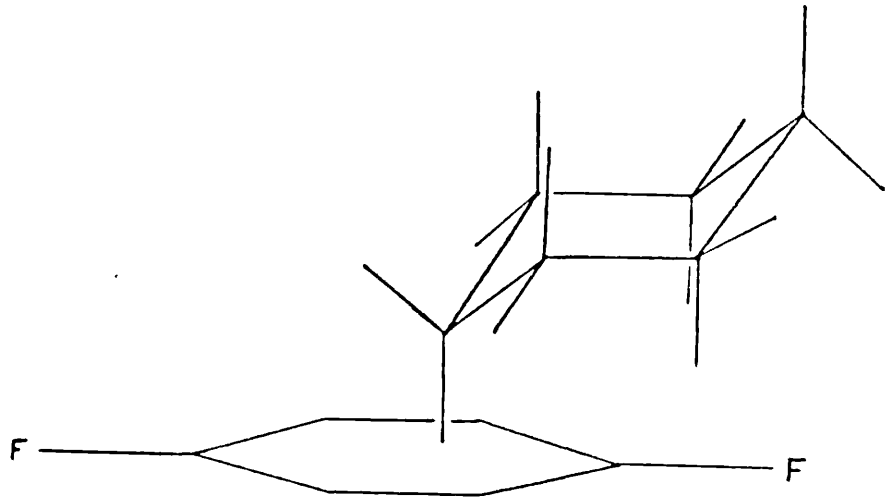

b) acetonitrile

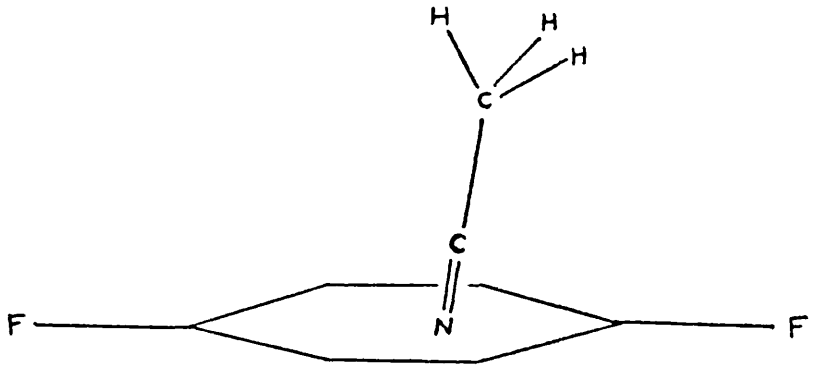

A possible explanation of the effects seen is as follows. The energy barrier to rotational relaxation is less in acetonitrile as indicated by the small effect of temperature on relaxation rate and the larger slope of the gradient. This is hardly surprising as Fig. 4.5 clearly shows that p-difluoro benzene will rotate more easily amongst the smaller acetonitrile molecules.

The gradient of the log of the Fourier transform against time is equal to the sum of the gradients due to the vibrational and rotational relaxation mechanisms, that is

$$G_{(C)} = G_{R(C)} + G_{V(C)}$$

$$G_{(A)} = G_{R(A)} + G_{V(A)}$$

for the solutions in cyclohexane and acetonitrile respectively. We have seen that

$$G_{R(C)} > G_{R(A)}$$

Therefore

$$G_{R(A)} - G_{R(C)} < G_{V(A)}$$

if we neglect $G_{V(C)}$, i.e. the vibrational relaxation due to interactions between cyclohexane and p-difluoro benzene. This is probably justified because the primary mechanisms of vibrational relaxation involve polar-polar interactions (i.e. dipole-dipole, dipole-quadrupole or to a certain extent transition dipole-dipole).[83, 84] In acetonitrile we have a large intensity i.e. large transition dipole interaction with a large dipole. It is well established that vibrational relaxation frequently shows a small temperature dependence compared with rotational relaxation and indeed this forms the basis of the oldest method of separating the

contributions of rotational and vibrational relaxation processes to the band width.[85] Even though the Rakov method appears to be of rather doubtful validity (see for example 86), the general conclusion that the temperature dependence of vibrational relaxation is small is compatible with our interpretation of our observations.

In acetonitrile the relaxation is mainly due to a random complexing effect and any temperature dependence is probably due to rotational relaxation effects. The presence of a small side band in acetonitrile solution may be due to the presence of a small amount of a more stable complex formation between p-difluoro benzene and acetonitrile.

In conclusion we can say that the main mechanism for relaxation in cyclohexane solution is due to molecular reorientation and the main mechanism in acetonitrile solution is due to molecular interactions.

List of References

1. R.R. Ernst, Adv. Mag. Res., 2, 1 (1966).
2. W.N. Haworth, The Constitution of Sugars, p.90, Edward Arnold and Co., London (1929).
3. D.H.R. Barton, J. Chem. Soc., 348 (1948).
4. R.M. Barrett, Ph.D. Thesis, University of London (1973).
5. J.A. Pople, W.G. Schneider, H.J. Bernstein, High-Resolution Nuclear Magnetic Resonance, p.458, McGraw-Hill, New York (1959).
6. F.R. Jensen, C.H. Bushweller, B.H. Beck, J. Am. Chem. Soc., 91, 344 (1969).
7. L.D. Hall, D.L. Jones, Can. J. Chem., 51, 2914 (1973).
8. E.L. Eliel, Chem. and Ind., 568 (1959).
9. J. Musher, J. Am. Chem. Soc., 83, 1146 (1961).
10. A.H. Lewin, S. Winstein, J. Am. Chem. Soc., 84, 2464 (1962).
11. F.R. Jensen, B.H. Beck, J. Am. Chem. Soc., 90, 3251 (1968).
12. F. Hruska, D.W. McBride, T. Schaffer, Can. J. Chem., 45, 1081 (1967).
13. J.B. Stothers, Can. J. Chem., 45, 2943 (1967).
14. F.A.L. Anet, J. Am. Chem. Soc., 84, 1053 (1962).
15. P. Laszlo, Progress in n.m.r. spectroscopy, Vol. 11, (1967).
16. L.W. Reeves, K.O. Stromme, Can. J. Chem., 38, 1241 (1960).
17. F.A. Bovey, E.W. Anderson, F.P. Hood, R.L. Kornegay, J. Chem. Phys., 40, 3099 (1964).
18. J. Reisse, J.C. Celotti, G. Chiurdoglu, Tetrahedron Lett., 397 (1965).

19. E. Breitmaier, G. Jung, W. Voelter, Angew. Chem., int. ed., 10, 673 (1971).

20. H-J. Schneider, R. Price, T. Keller, Angew. Chem., int. ed., 10, 730 (1971).

21. H-J. Schneider, V. Hoppen, Tetrahedron Lett., 579 (1974).

22. G. Gatti, A.L. Segre, C. Morandi, J. Chem. Soc. (B), 1204 (1967).

23. A.L. Anet, A.J.R. Bourn, J. Am. Chem. Soc., 890, 760 (1967).

24. A.J. Berlin, F.R. Jensen, Chem. and Ind., 998 (1960).

25. W.C. Neikam, B.P. Dailey, J. Chem. Phys., 38, 445 (1963).

26. R.F. Nystrom, W.G. Brown, J. Am. Chem. Soc., 69, 2549 (1947).

27. Chem. Ber., 88, 1053 (1955); Chem. Abs., 50, 13892c, (1956).

28. S.W. Pelletier, Chem. and Ind., 1034 (1953).

29. H. Stone, H. Shechter, Organic Syntheses, Coll. Vol., 4, 323 (1963).

30. H. Stone, H. Shechter, J. Org. Chem., 15, 491 (1950).

31. L. Larnaudie, Compt. Rend., 235, 154 (1952).

32. G. Chiurdoglu, L. Reisse, Bull. Soc. Chim. Belges, 70, 472 (1961).

33. I.O.C. Ekejiuba, H.E. Hallam, Spectroscopy Letters, 2, 347 (1969).

34. E. Fujimoto, K. Kozima, Y. Takeoka, Bull. Chem. Soc. Jap. 44, 2110 (1971).

35. A.R.H. Cole, R.N. Jones, K. Dobriner, J. Am. Chem. Soc., 74, 5571 (1952).

36. G. Chiurdoglu, L. Kleiner, W. Masschelein, J. Reisse, Bull. Soc. Chim. Belges, 69, 143 (1960).

37. R.G. Snyder, G. Zerbi, Spec. Acta., 23A, 391 (1967).

38. J. Aldous, I.M. Mills, Spec. Acta., 19, 1567 (1963).

39. O. Hassel, Research, 3, 504 (1950) and Quart. Rev. VII, 221 (1953).

40. P. Klaeboe, J.J. Lothe, K. Lunde, Acta. Chem. Scand., 10, 1465 (1956).

41. K. Kozima, K. Sakashita, Bull. Chem. Soc. Jap., 31, 796 (1958).

42. F.R. Jensen, L.H. Gale, J. Org. Chem., 25, 2075 (1961).

43. U. Kh. Agaev, S.Z. Rizaeva, A.T. Alyev, Yu. A. Pentin, Russ. J. Phys. Chem., 47, 583 (1973).

44. J. Stokr, B. Schneider, J. Jakes, J. Mol. Structure, 15, 87 (1973).

45. L.H. Scharpen, J. Am. Chem. Soc., 3737 (1972).

46. I.O.C. Ekejiuba, H.E. Hallam, J. Mol. Structure, 6, 341 (1970).

47. M. Hanack, Conformational Theory, Academic Press, New York (1965).

48. E.L. Eliel, N.L. Allinger, S.J. Angyal, G.A. Morrison, Conformational Analysis, Interscience, New York (1966).

49. J.A. Hirsch, Topics in Stereochemistry, 1, 199 (1967).

50. G.B. Robertson, Nature, 593 (1961).

51. O. Bastiansen, M. Traetteberg, Tetrahedron, 17, 147 (1962).

52. E.A. Braude, W.F. Forbes, J. Chem. Soc., 3754 (1955).

53. J. Dale, Acta Chem. Scand., 11, 650 (1957).

54. H. Suzuki, Bull. Chem. Soc. Japan, 32, 1340 (1959).

55. B. Tinland, Acta Phys. Acad. Sci. Hung., 25, 111 (1968); Theor. Chim. Acta, 11, 452 (1968); J. Mol. Structure, 3, 161, 513 (1969).

56. K. Mobius, Z. Naturforsch., 20a, 1117 (1965).

57. A.C. Littlejohn, J.W. Smith, J. Chem. Soc., 2456 (1953).

58. I.A. Bogdanov, M.F. Vuks, Zhur. fiz. Khim., 3, 46 (1965).

59. A. Unanué, P. Botherel, Bull. Soc. Chim. France, 1640 (1966).

60. J.Y.H. Chan, C.G. Le Fèvre, R.J.W. Le Fèvre, J. Chem. Soc., 2666 (1959).

61. A. Rousset, A. Pacault, Compt. rend., 238, 1705 (1954); C.L. Cheng, D.S.N. Murthy, G.L.D. Ritchie, J.C.S. Faraday 2, 1679 (1972).

62. A.D. McLachlan, Mol. Phys., 3, 233 (1960).

63. G. Casalone, C. Mariani, A. Mugnoli, M. Simonetta, Mol. Phys., 15, 339 (1968).

64. A. d'Annibale, L. Lunazzi, A.C. Boicelli, D. Macciantelli, J.C.S. Perkin 2, 1396 (1973).

65. V.J. Eaton, D. Steele, J.C.S. Faraday 2, 69, 1601 (1973).

66. G.B. Wheland, Resonance in Organic Chemistry, John Wiley (1955).

67. E.B. Wilson, J.C. Decius, P.C. Cross, Molecular Vibrations, McGraw-Hill, New York, 64 (1955).

68. O. Redlich, Z. Physik. Chem., (B) 28, 371 (1935).

69. E. Teller, quoted in J. Chem. Soc., 971 (1936).

70. R.A.R. Pearce, Ph.D. Thesis, University of London (1972).

71. J. Trotter, Acta Cryst., 14, 1135 (1961).

72. D. Steele, Spect. Acta , 22, 1275 (1966).

73. V.J. Eaton, Ph. D. Thesis, University of London (1973).

74. R.G. Gordon, J. Chem. Phys., 42, 3658 (1965).

75. R.G. Gordon, J. Chem. Phys., 43, 1307 (1965).

76. R.G. Gordon, Advances in Magnetic Resonance, Vol. 3 (Ed).

77. J.S. Waugh, Academic Press, New York (1968).

78. D. Steele, W. Wheatley, J. Mol. Spectry., 32, 265 (1969).

79. G. Jalsovsky, W.J. Orville-Thomas, Trans. Far. Soc., 67, 1894 (1971).

80. I.R. Hill, Ph. D. Thesis, University of London, 1975.

81. P. Dorval, Thesis, University of Brest, 1971.

82. I.R. Hill, D. Steele, J. Chem. Soc., Faraday Trans. 2, 70, 1233 (1974).

83. K.A. Valiev, Optics and Spectroscopy, 13, 505 (1962).

84. G. Döge, Z. Naturforsch, 28, 919 (1973).

85. A.V. Rakov, Opt. Spectry., 7, 128 (1959).

86. J.E. Griffiths and K.T. Gillen, Advances in Raman Spectroscopy, Vol. 1, Editor J.P. Mathieu, Published by Heyden & Son Ltd., 1973, p.472.